GENERAL ELECTRIC

MISSILE AND SPACE [illegible]

PARTIAL PRESSURE OXYGEN SENSOR, THE DESIGN AND DEVELOPMENT OF A PROTOTYPE ASSEMBLY

LIFE SUPPORT

NASA CR108510

PARTIAL PRESSURE OXYGEN SENSOR, THE DESIGN AND DEVELOPMENT OF A PROTOTYPE ASSEMBLY

CREW SYSTEMS DIVISION

NASA MANNED SPACECRAFT CENTER

HOUSTON, TEXAS

Contract Monitor: Mr. W. H. Bush

Prepared under contract No. NASA-9-1300

By

W. E. Funsch, F. Primiano, L. Cooper
General Electric Company
Missile and Space Division
Valley Forge Space Technology Center
P. O. Box 8555
Philadelphia, Pa.

GENERAL ELECTRIC

PARTIAL PRESSURE OXYGEN SENSOR

I. SUMMARY

A development program has been conducted to further develop a General Electric oxygen sensor utilizing the fuel cell principal of operation. The total weight of this sensor is 1.0 pound, while its volume is 15 cubic inches. The program objectives are outlined in NASA Contract NASA-9-1300. The work completed under this contract included conceptual studies, development testing; and the design, fabrication, and checkout of two prototype oxygen sensors.

As a result of this effort an oxygen sensor was developed which has a normal operating life of 30 days. The sensor has a useful range of 10 mm Hg to 760 mm Hg pO_2, with an accuracy of $\pm 5\%$. The sensor output voltage is essentially zero at zero oxygen partial pressure, and increases linearly with oxygen partial pressure in the sample atmosphere.

The sensor output voltage at any given partial pressure of oxygen (pO_2) increases about 1MV/°F. This thermal effect is compensated for by a thermistor network to provide an output which varies less than $\pm 3.6\%$ over a temperature range of 35 to 110°F. Humidity has shown little affect on the sensor output signal between 20-80% relative humidity.

However, above 80% relative humidity the output voltage decreases; and below 20% relative humidity the output voltage increases.

The detailed results of the test program are presented in Section III of this report. A tabulated summary of these results and the requirements specified in the NASA work statement are shown in Table I below:

TABLE I

TEST	REQUIREMENT	RESULT
Endurance	30 Days	30 Days
Temperature Compensation 35 - 110°F	± 3%	3.6% Total*
Response Time	3 - 5 secs.	25 - 32 Secs.△
Humidity	0 - 100%	20 - 80%
Accuracy	± 3% full scale	± 5% Full Scale
Linearity	± 2%	± 3%
Range	160 - 400 mm Hg.	80 - 460 mm Hg.
O_2 Mixtures	Single & Multigas	Requires Barrier Change+
Weight	13 ounces	16.7 ounces
Volume	12 cubic inches	15 cubic inches

* Hysteresis loop gives total variation (See Figure 22)

△ Rapid initial response with rate decreasing with time.

\+ 1 mil barrier required for multigas atmospheres and 4 mil barrier for pure oxygen.

II. SENSOR DESCRIPTION

A. Introduction

Oxygen concentration levels which will prevent physiological and psychological performance degradation are an important measurement for the control of a spacecraft atmosphere. The General Electric fuel cell principal of oxygen measurement shows much promise of providing a simple reliable oxygen measuring instrument to monitor this atmosphere.

The chemical combination of hydrogen and oxygen in the presence of a catalyst has been the subject of a major development effort by numerous organizations over the past several years. The ion-exchange membrane type fuel cell has been developed by the General Electric Company for space power applications. In the course of this work, engineers noted an apparent response of fuel cell output energy to changes in the mass density of oxygen. This fact brought forth the possibility of using the fuel cell principal to sense the partial pressure of oxygen as a direct reading instrument.

The General Electric oxygen sensor concept developed from this beginning, utilizes a miniaturized ion-exchange membrane (IEM) as the sensing element. The basic membrane material is procured from the production facilities of the Direct Energy Conversion Operation at Lynn, Massachusetts. The anode side of

the membrane is exposed directly, via a diffusion barrier, to the gas mixture whose oxygen partial pressure is to be measured, (see Figures 2 and 3). The purpose of the diffusion barrier is to limit the flow of oxygen molecules to a rate less than the ion-exchange membrane can utilize. In effect the ion-exchange membrane must use up oxygen as fast as it diffuses through the barrier. When the oxygen partial pressure reaches a value such that the amount diffusing through the barrier is greater than that required for the reaction, the sensing element saturates. Thin metal washers, i.e., current collectors, are pressed against the platinum black on the ion-exchange membrane to provide a conducting path for the electrons.

Product water accumulates on the oxygen side of the membrane until its vapor pressure allows it to permeate through the diffusion barrier. This product water is essential in that it prevents the ion-exchange membrane from drying out. The sensors developed operate at approximately 2 ma. at ambient atmosphere (pO_2 160 mm Hg). This low current density (.007 amp/cm^2) theoretically permits 3000 hours of useful life.

The General Electric oxygen sensor is shown in Figure 1 with an exploded view of this sensor shown in Figure 2. This miniaturized sensor supplies a self-generated current which can be applied directly to an indicating instrument. It will sense oxygen partial pressure continuously, to the exclusion of the other gases and vapors.

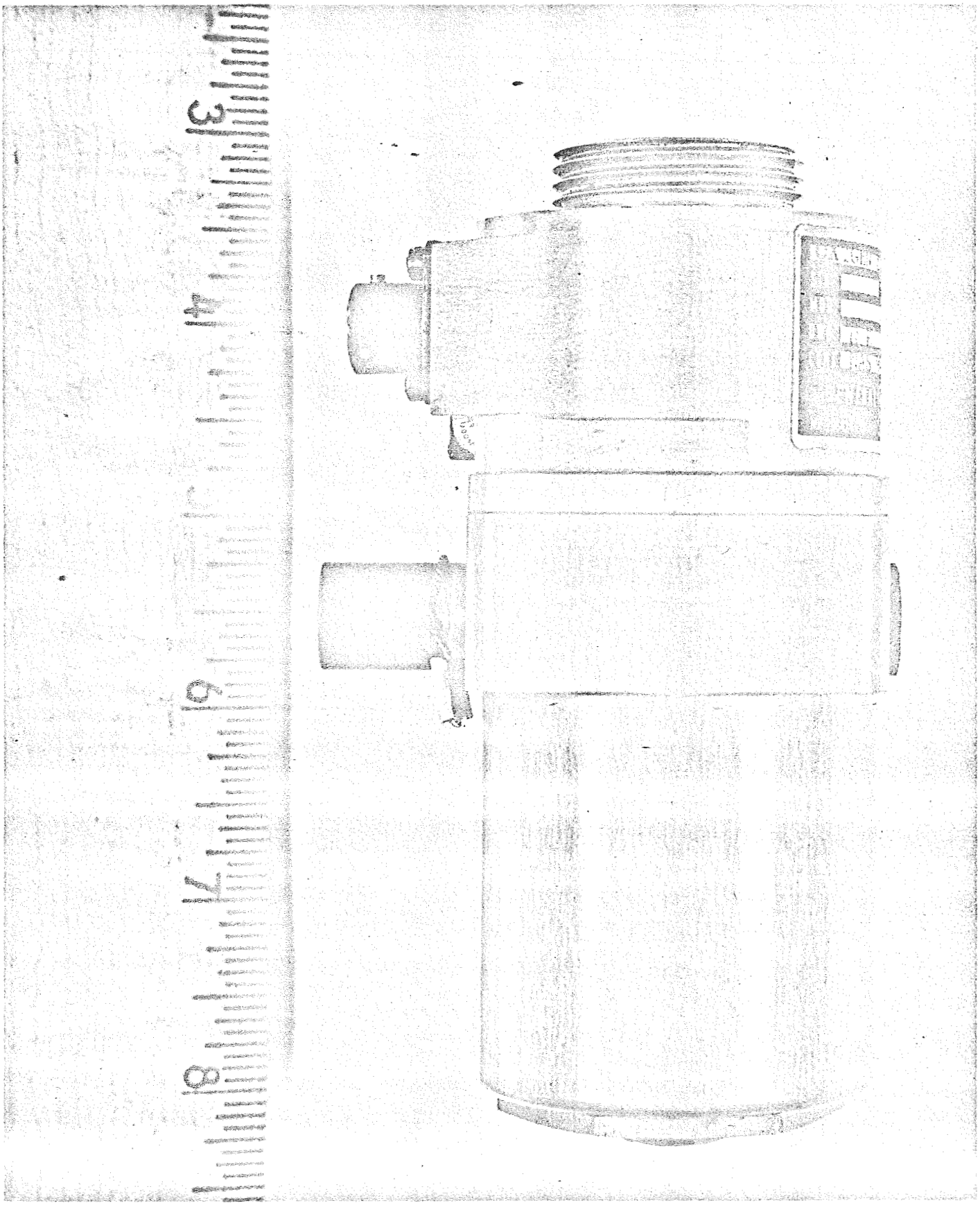

FIGURE I.: PROTOTYPE OXYGEN SENSOR

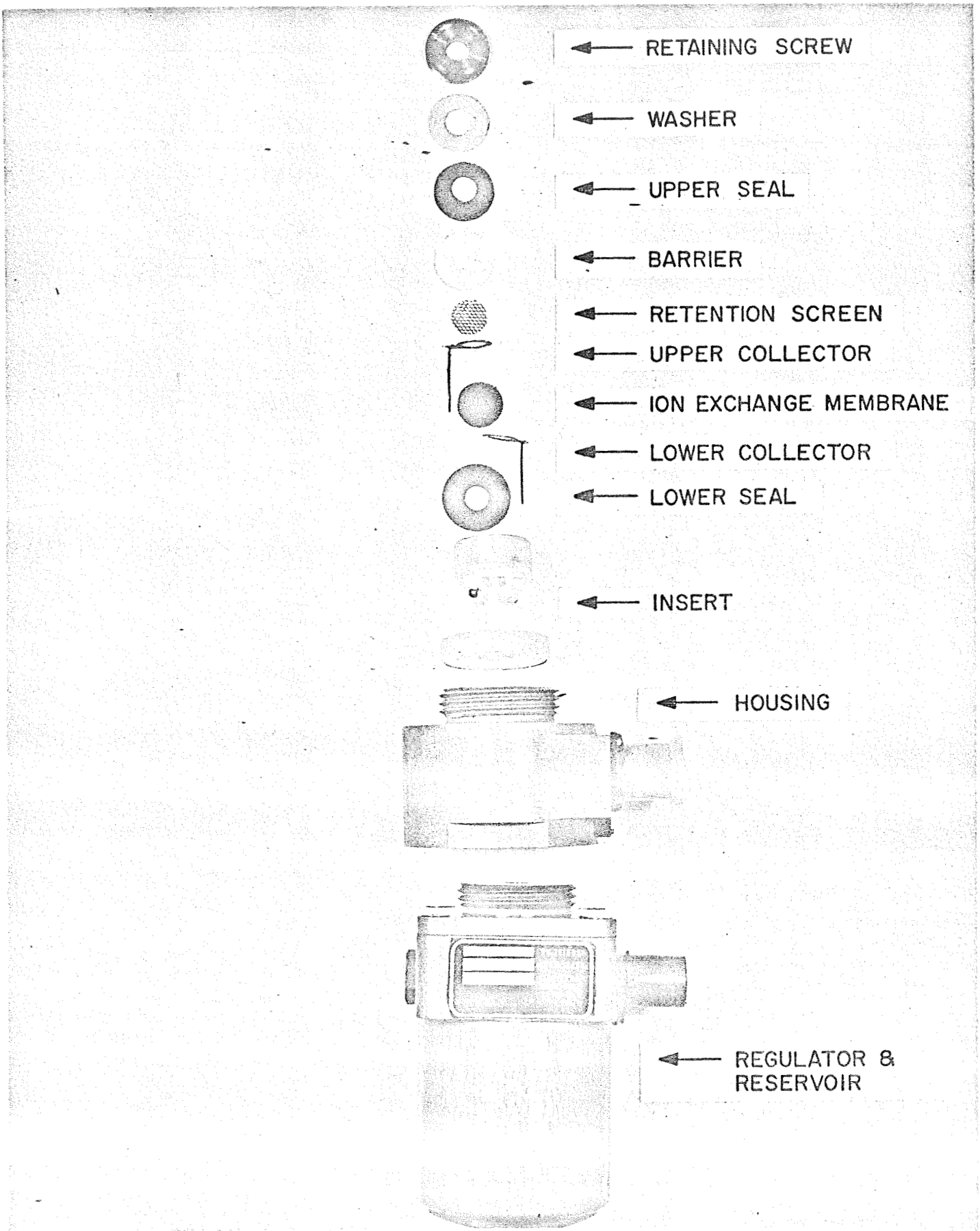

FIGURE 2.: EXPLODED VIEW-OXYGEN SENSOR

After initial calibration in the atmosphere to be measured, the sensor will provide an automatic, continuous, electrical output signal which is proportional to the actual pO_2 present. All components of the system are miniaturized and extremely rugged.

This sensor represents a new technique of polargraphic sensing of oxygen without exhaustion of the sensor through irreversible chemical reaction, and without the need for a polarizing electrical potential from an external source.

B. Detailed Description

The prototype oxygen sensor is designed to provide a given response to oxygen levels from 80 mm Hg to 460 mm Hg. The sensor is essentially a miniaturized concentration polarized fuel cell. Operating in the concentration polarized regime extends the range over which the sensor is affected by changes in oxygen partial pressure. For proper operation two items are essential, a dependable fuel cell assembly and a mass transport limiting mechanism.

A number of materials and sensor configurations have been tried in order to develop a reproducible, stable sensor with good accuracy, linearity, range and response time. Section III of this report describes this development effort.

Detail drawings of each component making up the sensor assembly are included in Appendix B. Figure 3, an assembly drawing

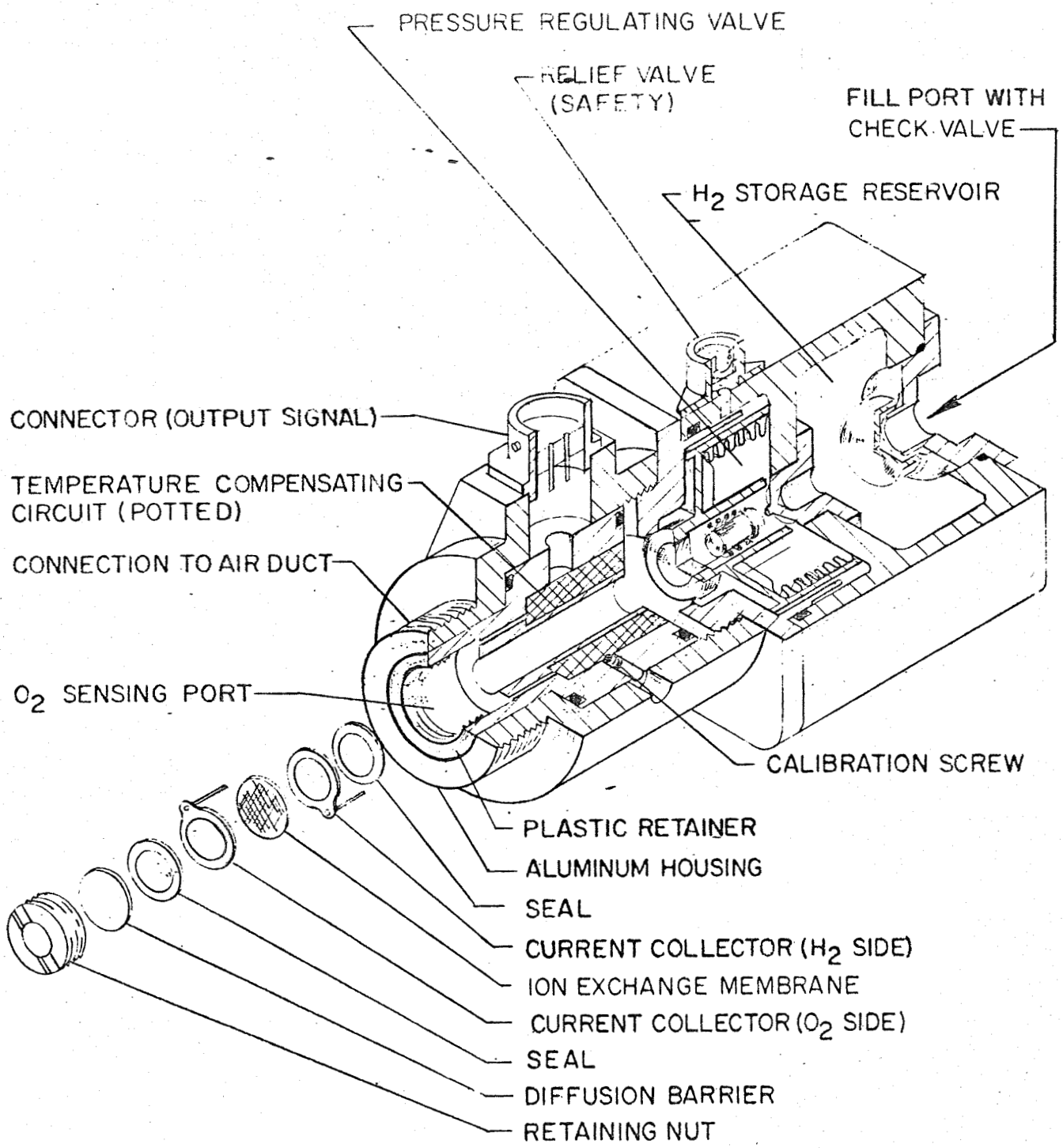

GENERAL ELECTRIC

PARTIAL PRESSURE OXYGEN SENSOR

of the oxygen sensor, illustrates the overall configuration of the instrument. The sensor assembly can be considered to be made up of seven major components: ion-exchange membrane, collectors, seals, barrier, housing, H_2 supply, and temperature compensation network. A detailed weight breakdown of the sensor assembly is shown in Table II.

TABLE II

pO_2 SENSOR WEIGHT BREAKDOWN

Regulator & Reservoir	332 grams
Housing	105 grams
Sensor Body	9 grams
Connector & Screws	8 grams
Retaining Nut	6 grams
Collectors	1 gram
Temperature Compensation Network	5 grams
"O" Rings	1 gram
Seals	2 grams
Barrier	0.5 gram
Ion-Exchange Membrane	0.5 gram
Lock Wire & Nameplate	2 grams
TOTAL	472 grams (1.041 lbs.)

1. Ion-Exchange Membrane: The ion-exchange membrane itself is a .009 thick solid polymer impregnated with an electrolyte, polystyrene sulphonic acid (PSSA). This membrane acts as a impermeable partition between the reactant gases. The electrodes are composed of platinum black deposited on each face of the membrane. This catalytic coating on each surface serves as the electrode for that gas exposed to it. At the hydrogen electrode, H_2 gas dissolves in the platinum to yield protons and free electrons which are transferred via the current collector as a negative current. The protons move from the H_2 side platinum directly to the membrane and are transported through it to the oxygen side. At the oxygen electrode these protons pass into solution with the platinum. Oxygen is adsorbed on the platinum surface and is available to combine with the proton and the free electrons transported from the H_2 electrode to form water. This type of membrane has an advantage in that the electrolyte remains non-diluted by H_2O formed as a result of the oxygen-hydrogen reaction. The IEM is approximately 60% water so that variations in water contact at the surface can result in significant changes in diffusion rates and conductivity of the desiccated portions.

An external circuit is provided to connect both electrodes to a fixed electrical load, in parallel with the EMF. A voltmeter across the load will indicate an output related to the pO_2, and can be calibrated in any units desired (mm Hg, psia, etc.).

2. Current Collectors: Metal plates, or current collectors, are pressed against the carbon black on the membrane to provide a conducting path for the generated electrons. Figure 3 illustrates the position of these collectors in relation to the membrane. The internal resistance of the cell depends not only upon the electrolytic conductivity, but also upon the resistance associated with the current collectors and lead wires. Tantalum has been used as the material for the current collector. This metal has some unique properties which could lead to difficulties. It is a refractory material and so non-corrosive; affected mainly by hydrofluoric acid. It protects itself by growing an oxide film on its surface at room temperature. Not only does this film serve as an inhibitor to further oxidation, it also increases the resistance to electron flow into the metal. Positively polarizing the film in the presense of 0_2 increases the film thickness and its resistance. Fortunately, in this cell, the 0_2 side is negatively polarized and the film does not grow. But the initial oxide layer caused by exposure to atmospheric air may have enough resistance to be troublesome. Minor abrasions on the surface tend to break the continuity of the film and, therefore, to lower its resistance. Testing shows that a cleansing with hydrochloric acid and a light buffing of the contact surfaces should eliminate any trouble. Tantalum wire is spot welded to the current

collector and used to conduct the output current to terminals on the outside of the plexiglas insert.

3. The seals consist of two Viton "A" washers .125 inch thick. Leakage of hydrogen to the oxygen side of the ion-exchange membrane causes polarization of the cell and reduces output significantly. Therefore, it is essential that all leakage paths around the membrane are eliminated. It is also important to make sure all of the oxygen flows through the barrier. Any oxygen that bypasses the barrier, will produce an increased non-linear response. The seals are positioned so that compression will extrude the seal around the current collectors assuring a leak tight system.

4. Barrier: In order to insure that the cell is current limited, (concentration polarized), a diffusion barrier is placed in the path between the oxygen supply and the oxygen electrode. This essentially creates a pressure drop in the 0_2 inlet, allowing the external pressure to be higher than the saturation pressure of the cell itself. The silicone barrier utilized on the oxygen sensor was selected for its high oxygen permeability. In order to achieve maximum sensitivity, this material was selected over many commercially available materials such as cast teflon, polyethylene, polypropylene, and polypropyl nitrate. For low pressure applications a screen has been inserted over the barrier, to prevent it from bulging outward and tearing. Pressure differentials in excess of 750 mm Hg can be tolerated with this design. The barrier is positioned directly over

the collector to minimize the volume between the ion-exchange membrane and the barrier. The shorter the gap between the barrier and electrode, the less water and gas that can be trapped in this volume. Any water that builds up on the oxygen side of the membrane must be kept to a minimum or the overall permeability will be greatly decreased as the diffusion rate of oxygen in air is a million times that of water. A one mil silicone barrier was selected as permeability is approximately a linear function of barrier thickness. Thus sensitivity and response time are affected by the thickness of the barrier.

5. Hydrogen Supply: A three cubic inch reservoir has been provided to store a 30 day supply of hydrogen at 2000 psig. The rate of hydrogen consumption is a direct relationship to the amount of current produced. The electro-chemical equivalent for hydrogen is 26.6 ampere-hours per gram, or 1 milliamp requires .007 cc/min of hydrogen. At atmospheric pressure the sensor will utilize .014 cc/min of hydrogen.

A single stage pressure regulator is provided to reduce the storage pressure to 15 psia for delivery to the ion-exchange membrane. The orifice of the regulator is sized to pass a minimum flow of 0.13 cc/min.

The specification for this regulator-reservoir is included in Appendix "D". A charging port at the bottom of the reservoir allows filling of the reservoir from a high pressure hydrogen source. A test

port downstream of the regulator allows access to the hydrogen side of the ion-exchange membrane for monitoring hydrogen pressure or evacuating the storage chamber.

6. Temperature Compensation Network: The temperature compensation network consists of a series parallel circuit. A thermistor and 20 ohm resistor are in parallel with a 51 ohm resistor and a 0 to 50 ohm trimming potentiometer. The thermistor chosen has a resistance of 150 ohms at 35°F, 50 ohms at 77°F, and 25 ohms at 110°F. Figure 4 shows an electrical schematic of the temperature compensation network. The network has been potted in place on the inside of the aluminum sensor housing. Three inch leads are utilized so that the plexiglas insert can be removed from the aluminum housing which contains the trim potentiometer and the connector.

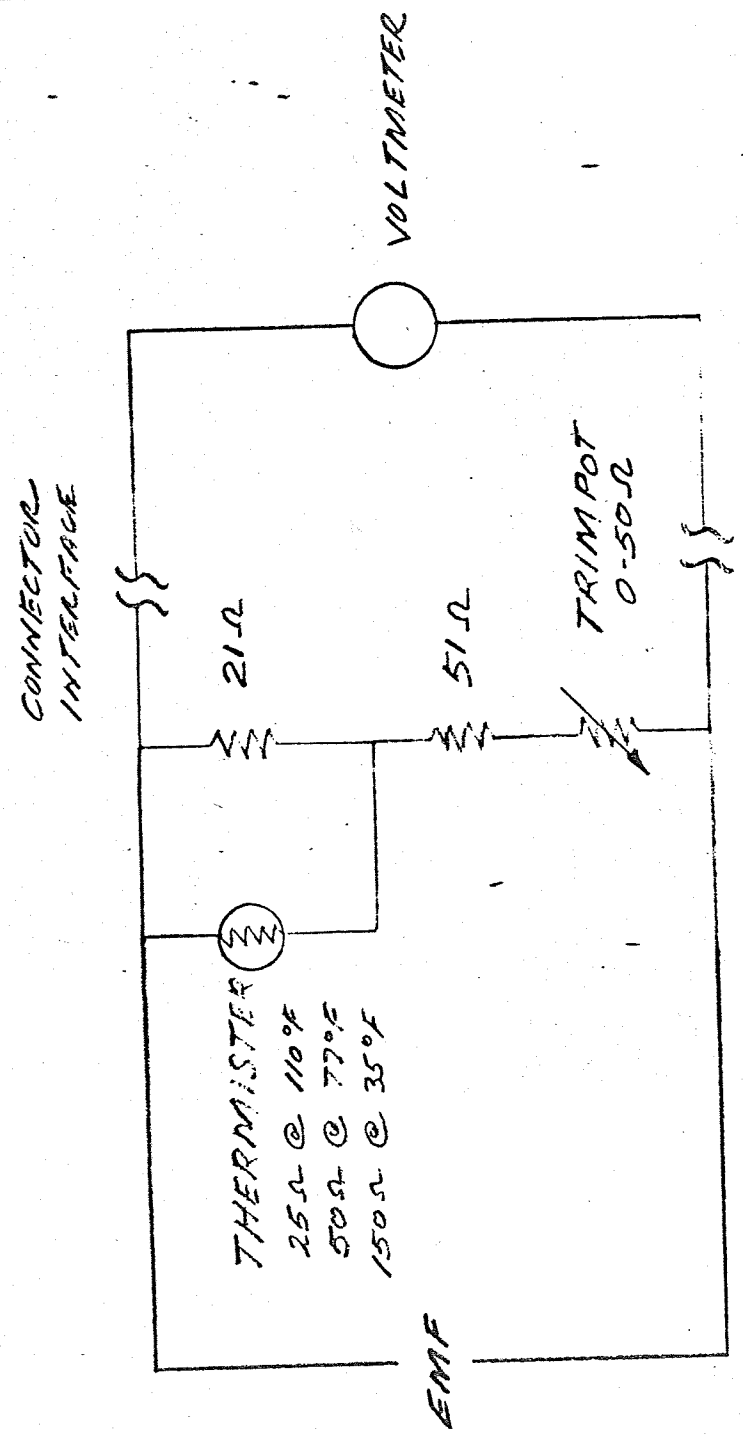

FIGURE 4. TEMPERATURE COMPENSATION CIRCUIT

III. DEVELOPMENT PROGRAM

The development program for the pO_2 sensor can be broken down into four hypothetical Phases (A, B, C, and D). The original experiments in Phase A, were conducted on test models made of stainless steel and gave unsatisfactory results. Phase B included a broader approach to the problem with many and varied approaches considered and tried. The decision to use tantalum current collectors and a plexiglas body with no reservoir or seals began Phase C. Phase D consisted of conducting the detailed development testing on the final configuration. Figure 5 shows a schematic of these phases with the tests performed in each.

Phase A: In the beginning of August 1963, the fabrication of two test model sensors, which had been designed on the basis of knowledge from prior programs, was completed and sensors were readied for testing. Since it was not known whether the cells would be run at currents high enough to produce the amount of water sufficient to maintain the necessary moisture state of the ion-exchange membrane (IEM), a liquid reservoir was included within the fuel cell. This reservoir was in the form of a conducting electrolyte path located in a plexiglas spacer placed between two membrane half cells, Type A (Figure 6). The half cells are membranes which have platinum black deposited on one surface only. The electrolyte connected the two uncoated surfaces of these membranes

12-12-63

pO_2 Sensor Experiment Development

Fig. 5

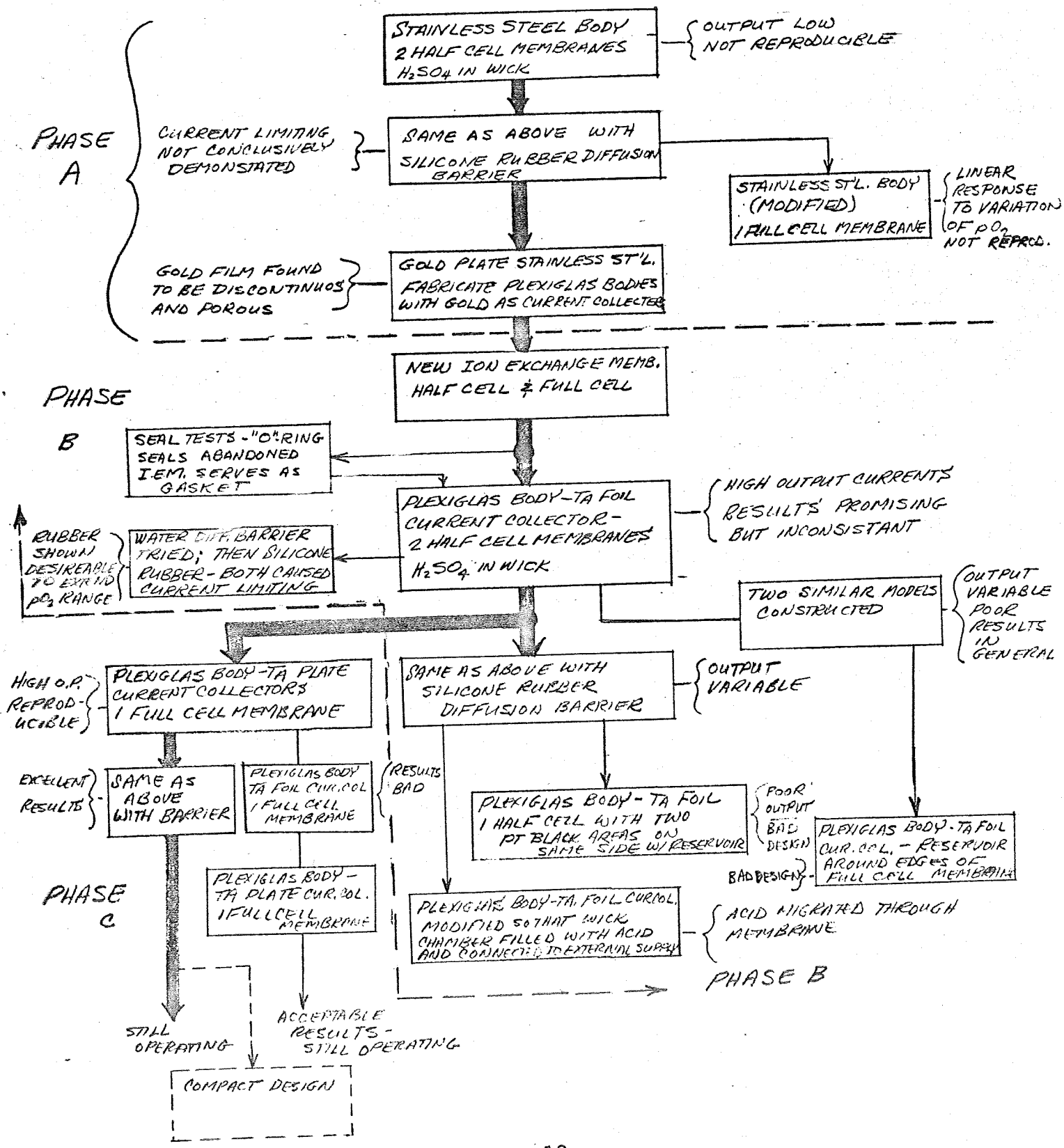

12-12-63

pO_2 SENSOR

BASIC CONFIGURATIONS

FIG. 6.

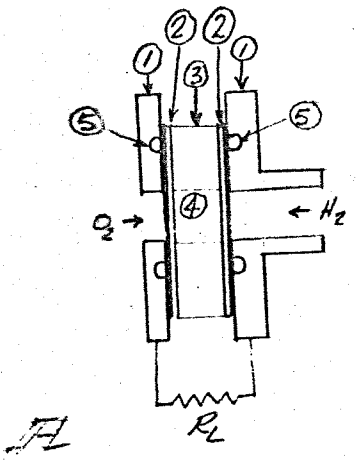

A

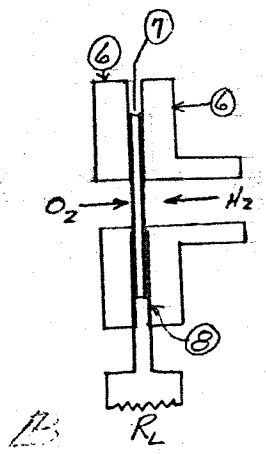

B

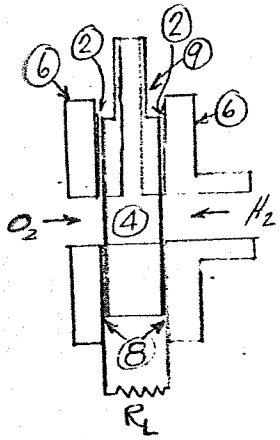

C

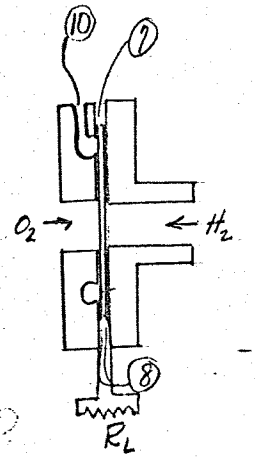

D

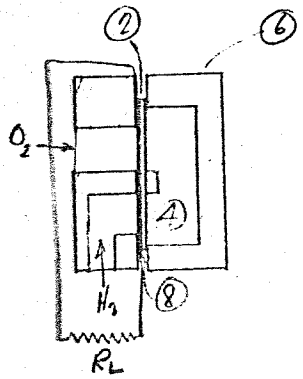

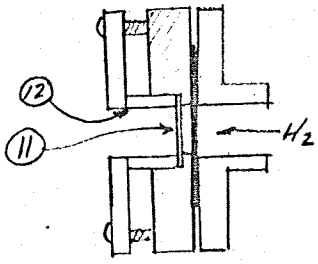

E

1. STAINLESS STEEL BODY
2. HALF CELL MEMBRANE
3. SPACER HOLDING WICK
4. ACID CHAMBER
5. "O" RING SEALS
6. PLEXIGLAS BODY
7. FULL CELL MEMBRANE
8. TA FOIL OR PLATE CURRENT COLLECTORS
9. SPACER MODIFIED FOR ACID INLET (NO WICK)
10. WATER RESERVOIR
11. DIFFUSION BARRIER
12. BARRIER RETAINER ASSEMBLY

FIG 2 TYPICAL OUTPUT CHARACTERISTIC OF pO_2 SENSOR USING 2-HALF CELLS WITH WICK BETWEEN. (NO DIFFUSION BARRIER) IN AIR. (STAINLESS STEEL BODIES — OLD T.E.M.)

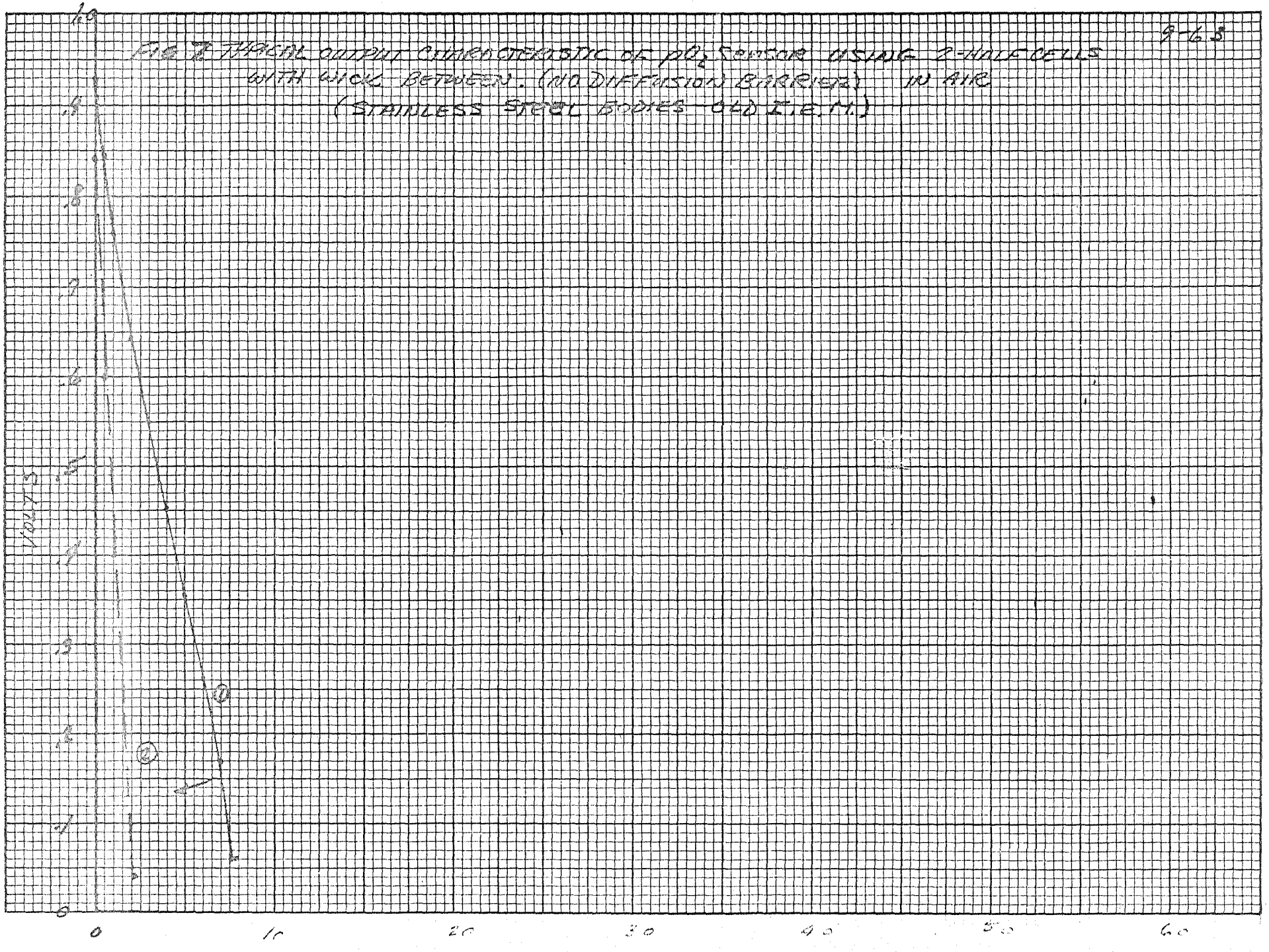

FIG. 8 TYPICAL RESISTANCE CURVES OF pO_2 SENSORS TO CHANGES IN ppO_2
USING OLD I.E.M. IN STAINLESS STEEL BODIES

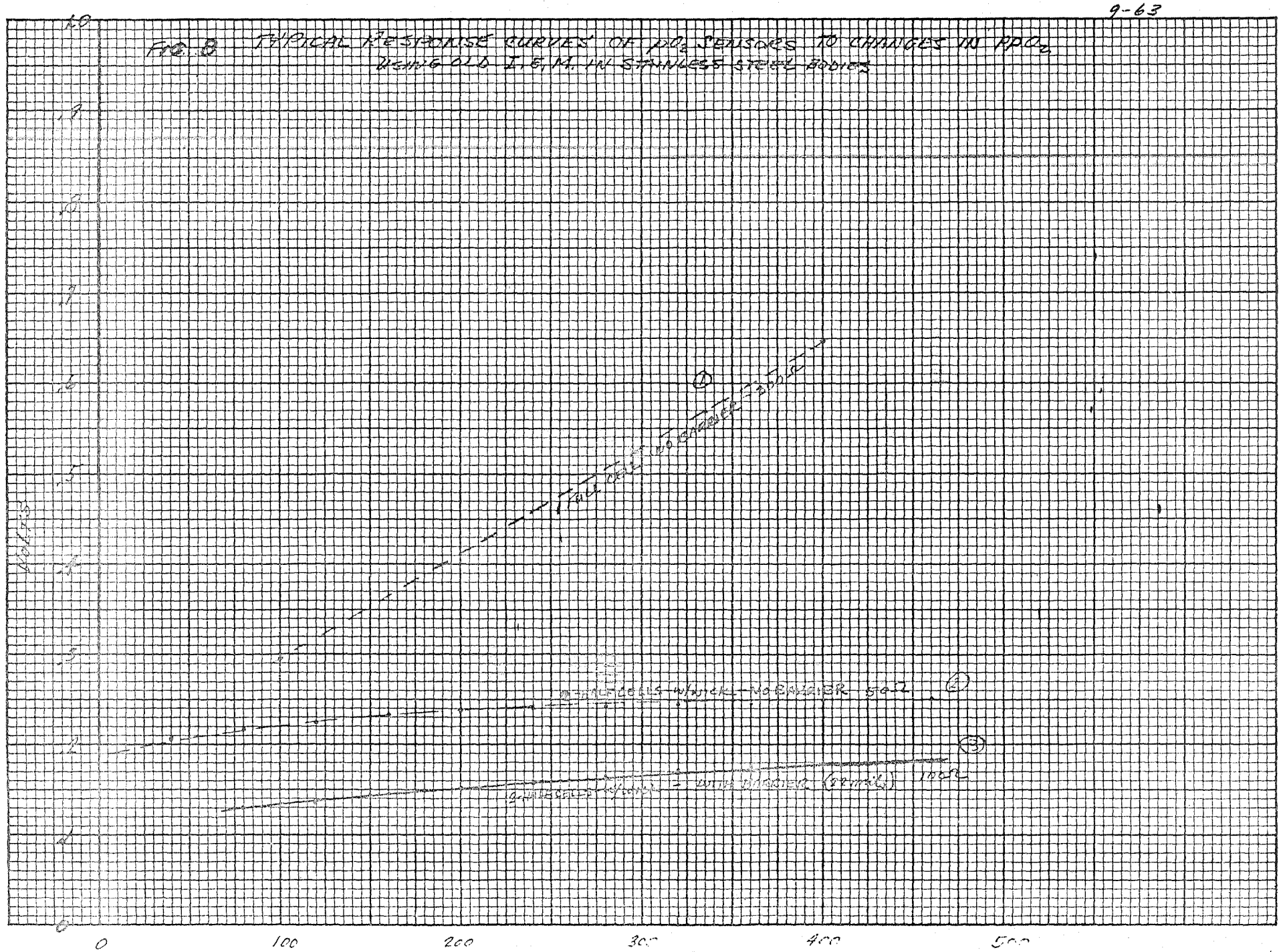

with each other while the platinum coated electrode surfaces faced the hydrogen and oxygen respectively. "O" rings pressing against the membranes on the coated sides served as seals for the acid and gases. The stainless steel body of the sensor which was made in two pieces, each insulated from the other, held the membrane-reservoir-spacer-membrane sandwich together and also served as the current collector at each electrode. Since the ion-exchange membranes are cationic acid membranes, H_2SO_4 was used as the electrolyte in the reservoir.

Curves of 1 and 2 of Figure 7 show the relatively low output achieved. Curve 1 shows the initial output of the cell and curve 2 the output a day later.

In order to test the cell without the acid electrolyte and since fuel cell membranes, coated with platinum black on both sides were available, a sensor was modified to accommodate this arrangement. The output was non-reproducible with time but it gave a linear response to pO_2. Whereas the cells with the reservoir had shown hardly any response to pO_2 and had given the impression the cells were O_2 saturated, this latter cell produced a very encouraging curve, Figure 8, Curve (1). Further testing showed that output signal variation and low values made these cells unacceptable. Proceeding under the assumption that constituents of the stainless steel were contaminating the membrane

and/or catalyst, it was decided to attempt to mask the steel so that it did not make direct contact with the membrane. A gold film was deposited on the current collecting surfaces of the steel body. This was expected to provide a shield for the IEM, but upon close examination, it was discovered that the film was discontinuous and very porous. In an effort to remove the possibility that the stainless steel would exert any influence on the cells' output, a sensor was made in the same configuration but with plexiglas replacing the steel members. Current collecting surfaces were made by depositing a gold film on the plexiglas. This film was also found to be discontinuous. For economic reasons and because of the fact that the gold and platinum diffused into each other during use, an extension of this approach was prohibitive. Phase A therefore ended without providing a working fuel cell let alone a pO_2 sensor, but it did serve to eliminate a number of possible blind alleys.

Phase B: After reviewing the test results it became obvious that the stainless steel in the original sensors, coupled with the possibility that the IEM may have been dried at one time, were mutually the basic causes of the erratic readings. Upon the delivery of fresh membrane, the sensor assembly was changed. A series of tests conducted on the membranes held in test assemblies which simulated the mechanical arrangement of the sensors, showed that the "O" rings were unnecessary as seals for the membranes. Under a sufficient pressure, the membranes acted as their own gasket, compressi

enough to seal. This knowledge allowed the "O" rings to be discarded, greatly simplifying the cell construction.

Since plexiglas was now used as the material for the sensor body, and the gold film was found inadequate, a current collecting material was needed. After a material investigation tantalum was selected. The only form of tantalum immediately available at the time was pure tantalum foil. This was used in conjunction with two half cells separated by a sulfuric acid reservoir. A photograph of the type "A" sensor described is shown in Figure 9. The output was markedly much higher than before but it was erratic, varying from day to day and even hour to hour. The sensors were assembled and disassembled until one or two were fabricated that had outputs constant for up to two days. A photograph of a typical test setup to evaluate performance is included in Figure 10. Performance testing was accomplished by evacuating a bell jar and admitting a mixture of oxygen and nitrogen to atmospheric pressure. A review of the literature revealed that current limiting could be accomplished by diffusion through all three physical states, gas, liquid and solids. In an effort to see if current limiting could be effected upon the cell, a layer of water was placed on the surface of the O_2 cathode covering it entirely. The effect was that the output voltage was reduced at high current. A silicone rubber diffusion barrier was next utilized and its effects were more severe than that of the

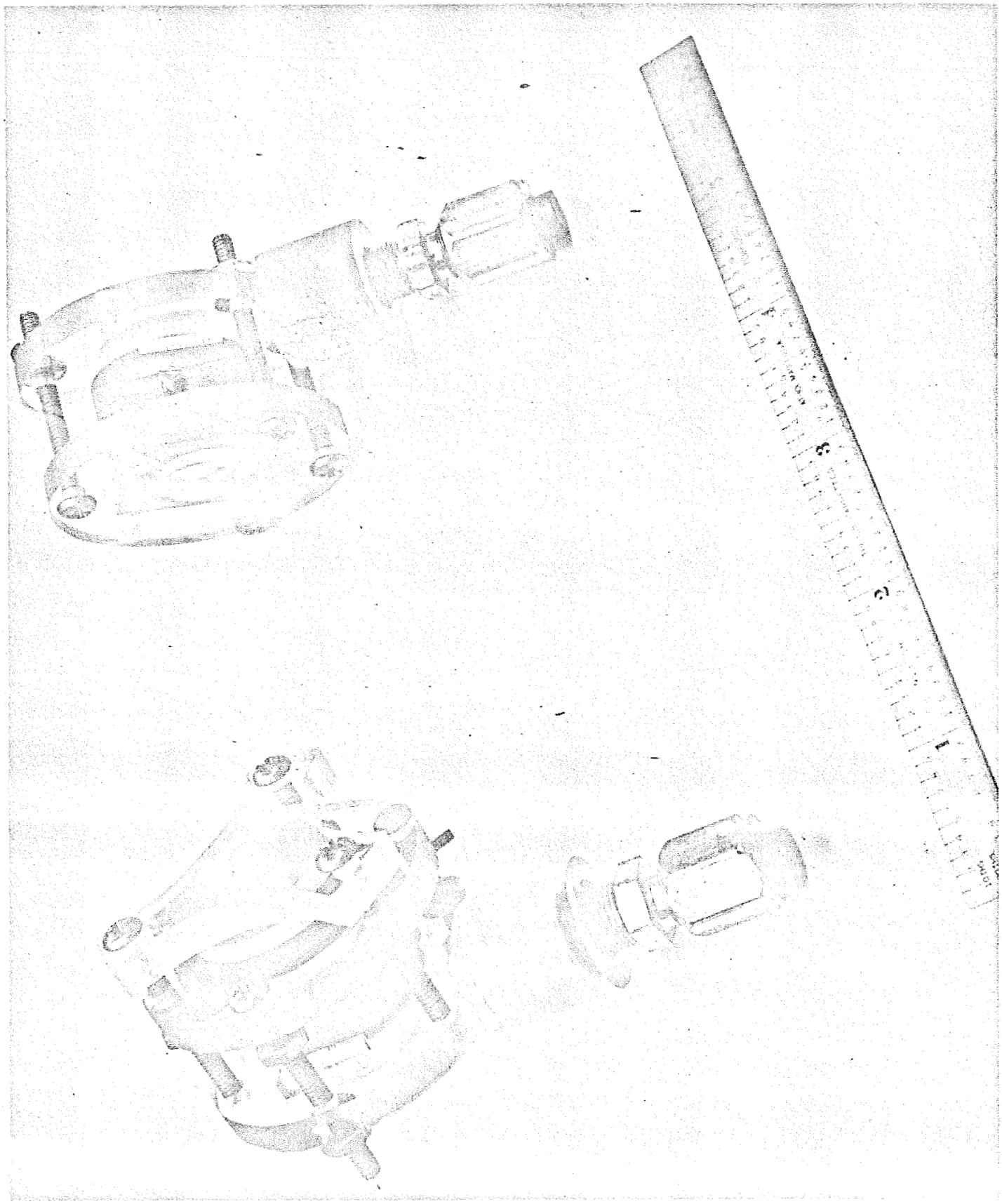

FIGURE 9.: INITIAL SENSOR DESIGN-TYPE "A"

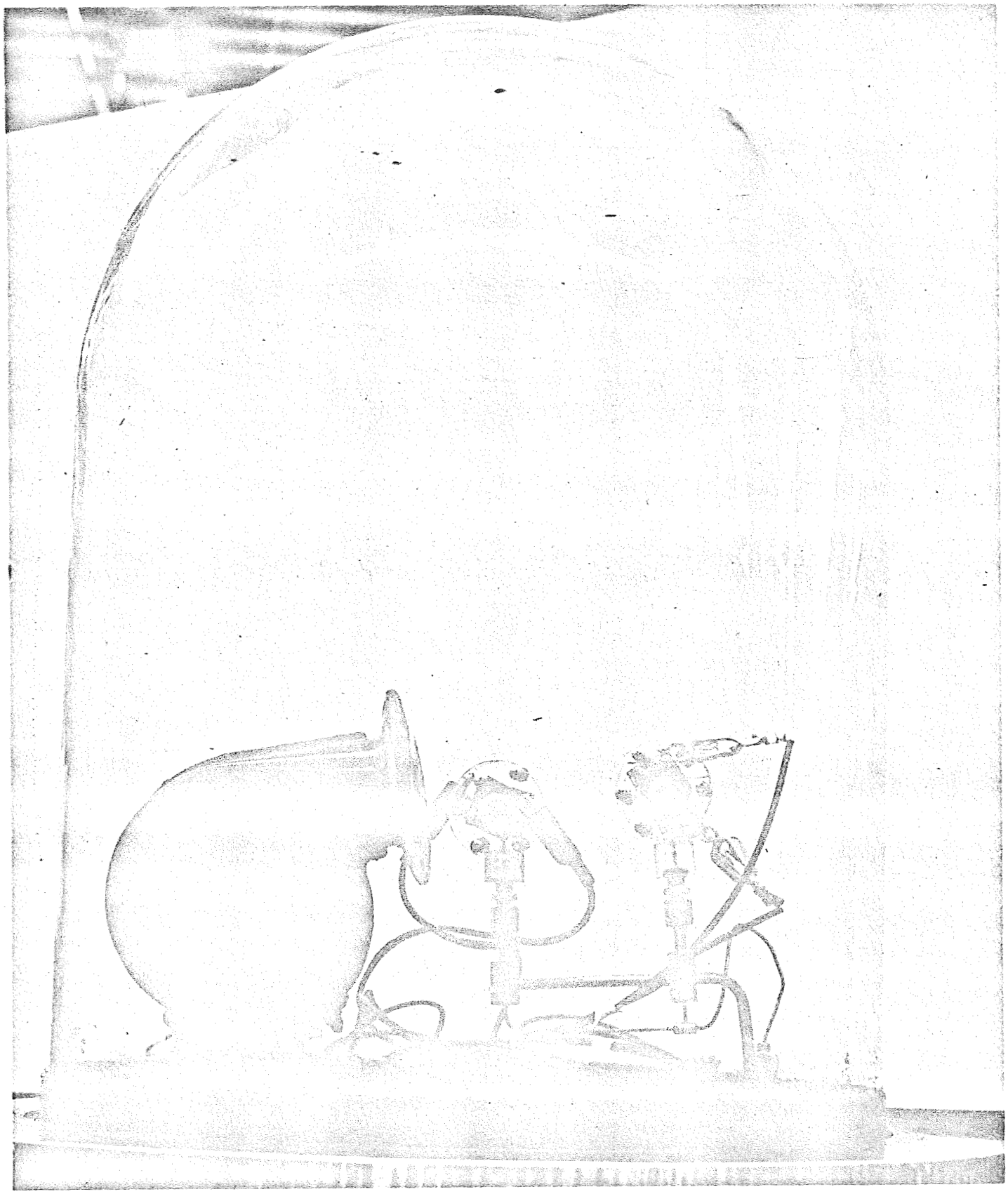

FIGURE 10.: TYPICAL PERFORMANCE TEST-TYPE "A" (CONTAINING RESERVOIR)

water, causing a greater degree of polarization at high current. Curve (1) of Figure 11 shows the general shape of the E-I curve under concentration polarization caused by the diffusion barrier.

With this improved performance, the next step was to produce a cell with a stable output. In order to accomplish this, a number of different cell configurations were tried. Two models similar to the above were made and tested but also gave poor results. A barrier was placed on these cells but the sensor gave variable long term results.

Modifications included a design with a double sided membrane and a reservoir around its edges, Figure 6, Type D; a single sided membrane with two separate platinum black patches on the same side and a reservoir behind, Figure 6, Type E; and two single sided membranes with a reservoir which was open to the outside so that acid could be added or subtracted, Figure 6, Type C. The first of these failed because air diffused through the water in the reservoir and reacted at the electrode surface to increase the cell output. Variation in water level varied the output. The second configuration failed because the path from one electrode to the other, lengthwise through the membrane, was not very conductive to protons. This may have been because the resistance along a path parallel to the surface of the membrane is higher than that perpendicular to it or because the sealing pressure applied between the electrode areas was

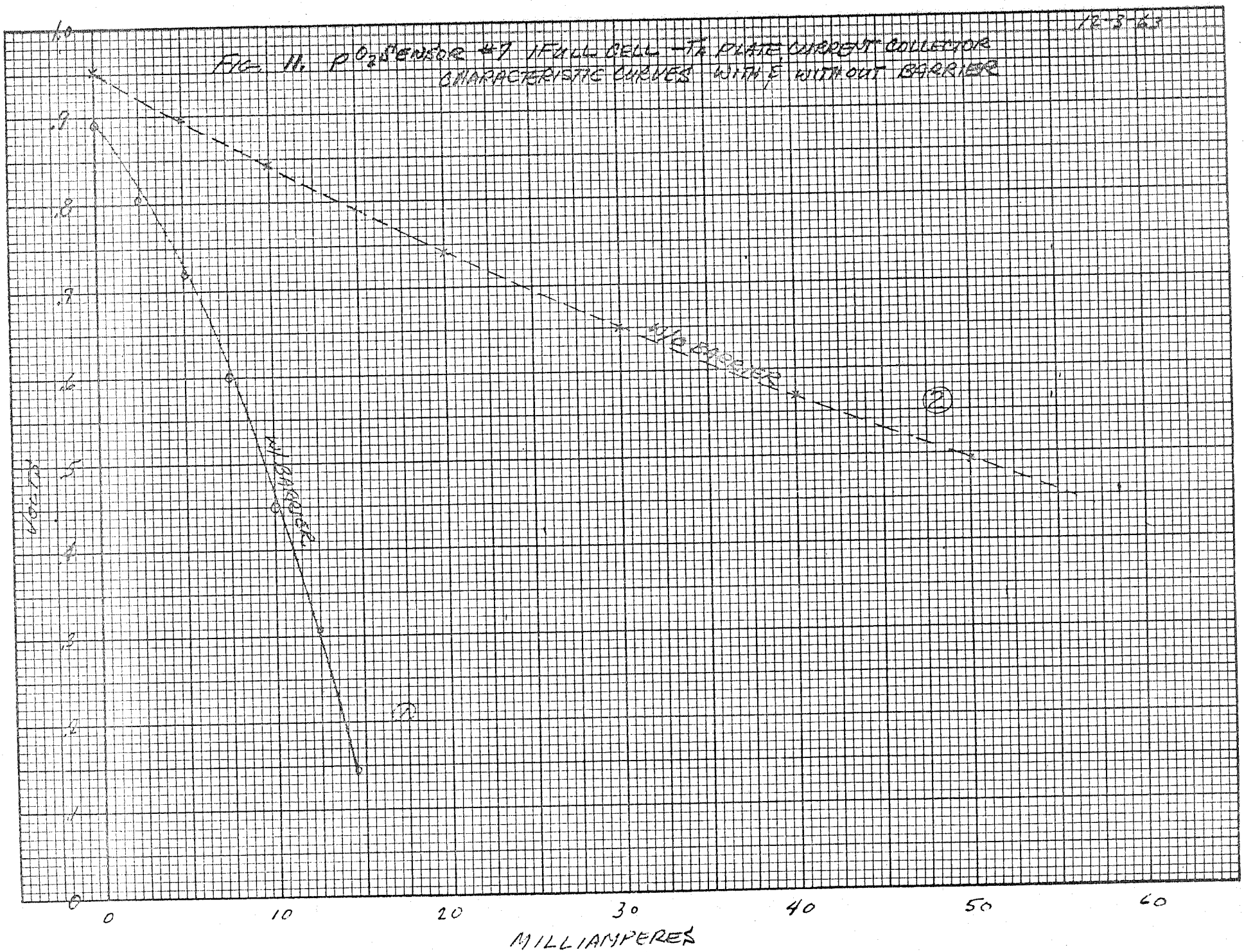
FIG. 11. P_{O_2} SENSOR #7 (FULL CELL — Ti PLATE CURRENT COLLECTOR) CHARACTERISTIC CURVES WITH & WITHOUT BARRIER
WITH BARRIER
WITHOUT BARRIER
VOLTS
MILLIAMPERES
0
10
20
30
40
50
60
.1
.2
.3
.4
.5
.6
.7
.8
.9
1.0

so great that it forced the water out of the membrane causing drying and therefore an increase in its resistance. When acid was used in the reservoir instead of distilled water the output was very high and stable as long as the acid level remained the same.

The third configuration allowed experimentation upon the acid in the reservoirs since it was now accessable. This cell displayed the same non-static outputs as did the earlier cells. A photograph of this cell appears in Figure 12.

Upon investigation it was found that the cell output varied with the concentration of H_2SO_4 solution. This was to be expected since the conductivity of the solution varies with concentration, being highest near 35% concentration and decreasing above and below this. The interesting fact discovered with this cell was that the acid freely migrated through the membrane and its volatile components evaporated. Water formed in the reaction was also probably entering the reservoir. Both of these phenomena varied the conductivity of the cell. Also the loss of electrolyte caused the contact area between electrolyte and membrane to be reduced so that uniform wetting was not maintained. All in all enough evidence was provided to discourage further use of cells with conducting electrolyte reservoirs.

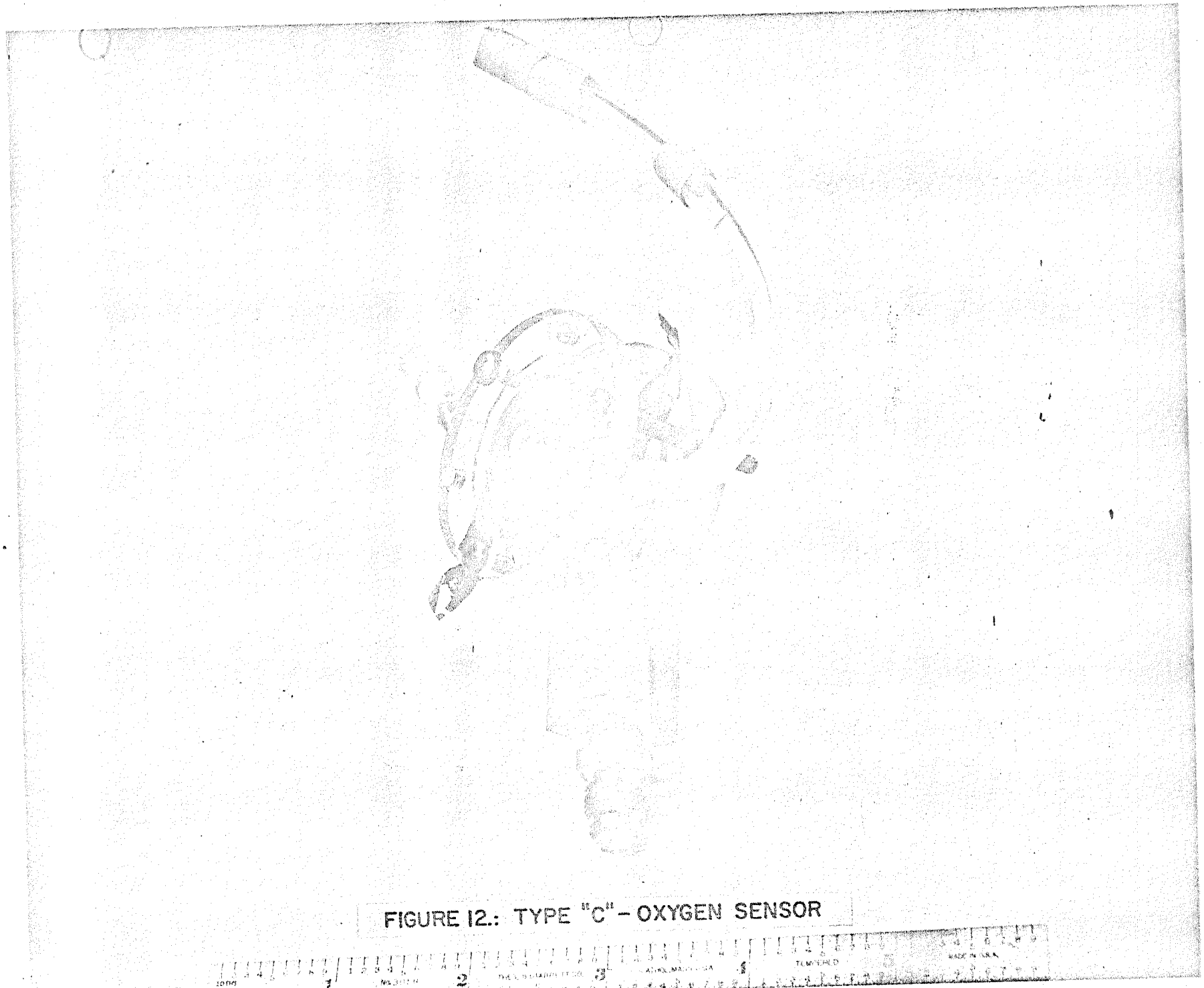

FIGURE 12.: TYPE "C" – OXYGEN SENSOR

The only alternative left was to eliminate the reservoirs completely by trying a full cell, (double sided membrane) instead of two half cells. In order to make the cells easier to assemble, thick, rigid, tantalum plate was shaped into current collectors and used as an integral part of the sensor body. This began Phase C, which utilized Type B and F, Figure 6.

Phase C: For the first time in the program a reproducible, high output was maintained by the test sensor. The original cell, once it was started, had a barrier placed on it and continued in operation for more than three months.

This success was followed by the assembly of a similar cell first using foil and then tantalum plate. That cell also operated for 2-3 months. The effect of the barrier is clearly shown by Figure 11. where the output of a very efficient cell was drastically reduced. Figure 13 shows the comparison of the output of another cell before and after the barrier was added. This later cell was more polarized before the barrier was added than the previous one. The apparent rise of output after the addition of the barrier came from the increase of moisture in the membrane caused by the water trapped between the barrier and the membrane. The shape of the curve, specifically the voltage drop at high current, indicates definitely that the cell is current limited.

11-7-63

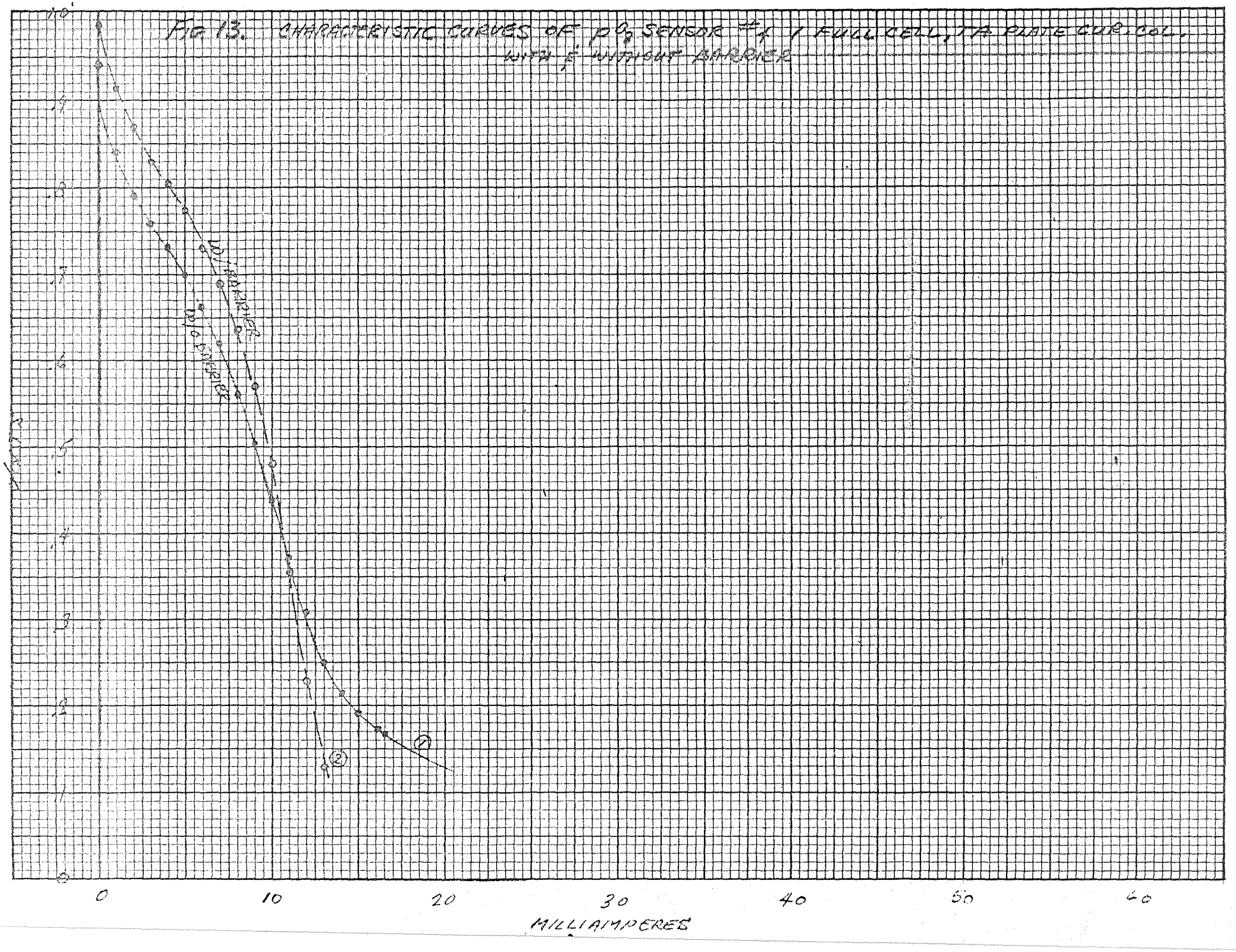
FIG 13. CHARACTERISTIC CURVES OF O_2 SENSOR #1 / FUEL CELL, 1% PLATINUM CAT. COL., WITH & WITHOUT BARRIER
WITH BARRIER
WITHOUT BARRIER
0
10
20
30
40
50
60
MILLIAMPERES

The response of a cell to pO_2 is shown in Figure 14. The flattened slope indicated the effect of the barrier. A comparison of response to pO_2 before and after current limiting is shown by Figure 15 curve B. The unpolarized cell has a fast rising logarithmic response the shape of which can be varied by the diffusion barrier used. In practice, when a rubber barrier is placed in front of the electrode, the water produced is trapped. After equilibrium is established between the liquid behind the barrier and the steam diffusing through it, the membrane assumes a steady state moisture level which usually enables it to produce an output slightly higher than the unshielded cell.

Now that an operating fuel cell with repeatable output was on hand, a number of tests were run to determine how this sensor responded to various stimuli. A family of E versus pO_2 curves were run at different load resistances, Figure 16. The high resistance, low current, lightly loaded curves continued to resemble the non-polarized curves in as much as they were basically expanded logarithmic curves. At low resistances and higher current densities the effects of concentration polarization were evident in the distortion of the logarithmic type response curve. These were reverse curvatures superimposed upon the logarithmic curve. The response to pO_2 should follow the equation:

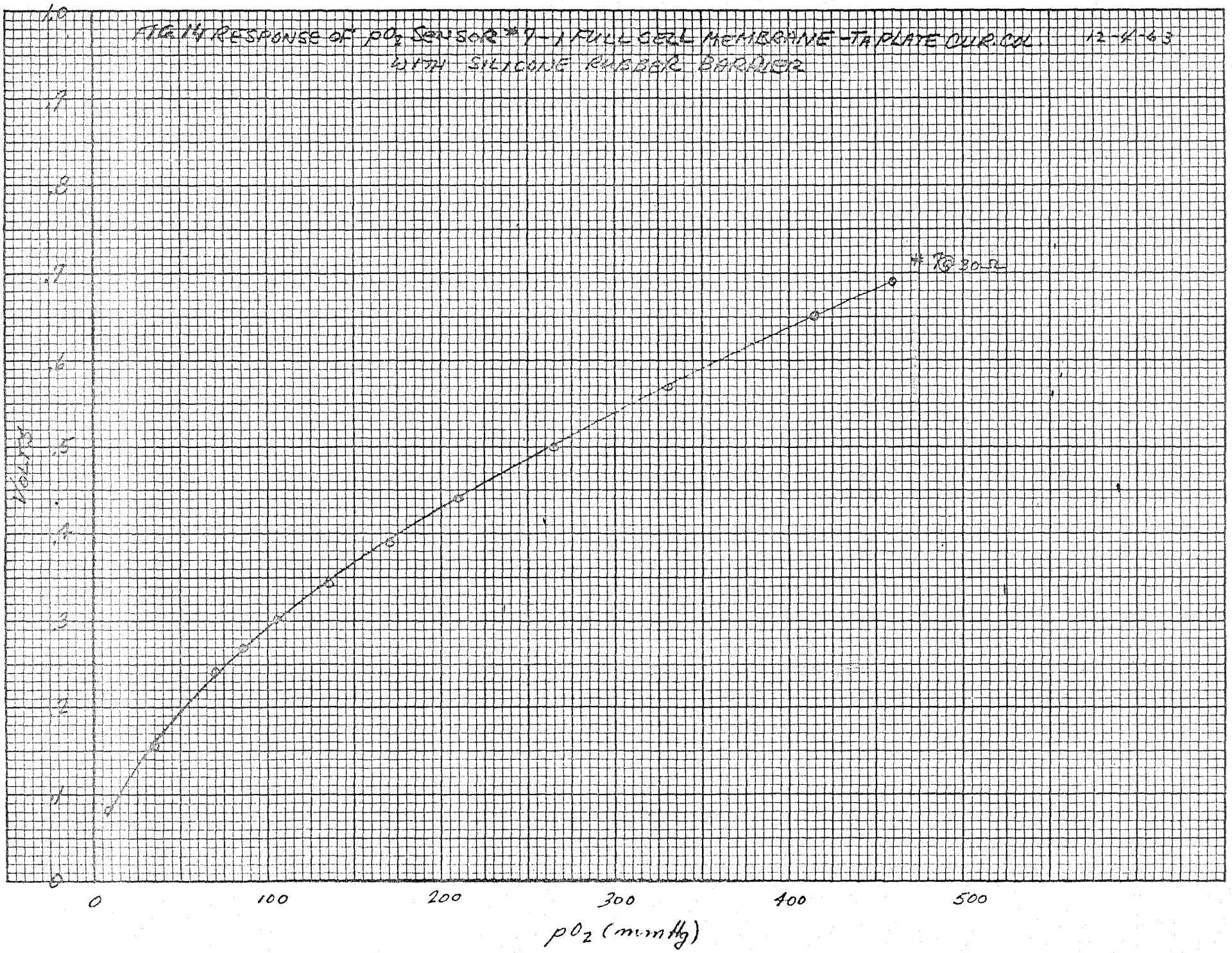
FIG 14 RESPONSE OF pO_2 SENSOR #9-1 FULL CELL MEMBRANE-TA PLATE CUP COL. 12-4-63
WITH SILICONE RUBBER BARRIER
#9-1 90-Ω
1.0
.9
.8
.7
.6
.5
.4
.3
.2
.1
0
Volts
0
100
200
300
400
500
pO_2 (mmHg)

12-12-63

GENERAL SHAPE OF O_2 SENSOR RESPONSE CURVES

FIG. 15.

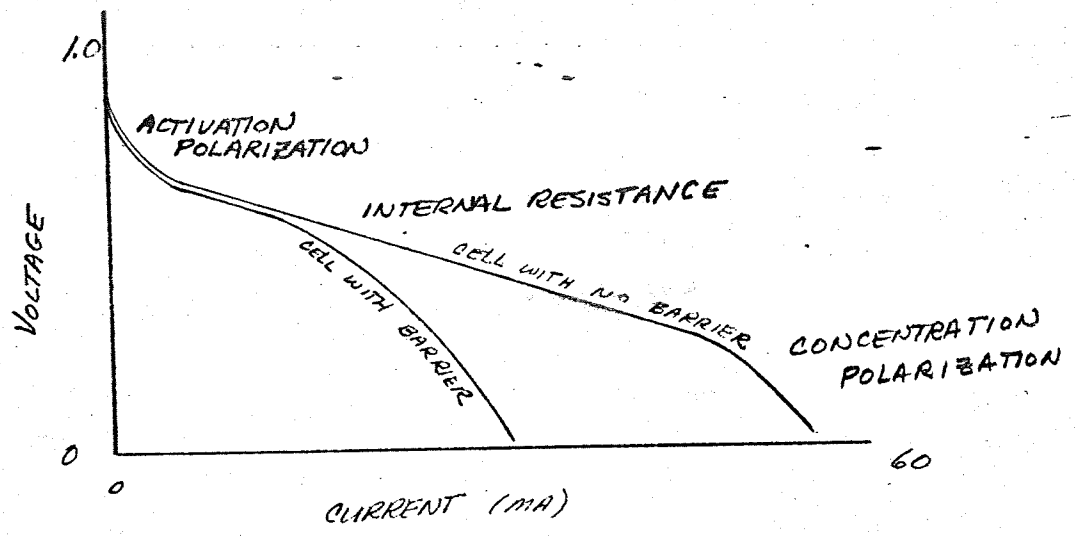

A.

V vs I FOR pO_2 SENSOR FUEL CELL

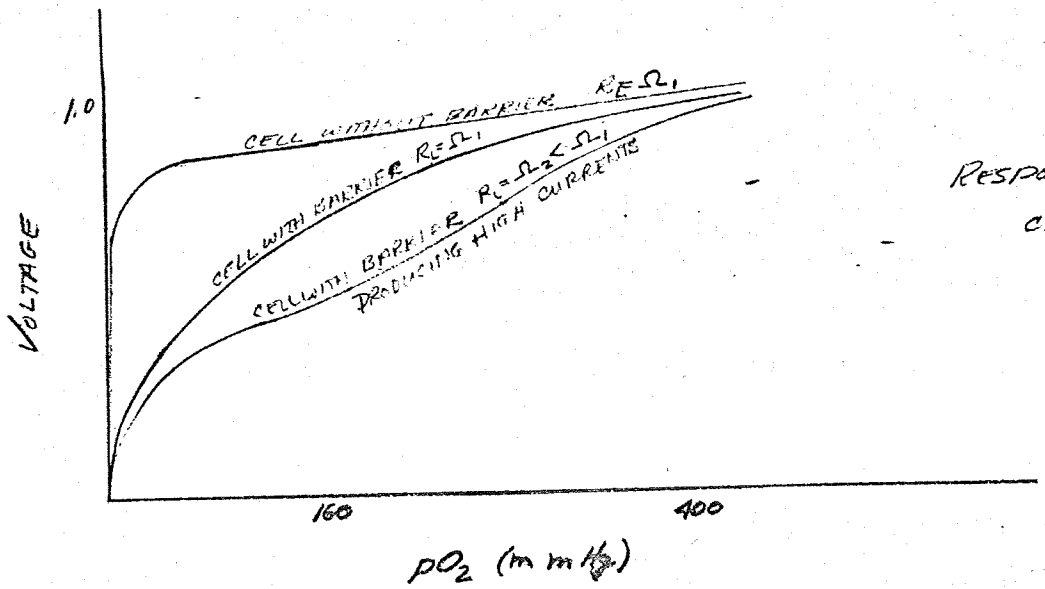

B

RESPONSE TO CHANGE IN pO_2

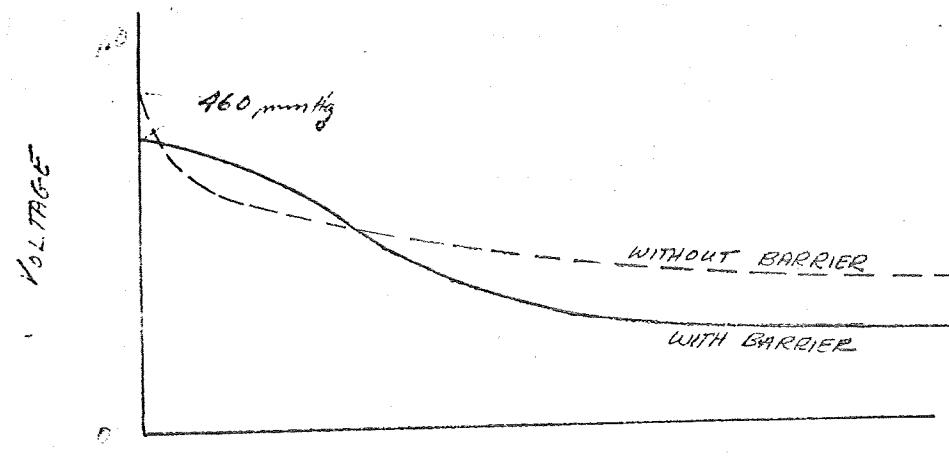

C

TIME RESPONSE TO STEP DROP IN pO_2

FIG 16. - RESPONSE OF pO_2 SENSOR #4 (IFULL CELL MEMB. - TA PLATE CUR. COL. - RUBBER BARRIER) TO VARIATION OF ppO_2

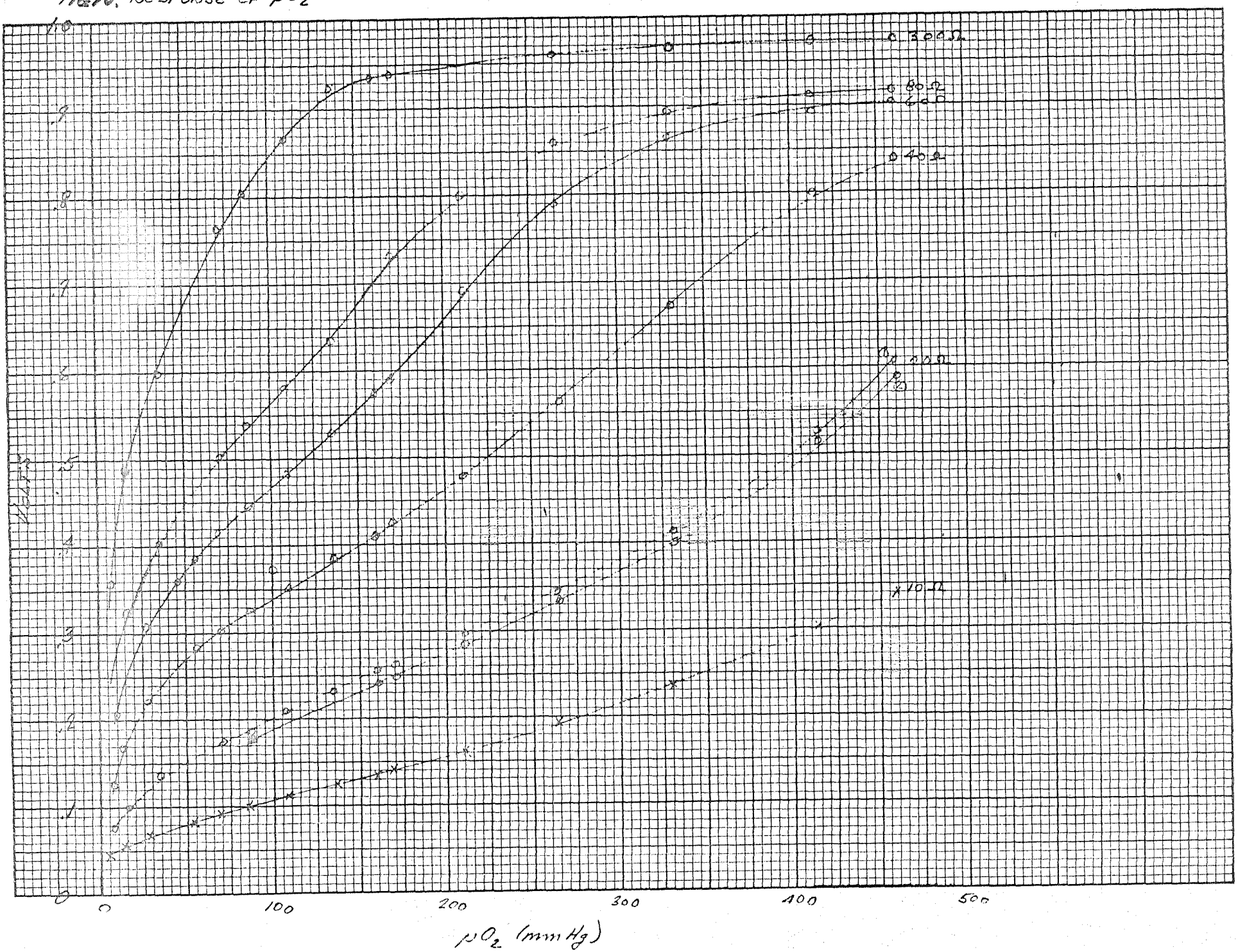

$$E_T = E_o + \frac{RT}{nF} \ln (pO_2)^r (pH_2)^r - \frac{RT}{nF} \ln \left(1 - \frac{E_T}{pO_2 R_i nF} \frac{\delta}{D}\right) - \dot{z}R - K_{AUT.}$$

where $\left(\frac{\delta}{D_{eff}}\right)$ is the composite diffusion coefficient for water and silicone rubber given by

$$\frac{\delta}{D_{eff}} = \frac{D_1 \delta_2 + D_2 \delta_1}{D_1 D_2}$$

The next area of interest was the time response. It was obvious from normal test runs to that date that the sensor responded immediately to pO_2 changes, but had a slow rate of change. The cell with no barrier responded rather rapidly when moderate or high currents were drawn. The time contant was on the order of 5 secs. as illustrated by Figure 17. With the barrier added, the response was slowed considerably. The time constant varies, depending upon whether pressure is being increased or decreased, (Figure 18 and 19). When the external pO_2 is increased the cell seems to respond faster than when it is decreased. No satisfactory explanation for this phenomena has been uncovered yet but it appears to be linked with the fact that the rate of change of flow into the electrode decreases as a function of pressure decrease and increases as pressure increases. Then the velocity with which the cell reaches a new steady state equilibrium decreases in the former case and increases in the latter. The time contraints would, therefore, vary.

12-11-63

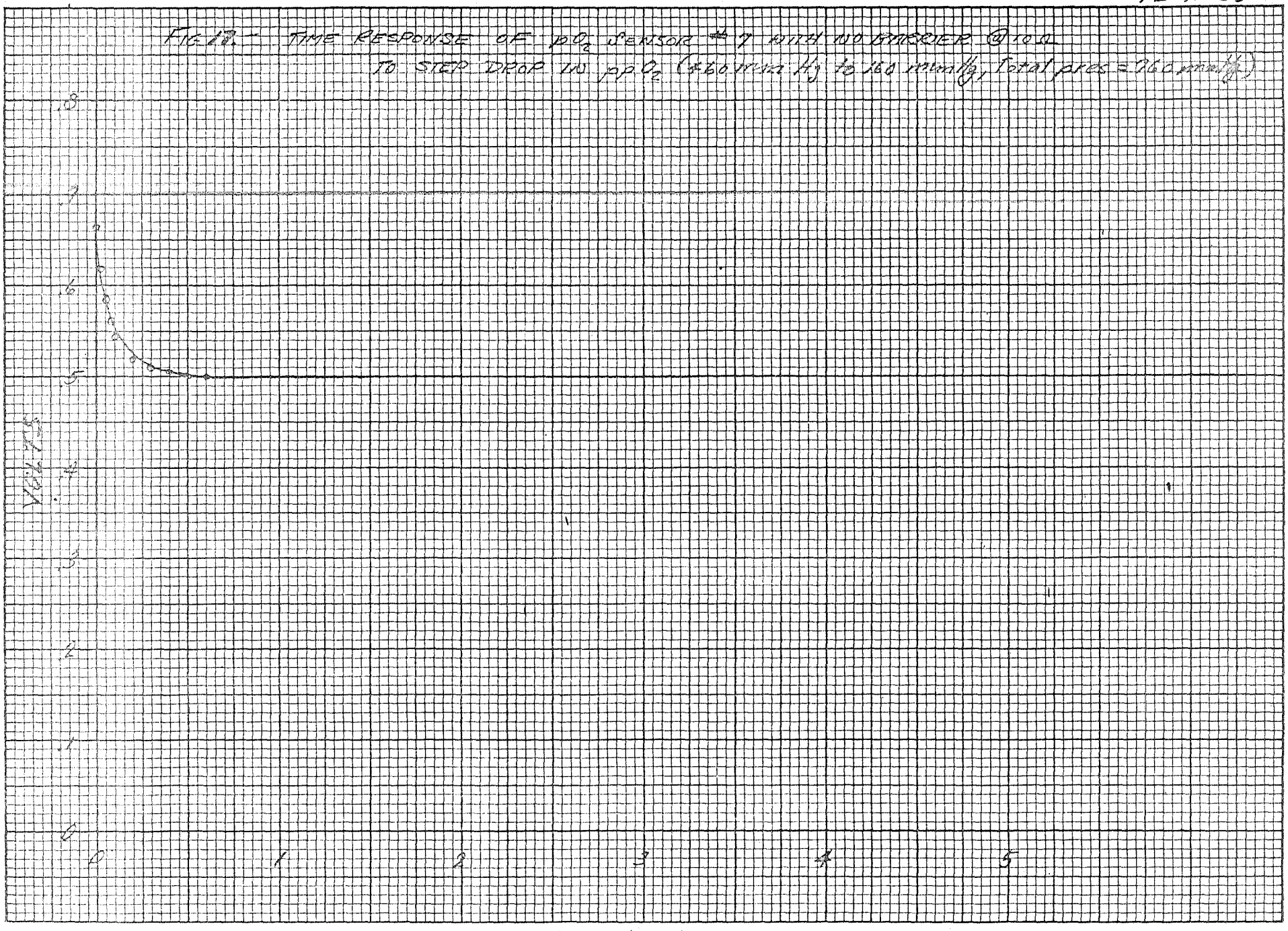
FIG 18. - TIME RESPONSE OF pO_2 SENSOR #7 WITH NO ANSWER @ 10 A
TO STEP DROP IN pO_2 (460 mm Hg to 160 mm Hg, Total pres = 760 mm Hg)
.8
.6
.5
.4
.3
.2
.1
0
0
1
2
3
4
5
Time (min.)

12-11-63

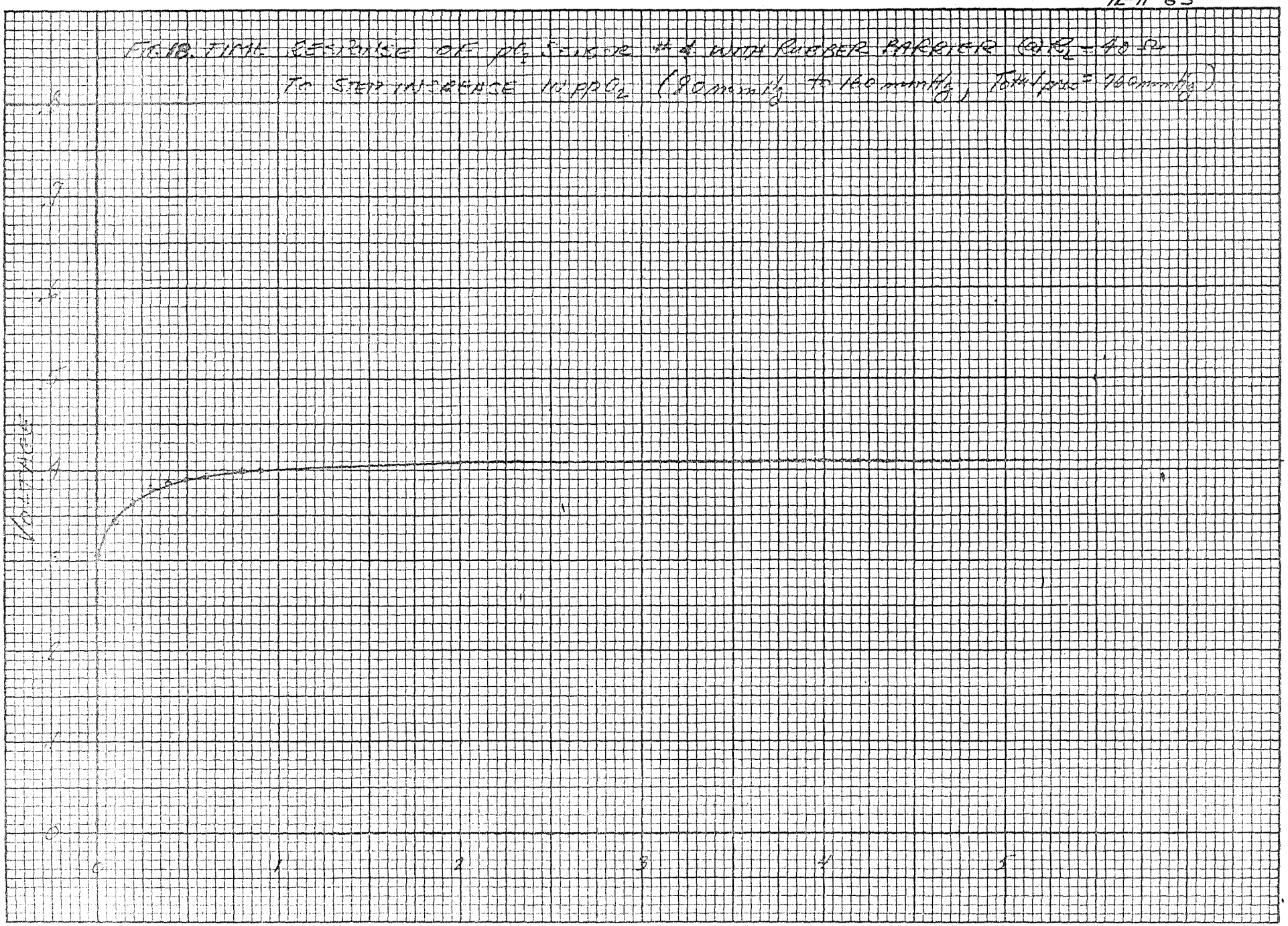
FIG 18. FINAL EQUILIBRIUM OF pO_2 SENSOR IN A MINI RUBBER BARRIER @ R_L = 40 Ω
TO STEP INCREASE IN pO_2 (80 mm Hg TO 160 mm Hg, TOTAL p = 760 mm Hg)
TIME (MIN)
0
1
2
3
4
5

12-11-63

FIG. 5 = TIME RESPONSE OF pO_2 SENSOR #4 WITH RUBBER BARRIER (K_L=40)

TO STEP DROP IN ppO_2 (460 mm Hg to 160 mm Hg)

(Total pressure = 760 mm Hg)

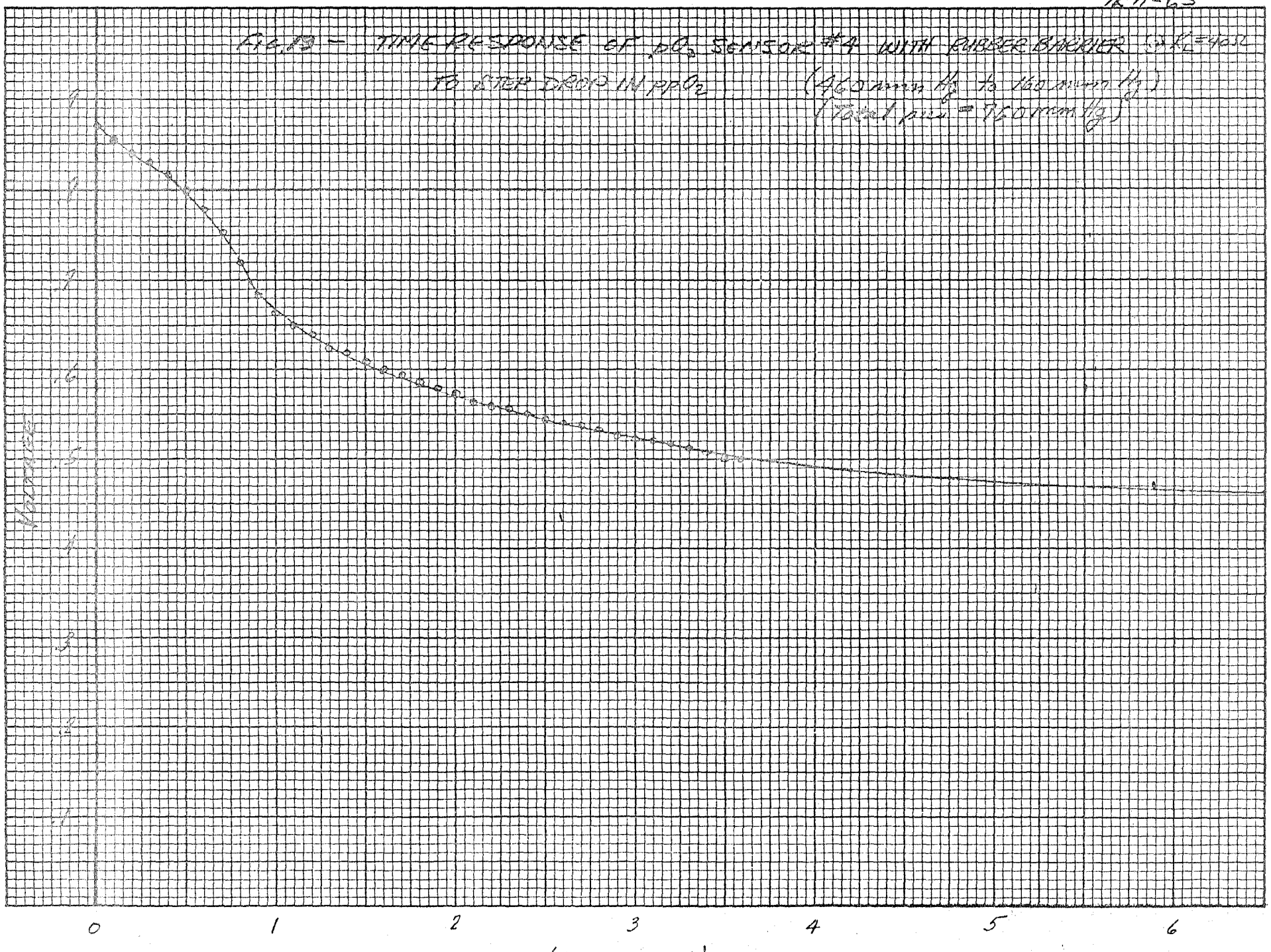

Phase D: Six new smaller, compact sensors were used for tests investigating and defining basic operating parameters of the sensor. An exploded view of the type "G" sensor appears in Figures 20 and 21.

1. Barrier Selection: Initial tests were directed at the selection of a suitable barrier. It was soon apparent that current outputs far exceeded theoretical values based on the permeability of the barrier being tested. It was suspected that oxygen was by-passing the barrier.

The type "G" sensors had current collectors protruding through slots in the sensor housing. It was thought that lapped surfaces on the current collectors and pressure due to torquing the retaining nut would effectively seal the ion-exchange membrane from atmospheric oxygen. However, it was proved that leakage was indeed taking place through the joint. Possibly minute scratches on the collector or platinum black allowed atmospheric oxygen to by-pass the barrier. Any molecules of oxygen that by-pass the barrier will tend to increase the output and saturate the load curve. Oxygen that penetrates the hydrogen side of the ion-exchange membrane will be adsorbed and polarize the cell. To eliminate this leakage a new housing and current collector was designed, and

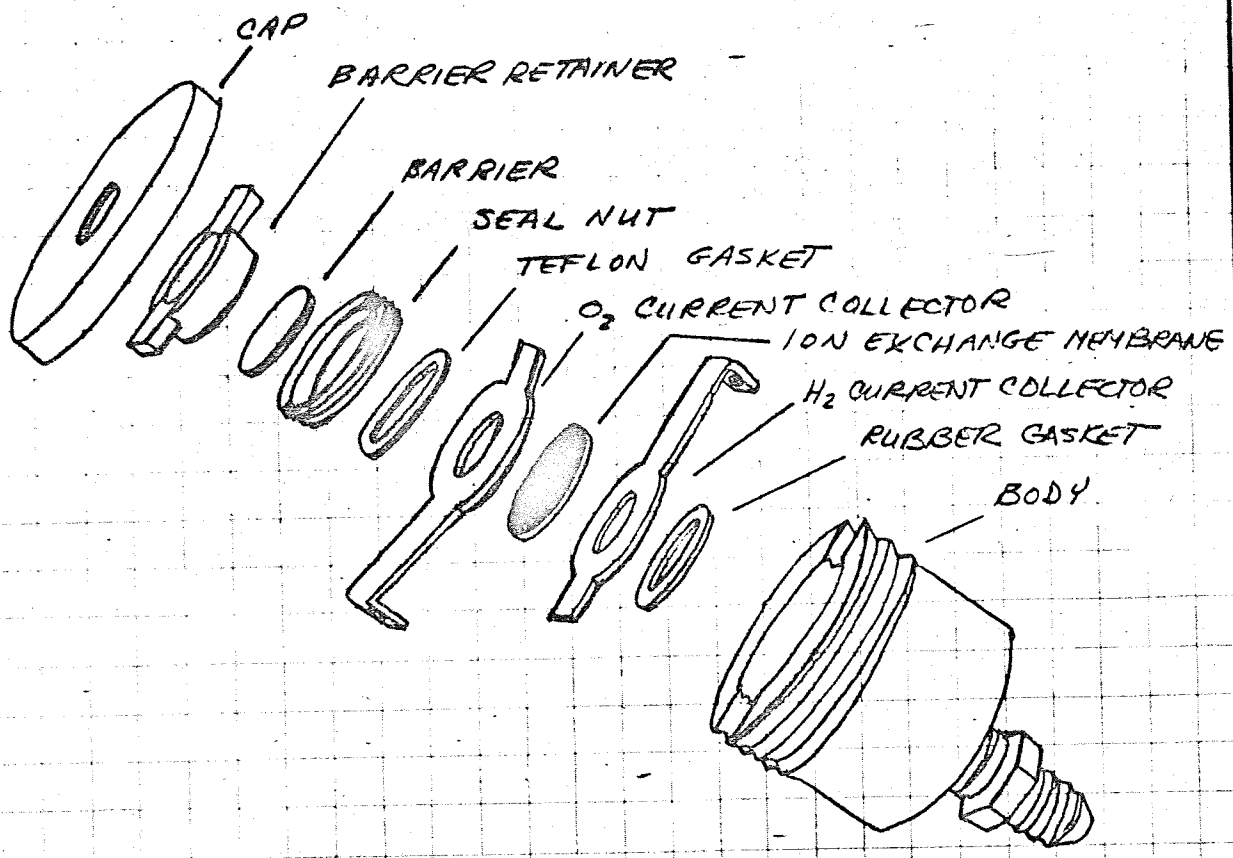

FIG. 20 - pO_2 SENSOR TYPE "G"

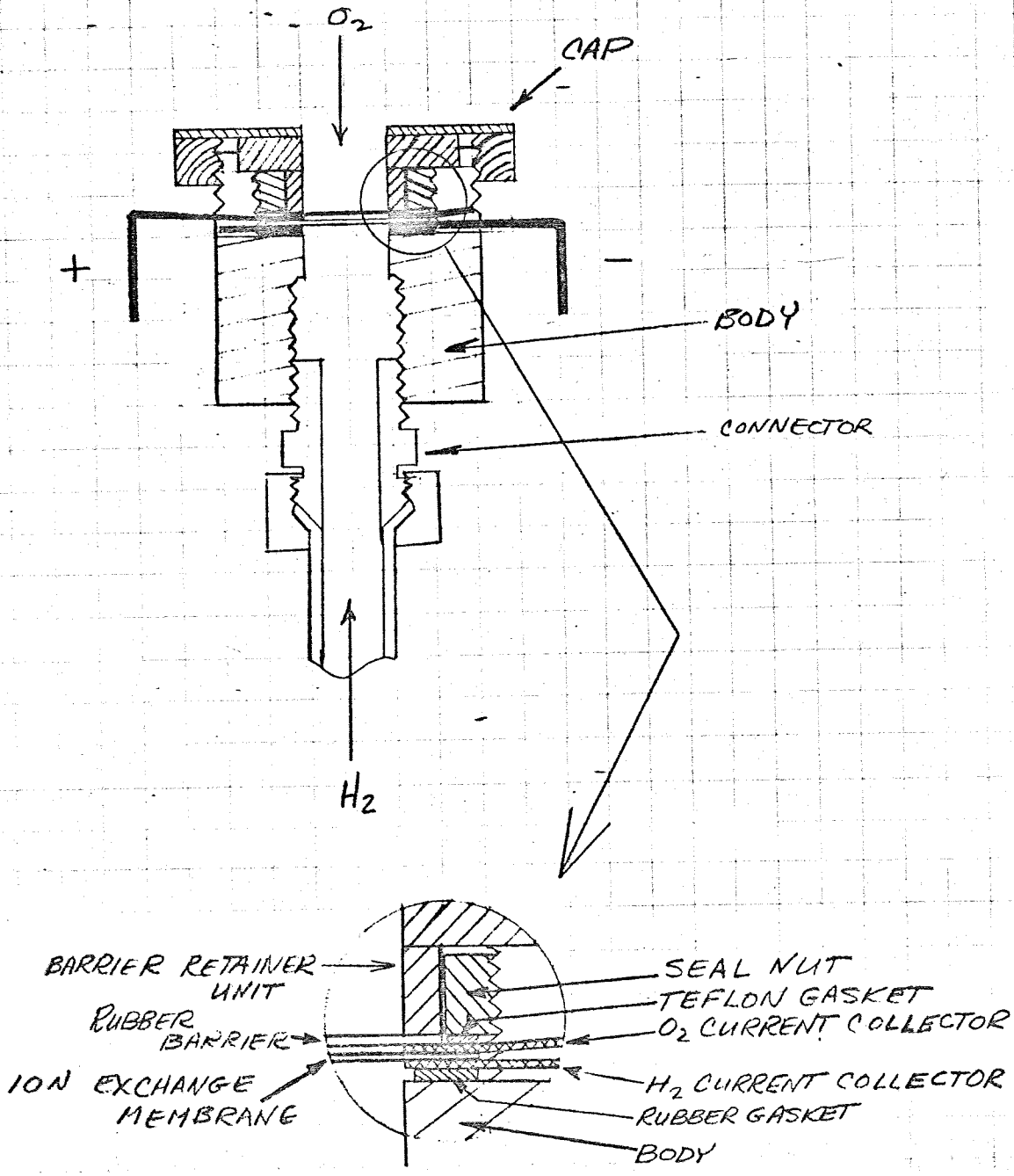

FIG. 21 - pO_2 SENSOR TYPE "G"

designated type "H". This sensor utilized .020" diameter wire for collector leads which penetrated the housing through small holes. A schematic view of this cell appears in Figure 22. Now current outputs of the sensor agreed with the theoretical outputs based on oxygen permeability coefficients for the material used as a barrier. A trade-off was now necessary between response time, CO_2 range, linearity, H_2 supply, and current. In order to maintain the moisture in the ion-exchange membrane a current of 2 ma was selected as a minimum current. Table III shows permeability coefficients for representative films surveyed. On the basis of its high permeability to oxygen silicone rubber was selected. Oxygen flow can be calculated by:

$$Q = \frac{P A \Delta p}{d}$$

Q = Total number of cc permeating per second through the film.

p = Number of cc (STP) passing per second through one cm^2 of a film one cm. thick under a partial pressure differential of one cm of mercury.

A = Area of film (cm^2)

ΔP = Partial pressure differential (cm of mercury)

d = Film thickness (cm)

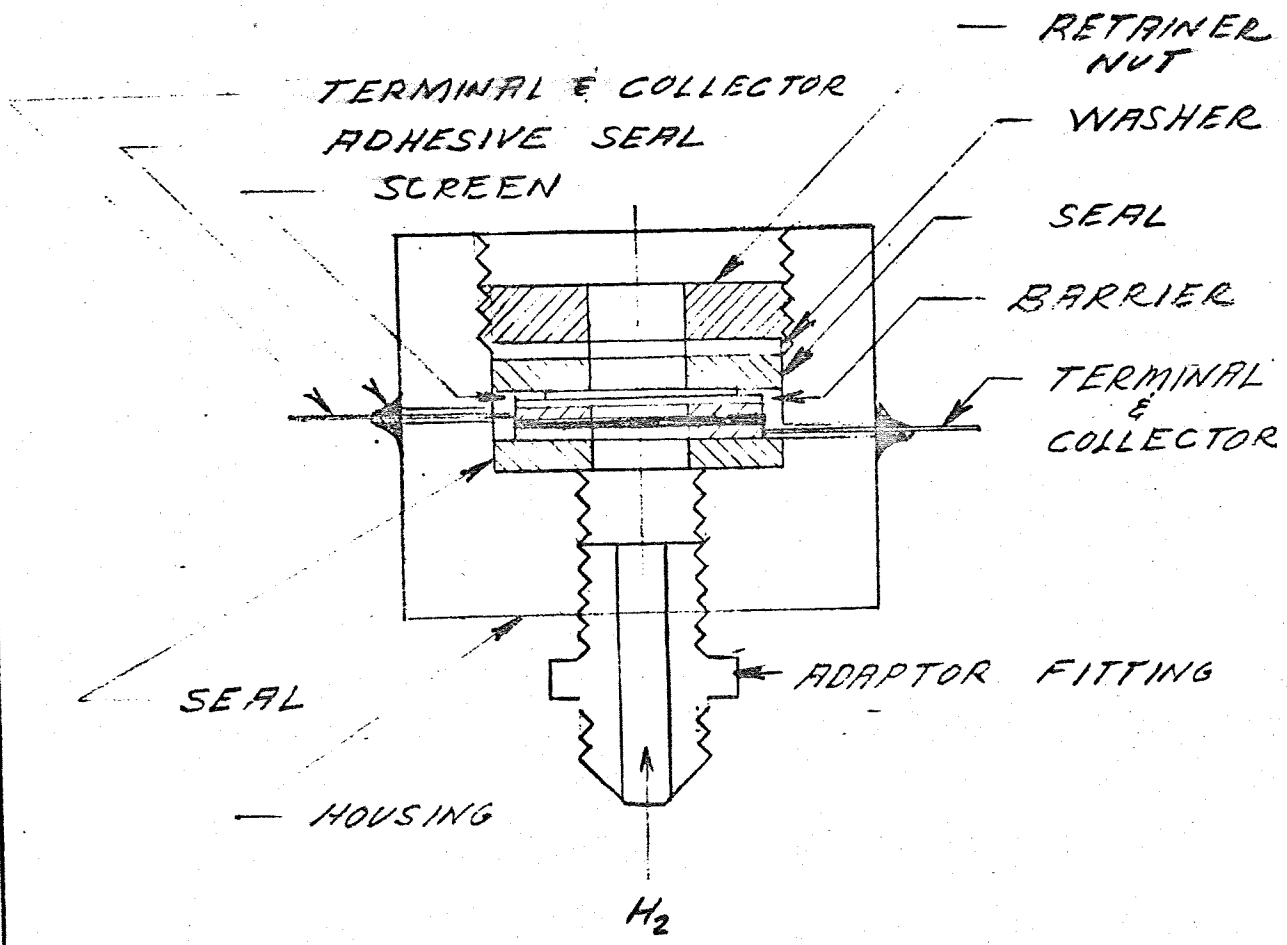

TYPE II

FIGURE 22

DEVELOPEMENT UNIT pO_2 SENSOR

$$Q = \frac{525 \times 10^{-10} \ (.316) \ (16)}{.00254} = 10.45 \times 10^{-5} \text{ cc/sec}$$

$$Q = 62.9 \times 10^{-4} \text{ cc/min}$$

$$1 \text{ ma} = .0035 \text{ cc/min of } O_2$$

$$\text{current} = \frac{62.9 \times 10^{-4} \text{ cc/min}}{35 \times 10^{-4} \text{ cc/min}} = 1.8 \text{ ma}$$

A practical consideration was that silicone sheet material cannot be procured under 1 mil. An exposed area larger than the .25 inch diameter presently used would have to be utilized if higher current values were desired.

TABLE III

PERMEABILITY COEFFICIENTS (p) OF VARIOUS FILMS TO OXYGEN

FILM	O_2 "P"
"Tedlar" Polyvinyl Flouride	$.02 \times 10^{-10}$
"Mylar" Polyester	$.02 \times 10^{-10}$
Cellulose Acetate	$.7 \times 10^{-10}$
Polyethylene	3.2×10^{-10}
Natural Rubber	23×10^{-10}
Silicone Polydimethyl-Silozane	525×10^{-10}
Polypropylene (Beckman)	$.02{:}06 \times 10^{-10}$
PPO (GE)	15×10^{-10}
Cast Teflon	18×10^{-10}
Ethyl Cellulose	$26{:}5 \times 10^{-10}$
Polystyrene	24.0×10^{-10}
Polybutadiene	19×10^{-10}

$$P = \frac{(\text{St'd. cc})\ (\text{cm thick})}{(\text{Sec})\ (\text{cm}^2)\ (\text{cm Hg. AP})}$$

$$Q = \frac{PA\Delta P}{d} = \text{cc/sec}$$

2. Hydrogen Leakage - Initially leakage tests were performed on all new sensor assemblies by subjecting the hydrogen side of the sensor to nitrogen at 20 psig, and submerging the sensor in distilled water. Since the hydrogen pressure is maintained at approximately eight inches of water for normal operation, this excessive pressure was deemed adequate. However, submerging the cell in water altered the permeability coefficient of the barrier and it required many hours before a reasonable value was achieved. In addition, this method did not show up leaks that possibly developed during the test. For these reasons an improved leakage test was initiated. Initially a bubbler was used on the hydrogen inlet which gave an indication of hydrogen consumption. Later a capillary "U" tube arrangement was used for precision measurements of hydrogen flow rates. A schematic of this test set-up appears in Figure 23. Test results showed that hydrogen consumption correlated with theoretical rates within 6%.

3. Electrical Leakage - The capillary "U" tube test apparatus shown in Figure 23 was also utilized to evaluate electrical leakage. At open circuit voltage (OCV) no current should flow; thus no hydrogen should be consumed. Tests showed OCV hydrogen consumption of .0014 cc/min. or leakage currents of 0.2 ma. This current leakage is attributed to low resistance through the area cleared of platinum

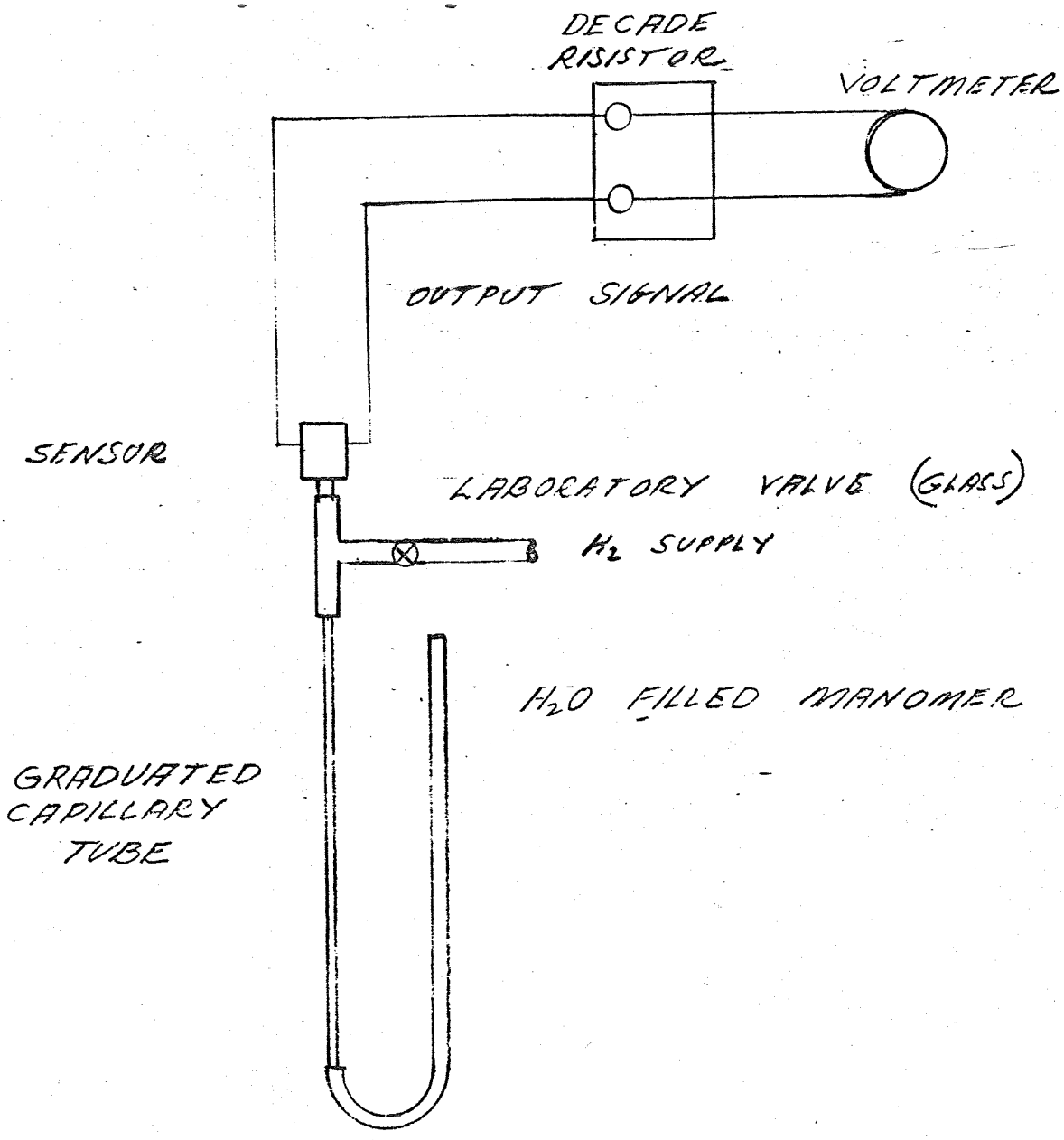

FIGURE 23.

HYDROGEN GAS CONSUMPTION SET-UP

on the periphery of the membrane. This area is scraped by hand to prevent a direct short between anode and cathode. Visual examination confirms that some of the platinum black is embedded in the interstices of the polystyrene membrane accounting for the current leakage. It is suspected that additional migration takes place with time and that this current leakage is progressively increased, accounting for the slow downward drift of the output signal.

4. Material Compatibility: During the course of development testing on the type "H" sensors it was evident that a major problem existed in a persistant downward drift of the sensor output. The downward drift was evident when pO_2 vs output curves were performed on successive days. Investigation of open circuit voltage (OCV) showed deterioration. After initially assembling a sensor an OCV of over 0.9 volt could be achieved with the barrier in place, however the value dropped off to 0.6 volt in less than 48 hours. It was evident that the decreased OCV brought about the lowered output curve. A check of the materials utilized indicated that the constantan wire used for a collector lead out and the butyl rubber seal washers were suspected as poisoning the ion-exchange membrane.

Constantan contains 60% copper and 40% nickel. Nickel is not a material recommended for use with the membrane. The isobutylene and isoprene, constituents of butyl rubber have unknown affects on

the IEM. The constantan was replaced by tantalum leads and Viton A was substituted for the butyl with good results. Two type "H" sensors assembled with the tantalum leads and Viton seals ran for over 30 days with untrimmed repeatability within ±6% (output voltage). These performance curves are shown in Figures 24 and 25 with a photograph of the test set-up included as Figure 26.

5. Platinum Migration: To prevent the ion-exchange membrane (IEM) from shorting out, assembly procedures called for removing platinum black along a 1/16 inch border around the periphery of both sides of the IEM. This eliminates the chance that a conduction path might allow current to short between the cathode and the anode. Examination of ion-exchange membranes after test showed that platinum black had migrated onto this cleaned area. Investigation showed that the electrical leakage of the unit had indeed increased. A disecting microscope was utilized to assure that all platinum black has been removed from the border. Subsequent testing showed that this migration is still a problem. In removing the platinum black some of the material is lodged in the pores and interstices of the polystyrene and cannot be removed. A "bulls eye" type of ion-exchange membrane is necessary to eliminate all current leakage. This would have to be manufactured in a special pilot run by the GE-Direct Energy Conversion Operation. Cost and schedule precluded obtaining these

INTERFORMATION CURVE
CO2 SENSOR
WATER
X-1
PRESSURE PSI
500
400
300
200
100
0

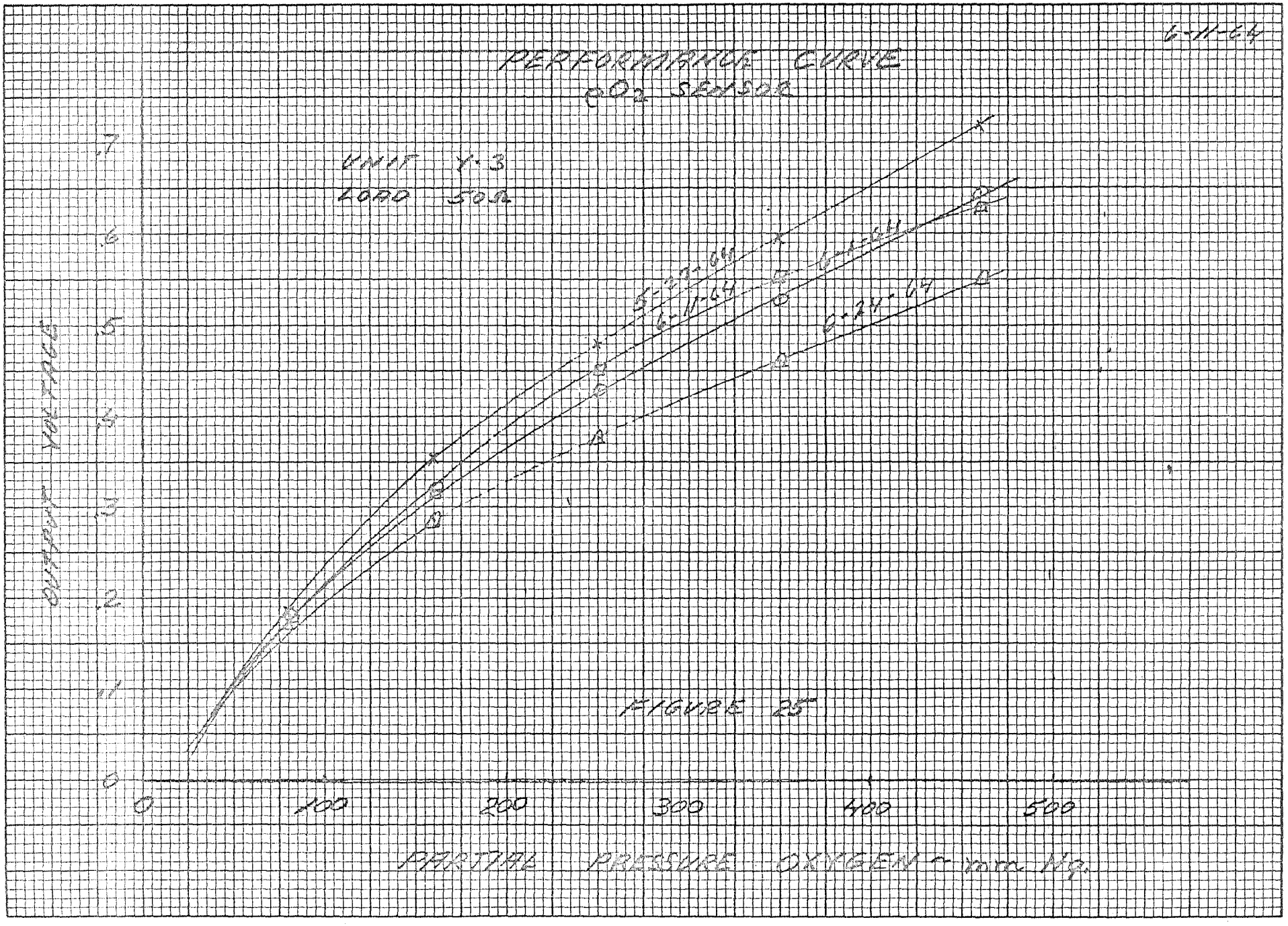
6-11-64
PERFORMANCE CURVE
O_2 SENSOR
EMF X.3
2080 505
5-23-64
6-11-64
6-24-64
OUTPUT - MV
.7
.6
.5
.4
.3
.2
.1
0
0
100
200
300
400
500
PARTIAL PRESSURE OXYGEN - mm. Hg.

FIGURE 25

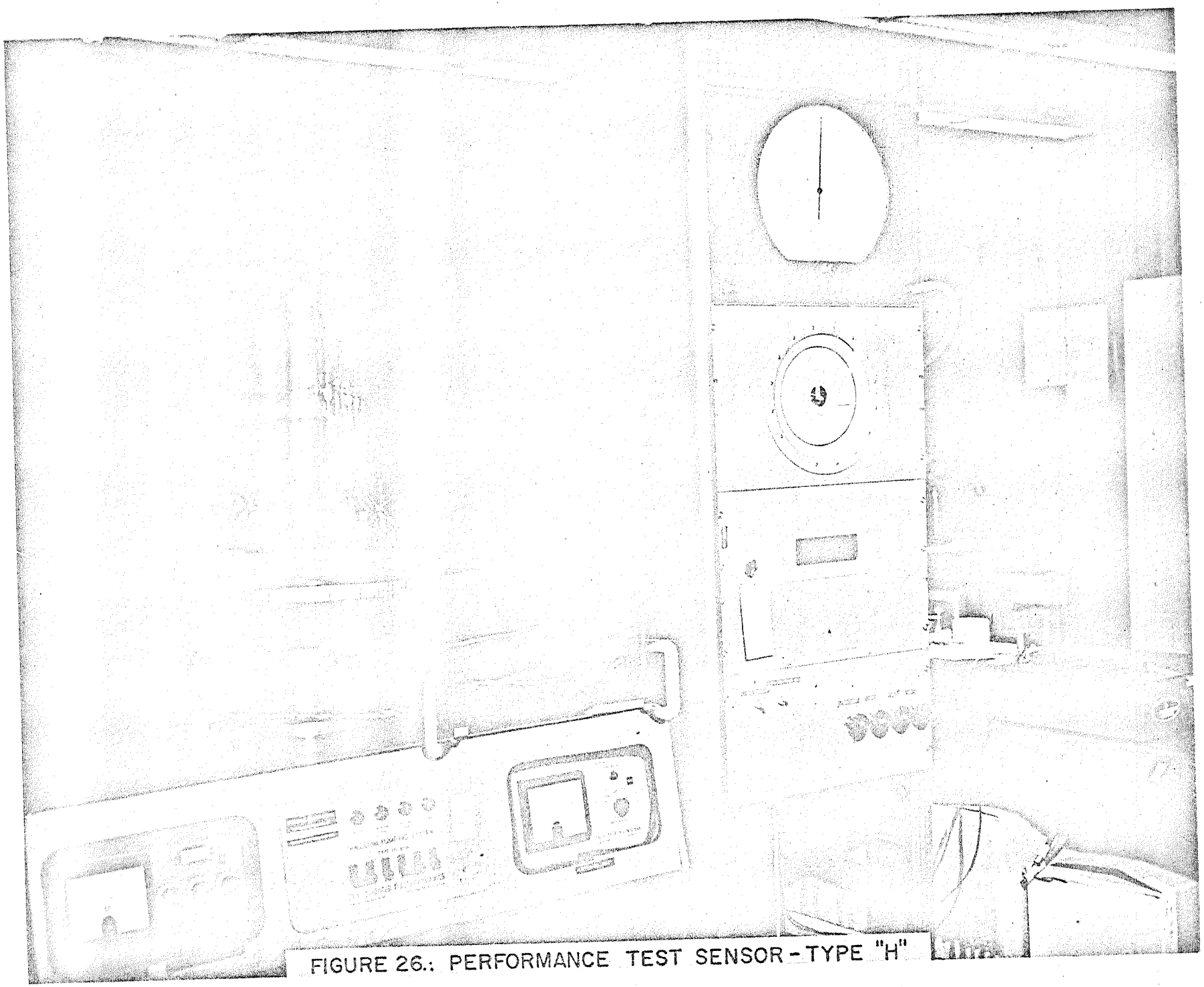

FIGURE 26.: PERFORMANCE TEST SENSOR - TYPE "H"

special IEM's under the present NASA contract.

6. Temperature Response: The temperature range in which the sensor must operate extends from 35°F to 110°F. It was anticipated that the output voltage would increase with higher temperatures. This would affect the entire E-I curve by shifting it upward with temperature increases and downward with temperature decreases. When a load resistance is chosen it must be low enough so that when the temperature drops the cell will continue to operate in the rate controlled region intended. Assuming, therefore, that the change in temperature allows the sensor to continue to be concentration polarized, the following equation can be applied.

$$E_T = -E_0 + \frac{RT}{nF} \ln (pO_2)^r (pH_2)^r - \frac{RT}{nF} \ln \left(1 - \frac{E_T}{pO_2 n R_L F}\right) \frac{D_{o1} C_{L2} e^{-\frac{E_{o1}}{RT}} + D_{o2} t_1 e^{-\frac{E_{o2}}{RT}}}{D_{o1} D_{o2} e^{-(E_{o2}+E_{o1})/RT}}$$

The terminal voltage, therefore, varies with the absolute temperature. The severity to which it is affected depends upon the constants in the equations. Initial testing over the temperature range 35°F to 110°F with a non-compensated sensor produced a curve

with a slope of 1 mv/^{o}F. Figure 27 is a plot of this curve. A temperature compensation network was designed and tested in a bread-board configuration using a constant voltage source to simulate the sensor output. This curve shown in Figure 28 confirmed the theoretical slope the circuit was designed for. With the slopes confirmed it remained to join the circuit to the sensor and check overall variations. A curve showing output voltage variations with temperature for the final configuration is shown in Figure 29. The overall temperature deviation has been held to .025 volts or 3.6% of full scale value. The hysterisis affect can be attributed to temperature lag or response time between the thermistor and the ion-exchange membrane.

7. Time Response: In order for the pO_2 sensor to be useful as an operational instrument a rapid time response is desirable. As O_2 flows through the barriers, both rubber and water, they become saturated with the gas according to the pressures involved. Also, if any gas-filled space exists between the barrier and the water, this is at a pressure corresponding to the flow through the membrane and into the cell. When the external pressure changes, especially a decrease, the O_2 trapped in the space and in solution must equalize with the new external condition. This is achieved by oxygen escaping to the atmosphere or being used by the cell. In order to speed this equilibration, several steps are possible.

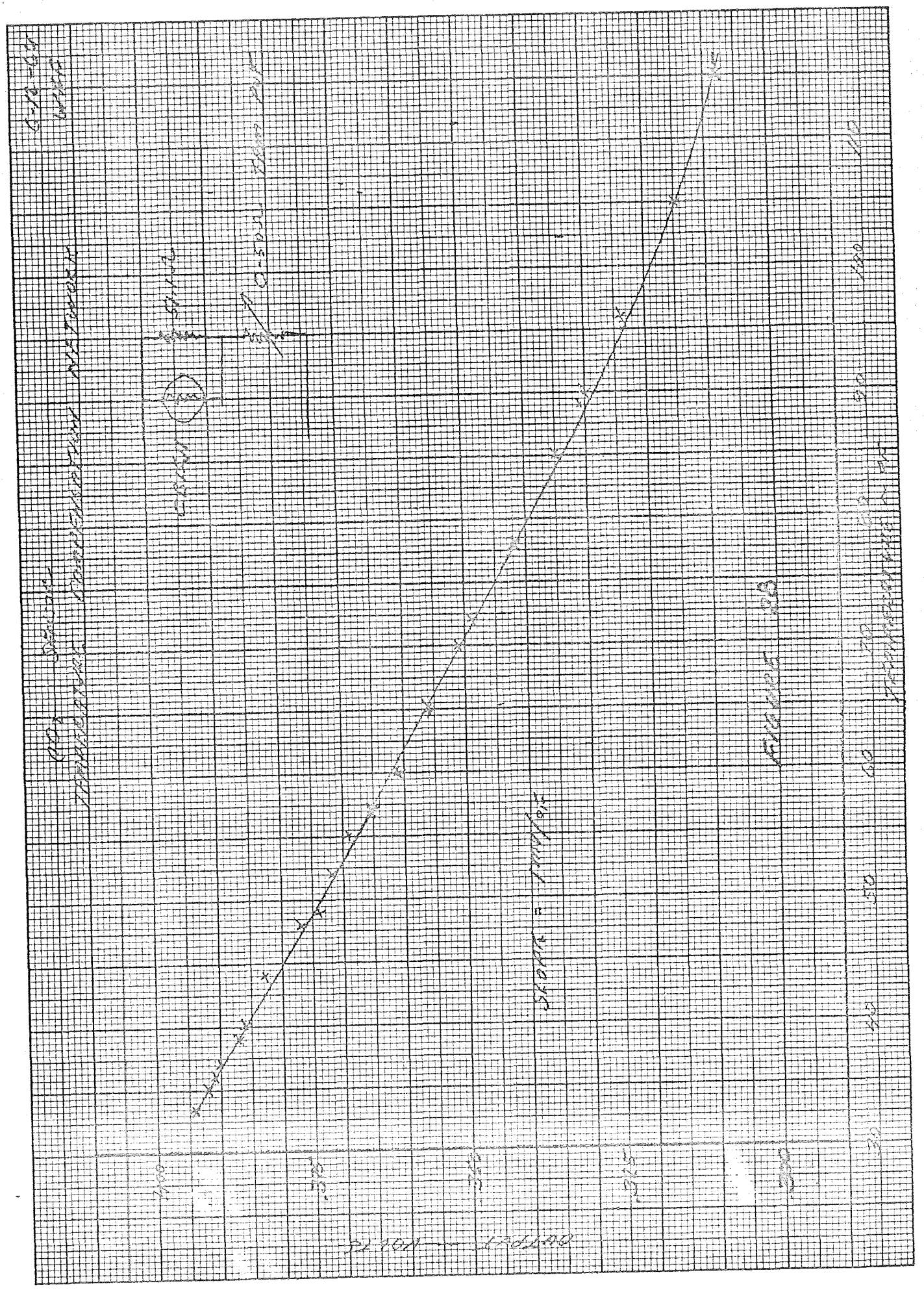

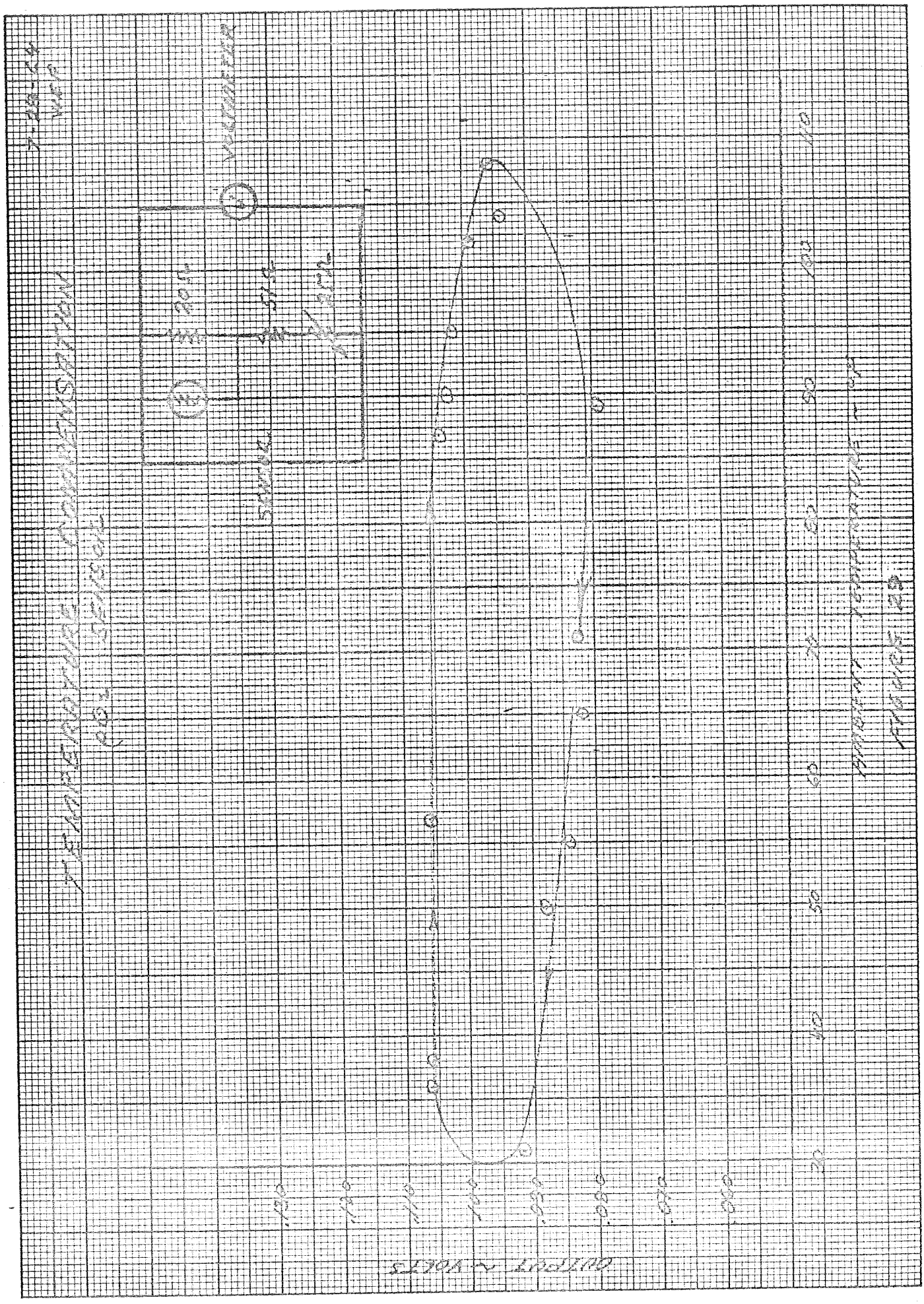

The more current produced, the faster the 0_2 is used, the faster the response. The thinner the barrier, the easier the 0_2 diffuses through it. The shorter the gap between the barrier and the electrode, the less water and gas trapped and therefore, the less quantity to be disposed of. These are valid, assuming that the cell, itself, has a very fast response to pO_2; i.e., the barrier arrangement is the rate controlling factor. The last two methods are the two which can be given the most attention since the amount of current produced affects both the amount of water produced and the amount of hydrogen used. Both of these must be kept to a minimum to have a practical instrument.

The time response then can be improved by making the diffusion barrier thin and the gap between the barrier and membrane small. Restrictions upon these two media are obvious. The barrier must remain thick enough to allow the necessary pressure drop so that the cell does not saturate below the desired upper end of the pO_2 range. Also, if the barrier comes in contact with the membrane, it appears to block off the active sites of the catalyst, thus completely polarizing the cell. This became apparent when with the barrier in contact with the membrane, gas was trapped between them. When the external pressure was reduced, instead of the output being reduced, as would be expected, the output increased. This is assumed to be due to an expansion of the trapped gas and a consequent

separation of the barrier and membrane. The active sites were thus free to react with the 0_2 and the output increased. A trade-off is therefore necessary between the barrier thickness, its distance from the membrane and the current drawn. The barriers tested up to now have been made of silicone rubber which is very flexible and distensible. A support is needed on both sides of this to provide it with rigidity to retain its shape. If it were unsupported, every change in pressure would cause it to deflect either inward toward the IEM or outward. This allows the trapped 0_2 to contract or expand immediately, but the cell doesn't come to equilibrium. The time delay of this system is very long indicating that a rigid barrier is necessary.

A schematic of the time response test set-up is shown in Figure 30. The two valves utilized were quick opening ball type valves which were actuated by hand. A series of runs on the type "H" sensors with the 1 mil barrier placed over the cathode collector and supported on both sides by 5 mil tantalum screen were performed. A step change was made from 400 to 160 mm Hg pO_2 with the sensor output recorded on a Sanborn recorder set at 1 mm/sec. Response times of 25 to 32 seconds were recorded for a 62% value of the delta output between 160 and 400 mm Hg pO_2. This time could be decreased by increasing the current. Reducing the load resistance or increasing the effective area of the barrier, would increase the current. The latter

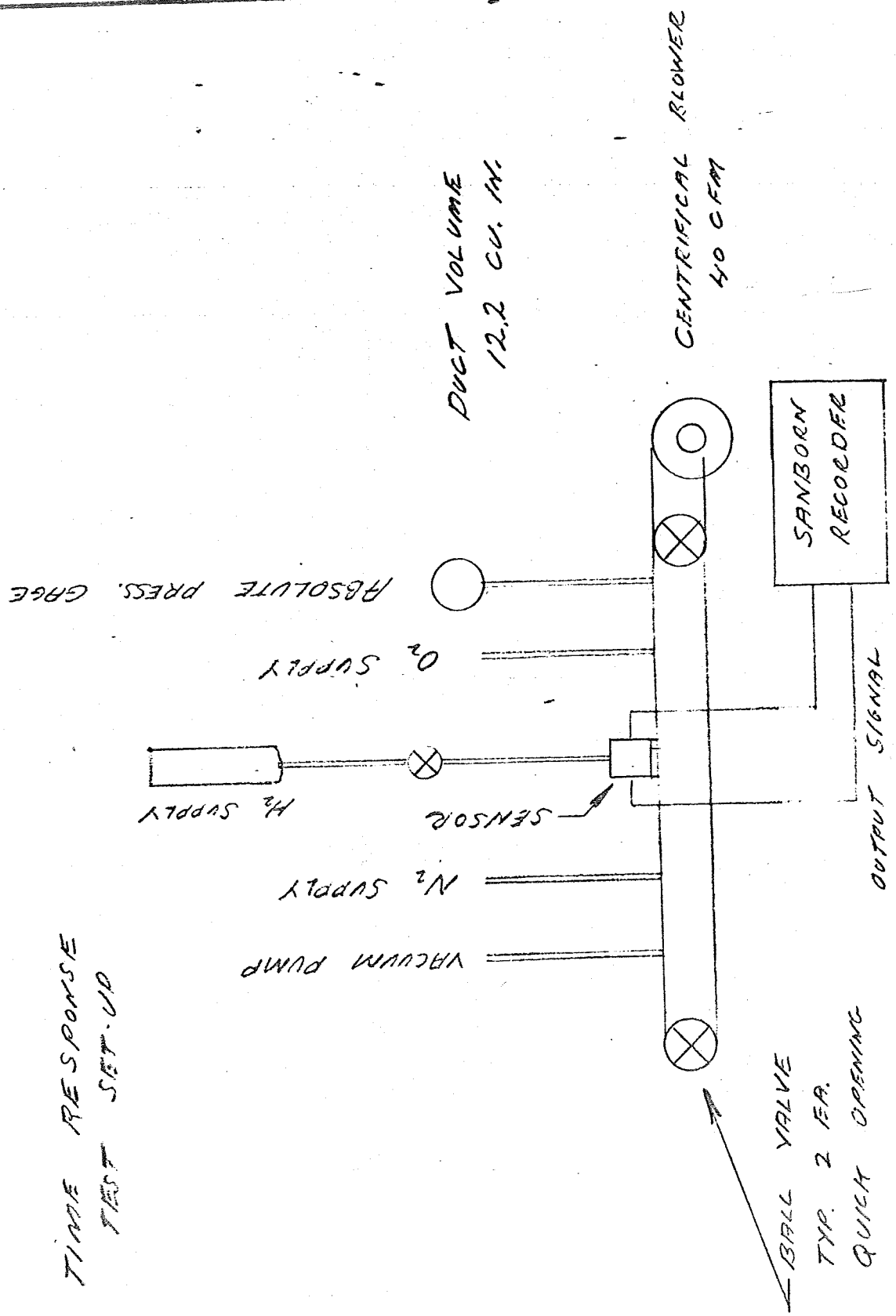
CENTRIFUGAL BLOWER
40 CFM
DUCT VOLUME
12.2 CU. IN.
SANBORN RECORDER
ABSOLUTE PRESS. GAGE
O2 SUPPLY
H2 SUPPLY
SENSOR
OUTPUT SIGNAL
N2 SUPPLY
VACUUM PUMP
TIME RESPONSE
TEST SET-UP
BALL VALVE
TYP. 2 PLA.
QUICK OPENING

FIGURE 30

approach is deemed more desirable as linearity, and stability are affected by the load.

8. Dead Ending of H_2: When hydrogen is produced commercially it contains some impurities. Initial testing was performed with the hydrogen under a constant purge so that water and contaminants were carried away. This eliminated any possible build-up of impurities on the H_2 reaction site. All phase D testing was accomplished with the H_2 supply dead ended. No evidence of chemical debris or excess water occurred except when water bubblers were in use on the hydrogen inlet. With the very low current densities in effect the build-up of impurities should not be a problem. Examination of the H_2 side of ion-exchange membranes after extended runs showed excessive dryness. As a precaution against dryout, a small doughnut of polyurethane was saturated with distilled water and inserted in the hydrogen reservoir of the prototype units.

9. Response to pH_2: Hydrogen pressure testing was performed early in the development program to establish a design point for the H_2 pressure regulator. A plot of H_2 pressure vs sensor output voltage appears in Figure 31. It can be seen that sensor output does not fall off until the H_2 pressure is reduced below 24 inches of Hg. absolute. H_2 pressures above this value have little effect on

FIGURE 31.
HYDROGEN PRESSURE vs. TIME
HYDROGEN SUPPLY PRESSURE
HYDROGEN OUTPUT VOLTAGE
Constant Load
Constant Current

the output of the sensor. Since extremely fine pressure control was not necessary, a nominal regulator outlet pressure of 15 $\pm$0.5 psia for the hydrogen supply was designated. A relatively low pressure was selected to minimize leakage problems on the H_2 side of the ion-exchange membrane.

10. Humidity: Since the ion-exchange membrane contains 50 - 60% water by weight it was suspected that humidity would have a significant affect on sensor performance. Humidity tests showed that relatively stable output was achieved at relative humidity levels from 20% to 80%. Humidity levels below 20% caused the membrane to dry out and increase the output voltage significantly. At 16% R.H. (110-70°F) the output started to increase after a period of 2 hours. The output increased at a constant rate from .220 to .436 V over a period of 1½ hours. It remained at .436 V for the remainder of the run (5 hours).

Desiccation in all likelihood occurred as a result of the extremely dry atmosphere. The dry hydrogen gas used tended to increase the rate of evaporation from the pores of the ion-exchange membrane. A test at 88% R.H. (73-70°F) produced a very gradual decrease in output from .281 V to .054 V after 50 hours. Even though the barrier was within .010 of the IEM, trapped water apparently decreased the overall permeability of the sensor a significant amount.

A humidity run of 15 hours at 50% showed no tendency to increase or decrease the output signal. If humidity variations are objectionable below 20% R.H. and above 80% R.H. a design change must be implemented to counteract this effect. However, between the relative humidity ranges of 20 - 80% the sensor is relatively unsensitive to variations in humidity levels. Figure 32 shows a photograph of the humidity set-up utilized for the above testing.

11. Multigas Atmospheres: When O_2 is mixed with other gases, as in air, it is theorized that the diluent gas tends to block off active reaction sites on the ion-exchange membrane causing some polarization. In practice it can be seen that the sensor produces less current for the same pO_2 when in air than when in pure oxygen. Figure 33 shows a plot of output vs total pressure for various oxygen partial pressures. It can be readily seen that as more diluent gas (nitrogen) is added to the atmosphere, the sensor output is reduced. Tests with CO_2 produce an identical effect. The G.E. Missile and Armament Department has done extensive development work on the diffusion of gases through thin porous membranes. Discussions with this group substantiated the fact that diffusion of oxygen through a diluent gas is not rate determining. Their testing showed that O_2 permeability coefficients do not vary in air or in 100% O_2 atmospheres. The fact that the sensor output is lowered by a

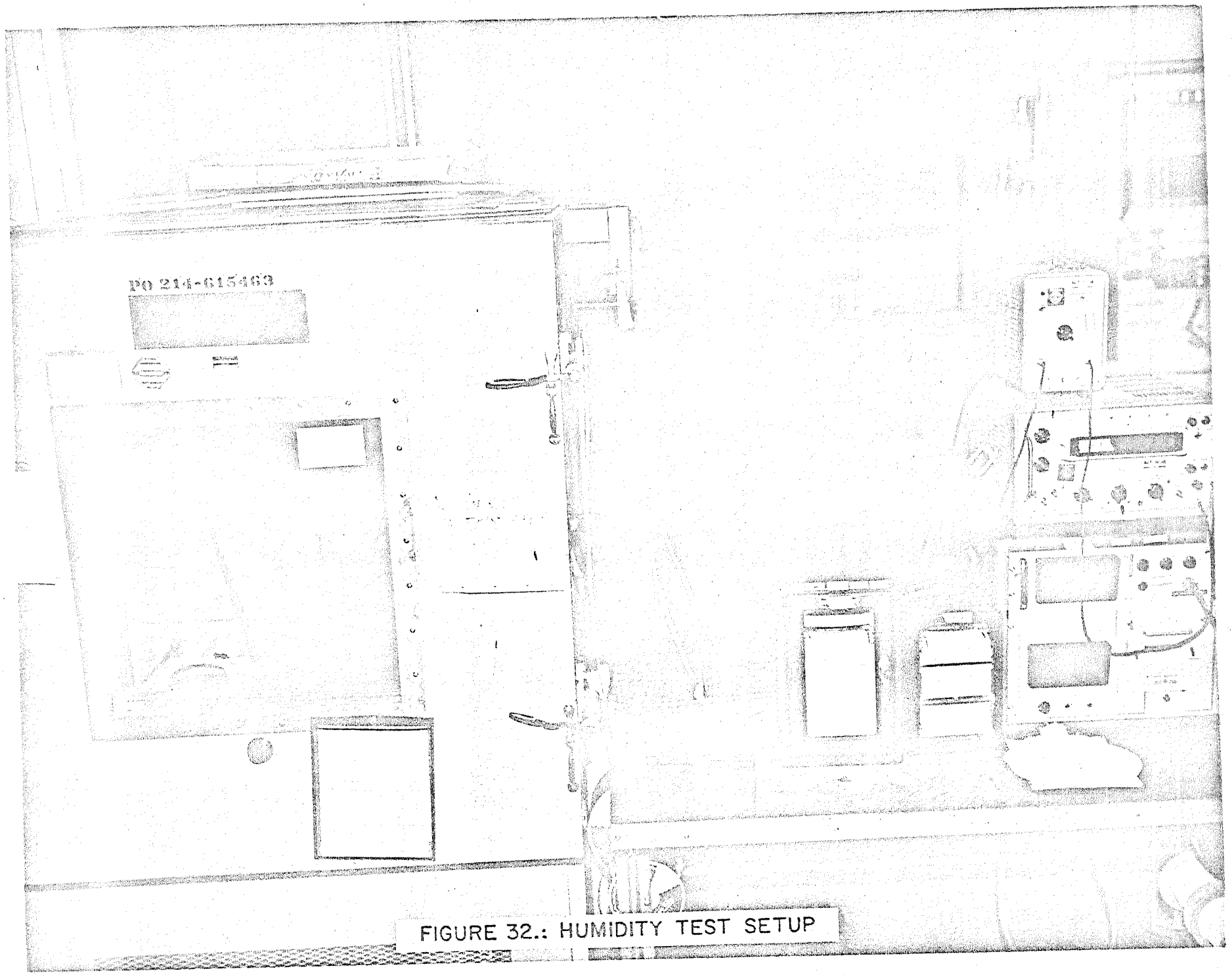

FIGURE 32.: HUMIDITY TEST SETUP

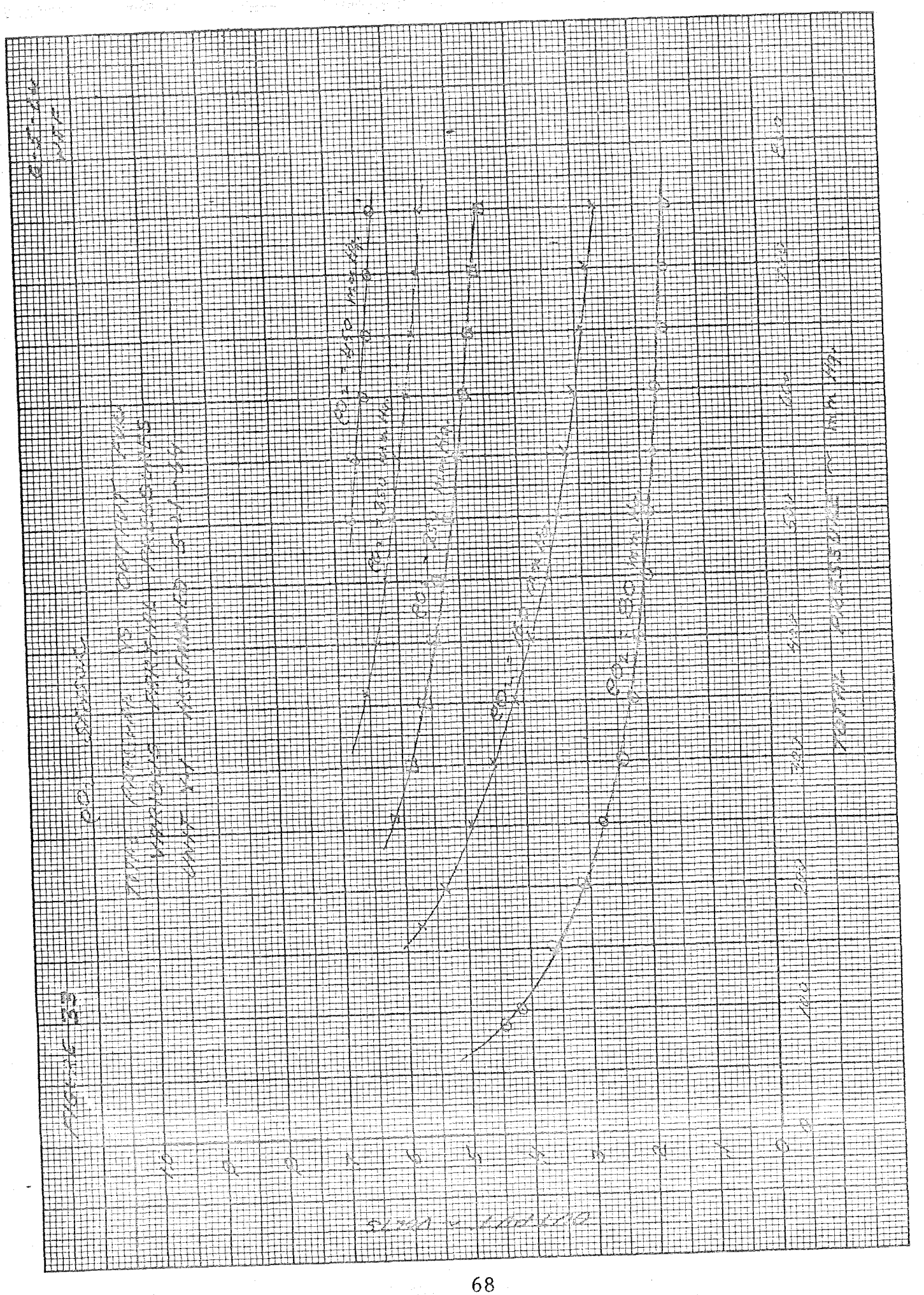

diluent gas requires the use of different barriers for a single gas and multigas atmospheres to achieve maximum sensitivity in both cases. A 1 mil barrier gives maximum sensitivity for a multigas atmosphere; whereas, a 4 mil barrier is necessary to prevent saturation in the pure oxygen atmosphere.

12. Storage Methods: As previously mentioned, the moisture state of the IEM affects its output. Irreversible damage takes place when the cell dries out completely or partially. It has been established that the cell must remain operating at all times at a moderate current once it has been started so that moisture is continually produced. Thus the sensor can be stored in an operating mode by supplying hydrogen either from the reservoir or externally. Also the sensor has been designed so that the IEM insert element can be disassembled from the remainder of the assembly and stored in distilled water.

Several tests were performed to prove that sensor performance does not deteriorate when stored in distilled water. Storage periods ranged from 3 to 6 weeks with no drop-off in sensor output at room ambient conditions. However, calibration curves could not be duplicated and varied by 25% at the high end of the curve (pO_2 = 460 mm Hg). This variation exceeds the maximum trimming capability of the prototype units, so that sensors would have to be recalibrated after prolonged storage.

IV. CELL ASSEMBLY

The storage of the ion-exchange membrane should be accomplished in a clean, sealed, polyethylene envelope and stored in a darkened chamber controlled at a minimum 90% relative humidity. The membrane is sensitive to ultraviolet light and can be artificially aged by exposure. All components of the cell must be completely cleaned before assembly. Parts that come in contact with the IEM should be rinsed in a 2% solution of sulphuric acid to prevent any hydroxide from coming in contact with the IEM. Any soap on hands, working surface of bench, or fixtures, will deteriorate the IEM. Rubber gloves washed in the acid solution are worn when removing the platinum black from the perphery of both sides of the 1/2 inch IEM wafer. A 3 power illuminated magnifying glass is used as an aid, with a dissecting microscope used for final inspection. Care must be taken to keep the IEM moist at all times during the scraping operation. The current collectors should be checked for flatness, pickled in HCl for 15 - 20 minutes, and washed in distilled water. In building up the cell, the collector lead out wires are sealed to the plexiglas housing as a precaution against oxygen leakage. Bostak #1142 adhesive was used where the tantalum wire protruded through the housing. When the barrier is placed on the collector, the only path for oxygen to get to the IEM must be through the

barrier. Most trouble of this type can be avoided by tightening the retaining nut sufficiently to maintain a good seal. When a sensor is put into operation, a break-in period is necessary (1 day). Initially the output will drop from open circuit voltage to a very low value, 1 - 2 mv. After 6 - 8 hours the output should increase to a nominal value of .120 V with a 1 mil barrier and the trim pot set at a nominal value of 25 ohms.

If it is necessary to install a new ion-exchange membrane, the fuel cell portion of the sensor must be detached from the H_2 reservoir. Once the sensor housing is removed the plexiglas insert can be pushed out from the sensing end. Care should be exercised not to harm the circuitry placed between the insert and the housing. A terminal screw on the insert can be loosened allowing the collector lead to be pushed up through the hole in the plexiglas housing. Only the upper most collector need be raised approximately one half inch. This will permit the ion-exchange membrane to be removed and replaced. This procedure should not be necessary for several months unless drying out occurs.

The barrier consists of 4 mil thick silicone rubber for a 100% oxygen atmosphere and 1 mil thick silicone rubber for a two gas atmosphere. Replacement of the barrier is accomplished by

removing the retaining nut at the sensing end of the sensor. The teflon and viton washers are removed, which will expose the retention screen and barrier. Since only a few inches of water Δ p exists across the membrane the barrier may be removed while the hydrogen supply is attached.

V. SENSOR OPERATION

A. Discussion of Fuel Cell Function

Fuel cells are usually tested in the laboratory by applying a potential across the terminals of the cell and then observing the current which the cell will produce or vice-versa. The instrument used for this potential-current measurement type of experiment is the potentiostat which maintains a given terminal voltage under varying current. Most fuel cell data presently available has been gathered in this manner.

Since the subject cell is to be used as its own source of power and is to be run with a load on it, i.e., current being drawn, the approach taken to determine its voltage-current characteristic was to vary a resistance placed across its terminals. This, in effect, placed a voltage across the cell, but in such a way as was determined by the equilibrium which the cell maintained between its own E-I relationship and Ohm's law. This approach was more meaningful, since it was a close approximation to the conditions under which the cell would be used.

Once the E-I curve had been plotted, it is usually easy to deter mine the range of resistances at which the cell operates under the influences of the various polarizing mechanisms. Since the fuel cell will saturate, or reach a nearly constant output potential at very low partia

pressures of oxygen, it is necessary to make the cell more responsive to changes in pO_2. To do this the cell was designed to operate under the influence of concentration polarization. In order to insure that the cell would operate in this current limited region, a mass transport barrier was used to impede the movement of oxygen to the reaction site. The barrier seals the cathode from atmospheric oxygen and also traps the water vapor and condensed water produced in the reaction between the oxygen and the electrode. Both the barrier and water act as impediments through which the O_2 must diffuse. When sufficient current is drawn from the cell, it becomes concentration polarized.

After a fuel cell is constructed and its operation begun, various pehnomena can occur which lead to undesirable cell output. When hydrogen and oxygen are introduced to their respective electrodes, the cell should generate open circuit voltage which is in the range of one volt. Measured with a high impedance voltmeter, this initial output should surge to a peak value as the gases reach the catalyst and then should remain constant there. Often times, though, the voltage falls from the peak as fast as it has risen. This open circuit polarization is often due to impurity currents caused by the leakage of either of the gases to the other electrode. For instance, if the seal between the H_2 and O_2 sides of the

membrane was not secure and H_2 got to the O_2 side, the H_2 would combine with any O_2 present on the nearest catalytic surface, thus polarizing this area of the catalyst. Since the OCV is a function of the active area of the catalytic surface, this decrease in area cuts down the cell's output.

Also, under certain circumstances, concentration polarization may occur at low voltages. This could be caused by some small concentration of reaction products or other impurities which may coat or adhere to the surface of the electrode. The reactants must be transported through them to reach the reaction site. Impurities may also be adsorbed onto the active sites of the catalyst, thereby reducing the active area and polarizing the cell. In any event, not too infrequently, when a cell is initially put into operation, its OCV is much less than expected. A method usually found adequate to remedy this situation consists of putting the cell through a breaking-in period in which a high current is drawn for a short period of time. This seems to burn off any masking elements and upon its return to an unloaded state, its OCV is invariably higher. This procedure can be repeated a number of times until a maximum OCV is attained.

The usual E-I curve for the sensor has an OCV between

0.95 and 1.05, and initial activation polarization drop to 0.8 - 0.85 at about 2 or 3 ma., then a gradual IR type drop to 0.4 or 0.5 at 30 ma. and finally concentration polarization takes over. Occasionally, the OCV starts at 0.8 - 0.85, has no activation polarization drop and continues with a slight IR drop normally through the rest of the curve, Figure 3. This means that the cell has been polarized by some means and that activation polarization has been masked by some other mechanism. This can probably be attributed to an inefficiency of the catalyst, contributing to a $T\Delta S$ loss of free energy.

The water produced by the cell is a necessary detriment since the membrane must remain moist to maintain its integrity. The water which is trapped by the barrier is beneficial in this way as well as in the form of a polarizing agent. Its evaporation seems to be kept at equilibrium by the barrier which will pass water vapor easily. One difficulty arises with the formation of water at high currents. Since the vapor is produced on the O_2 side only, it condenses on that side of the electrode starting at the junction of the membrane and current collector. The liquid water collects around the cooler periphery of the electrode and covers the outer exposed edge of the electrode surface. As more water

condenses, the covered area gets larger and the exposed active area is reduced until a pinpoint of area in the center of the electrode is all that is unshielded. Because the hydrogen side of the membrane is saturated with H_2 and the cell is producing a relatively high current, this one spot, being all that is directly exposed to O_2, produces the brunt of the current. As the process is nearly totally irreversible at high outputs, the reaction is no longer isothermal and the temperature of that one spot may rise enough to burn through the membrane. In this case the membrane is irrepairably damaged, since the O_2 and H_2 mix and can burn in thepresence of the catalyst.

The cell can be current limited not only by solid and liquid diffusion media, but also by gases. When the cell is operated in air of a certain pO_2 its output is lower than if it were operated at the same pressure of pure O_2.

B. HYDROGEN CHARGING

Periodically it is necessary to replenish the hydrogen gas in the reservoir of the sensor. A charging port with a check valve is incorporated in the bottom of the reservoir. A charging line can be attached to this fitting and hydrogen admitted to 2000 psig. Care should be taken to evacuate the charging line before admitting any hydrogen gas.

C. CALIBRATION

Before operating the sensor it should be calibrated with the mixture of gases it will be exposed to. If oxygen and carbon dioxide are to be monitored the partial pressures of each gas should be included in the calibration mixture. After an initial calibration curve is obtained the trim potentiometer is used to adjust the output signal to agree with the curve. The trim potentiometer varies the total resistance from 65.6 to 115.4 ohms.

VI. RECOMMENDATIONS & POST DEVELOPMENT TESTING

During the development program for the oxygen partial pressure sensor many serious problems were encountered and resolved. Several other problems affecting performance have been recognized but not corrected due to budgetary and schedule limitations. These problems are outlined in the following paragraphs and recommendations made for improving overall sensor performance.

1. During the course of the development program on the oxygen sensor it was evident that the sensor output drifted over long periods of time, i.e., 30 days. This drift was evident when pO_2 vs. output curves were obtained on successive days. The drift amounted to as much as 10% decrease over a 30 day period. Variations in water content at the surface of the ion-exchange membrane result in significant changes in diffusion rates and more importantly, in the conductivity of the desiccated portions. Also internal resistance of the cell can change with time. To minimize the above effects, an increased load resistance could be used; i.e., 1000 ohms, which will offer the major resistance in the cell circuit. Minor changes in water content or cell resistance would then have little affect on the output signal.

2. Electrical leakage as described in the Phase "D" Development Program has a significant effect on the repeatability of the oxygen sensor. Platinum black remaining in the cleared

peripheral area of the ion-exchange membrane will cause output to vary between sensors. Platinum migration into this cleared area can cause sensor drift.

Elimination of this short circuit could be achieved by having special "bulls eye" type ion-exchange membranes fabricated by the G.E. Direct Energy Conversion Organization. This would entail applying the platinum black only to the 5/16 inch diameter center protion of the 1/2 inch diameter membrane, thus eliminating any potential current leakage around the electrodes.

3. Introduction of nitrogen or any diluent gas into an oxygen atmosphere decreases sensor output significantly. This effect necessitated the use of two thicknesses of barrier; a 1 mil thick barrier for multigas, and a 4 mil thick barrier for a 100% oxygen atmosphere. It is hypothisized that the diluent gas blocks off active sites on the ion-exchange membrane thus preventing the molecules of oxygen from taking part in the reaction. This phenomenon should be investigated further to resolve whether all gases behave similarly. Also the effects of trace contaminants should be investigated.

4. The prototype designs supplied under contract NAS-9-1300 are by necessity crude in comparison to an operational instrument. The sensor could be simplified by providing a plug-in IEM module, so that replacement would merely consist of

unplugging the old IEM and substituting a fresh one. Reliability and ease of maintenance would be greatly increased with this modular concept.

5. The possibility of casting silicone rubber barriers directly on the ion-exchange membrane offers several attractive benefits. Decreased response time would result from reducing the volume between the barrier and IEM to a minimum; thus eliminating any time lag for the pO_2 to stabilize after a step change to the exposed atmosphere. Another advantage of the integral barrier IEM is the reduced effect of humidity on sensor output. Elimination of a volume for water to accumulate should reduce the effect of water build-up on the IEM. A third advantage would be the inherent sealing afforded by this approach. Oxygen leakage paths could effectively be eliminated from the sensor. Preliminary testing has indicated that blockage of active sites would not be a problem.

6. It is estimated that the volume of the oxygen sensor could be reduced by 40% and the weight by 50%. Thus, a sensor package could be developed which would weigh 8 ounces and fit within 9 cubic inches.

POST DEVELOPMENT TESTING

Prior to the delivery of the two prototype sensors to the Manned Spaceflight Center, it was learned that a joint Air Force,

General Electric, manned space cabin test was scheduled for the later part of August. Permission was obtained to utilize one of the NASA oxygen sensors as a "back-up" instrument during this test. Prototype sensor, Number 2, was installed in the environmental control console located outside the thermal-vacuum chamber. The ECS was connected with the cabin through two 6" lines. The atmosphere inside the cabin was thus circulated through the ECS where the gas was cooled; and moisture, CO_2, and odors were removed. Total pressure was maintained at 360 mm Hg with oxygen partial pressure held at 170 $\pm$5 mm Hg. The calibration curve for the Number 2 sensor utilized during the 15 day test is included as Figure 34. A 1 mil barrier was utilized for the O_2, N_2 and CO_2 gas mixture. Ambient signal output remained at .110 - .111 for eight days prior to the start of the manned test. For the first two days of the test, sensor output correlated closely ($\pm$2%) with the prime O_2 sensor. However output proceeded to drop on the third day and continued until an output of .050 volts was achieved. This output stayed constant for the remaining 10 days of the test. When the sensor was removed from the canister where it had been mounted it was discovered that the internal volume of the canister was filled with water. Apparently ice accumulating on the evaporator of the system was blown into the

8/19/94
CALIBRATION CURVE
PORTABLE SAMPLE
1 mM SOLUTION
1000 mM KH2PO4
1000 mM K2HPO4
30 mM KCl
pH = 7.00
SETRA - 7 PORTS ISOLATED
DRY GAS ATMOSPHERIC PRESSURE = 760 mm Hg
FIGURE B4

canister where it melted and remained. The relative humidity in the canister must have approached 100% so that the sensor built up a layer of product water, this reducing the amount of oxygen available to the ion-exchange membrane. Testing of the prototype sensor immediately after removal from the system showed an increase in output to .110 volts. Monitoring of the pO_2 sensor Number 2 was continued November 2, 1964, with the ambient output still holding at the .110-.116 volt level for a total of 54 days of continuous operation. At this time the output voltage climbed to .129 volt on October 1, 1964, and .175 volt a day later, where upon the output ceased.

Delivery of sensor Number 1 to NASA Manned Spaceflight Center, Houston, Texas, was made initially on August 10, 1964. Response to oxygen was good but a definite downward drift persisted at all oxygen partial pressures. The rate of this voltage drop was approximately 2 millivolts per minute. The sensor was exposed to various oxygen partial pressures by attaching it to a closed aluminum cylinder which was evacuated and pressurized to any given pO_2. After returning the sensor to GE-Valley Forge this drift could not be reproduced when tested in the conventional bell jar test

set-up used previously. However, when the cylindrical calibration fixture was tried a definite reduction in output was evidenced. An odor was evident from this calibration chamber which probably resulted from the acidic acid contained in the RTV silicone adhesive utilized in sealing the chamber. It is theorized that this constituent of the adhesive vaporized and poisoned the ion-exchange membrane, resulting in a lower reading. Subsequent monitoring of the sensor continued until December 1, 1964, when sensor Number 1 failed. This sensor had low (.010 volts) readings just prior to failure, so that a definite mode of failure (high or low output) cannot be predicted. Failure analysis on this sensor showed considerable migration of the platinum black to the edge of the membrane. This current leak increased until a short circuit existed across the electrodes. The P-1 sensor had run continuously for 90 days. The hydrogen reservoir was recharged to 1200 psig three times during this period.

APPENDIX A

1.0 THEORETICAL CONSIDERATIONS

An initial study of mass transport and electrochemical processes was undertaken to develop a fundamental understanding of the basic design parameters involved in a fuel cell type oxygen sensor. The data presented below shows the effect of oxygen partial pressure on the polarization of the cathode in an ion-exchange type system.

2.0 BASIC CONCEPT

A. Description of a Fuel Cell

A fuel cell is an electrochemical energy conversion system in which a controlled oxidation-reduction reaction between reactants, fed continuously from an external supply, takes place in the presence of a catalyst so that the energy change in the reaction is released nearly isothermally in the form of an electric current instead of heat. This definition applies also to consumable electrode cells. The basic components in a fuel cell are oxygen or air inlet, fuel inlet, catalytic electrode, electrolyte, current collectors and necessary seals.

According to physical chemistry literature,[1] a fuel cell can be regarded simply as a bielectrode system in which a net rate of oxidation takes place at the anode and a net rate of reduction at the cathode when the electrodes are coupled, resulting in a flow of electrons through an external resistance or load. In the pO_2 sensor the fuel used is hydrogen. Ignoring any intermediate reactions which take place as the ions pass into solution and are transported through the electrolyte, the reactions at each electrode are as follows:[2]

at the anode

$$2H_2 \rightleftharpoons 4H^+ + 4e^- \qquad (1)$$

releasing ions which pass through the electrolyte to the cathode and electrons which are picked up from the anode, pass through the load and reappear at the cathode.

At the cathode

$$4e^- + 4H^+ + O_2 \longrightarrow 2H_2O \qquad (2)$$

producing water as the end product of the reactions.

The over-all reaction in the cell representing the combination of the half cell reactions is

$$2H_2 + O_2 \longrightarrow 2H_2O \qquad (3)$$

The above definitions for anode and cathode can be seen to be the reverse of common electrical engineering terminology in which current flow is opposite to electron flow. In EE terminology, the hydrogen side would be the cathode (-) and the oxygen side, the anode (+). The cathode is, by definition, a source of electrons. From an external load looking at a fuel cell, the electrons are supplied from the hydrogen side which makes that electrode the cathode. Internally, the hydrogen sees the electrode as a sink for electrons, thereby making it the anode.

B. Electro Chemical Background

Various thermodynamic formulae can be used to describe and predict the performance of a fuel cell. Faraday defined the equivalent weight of a substance as its molecular weight divided by the number of charges it bears when ionized (valence). He found that the amount of electricity used or produced in an electrochemical reaction is proportional to the number of equivalent weights of the substance involved in the reaction.

Thus Faraday's Law can be summarized in the equation

$$It = Q = F \frac{m}{M/Z} \tag{4}$$

where I is current in amperes, t is time, Q is quantity of electric charge in coulombs, m is the weight of substance involved, M is molecular weight of the substance, Z the number of charges on the ion, and F is the constant of proportionality called Faraday's constant.[3]

The amount of energy which can be liberated by a chemical reaction at any particular temperature, called the Gibbs Free Energy, is given by the expression

$$\Delta G = \Delta H - T\Delta S \tag{5}$$

This simply states that the change in free energy must equal the corresponding change in heat content less the heat exchanged with the surroundings for a reversible, isothermal, isobaric reaction. The $T\Delta S$ term in the case of hydrogen and oxygen represents a loss which reduces the maximum theoretical efficiency to 83% when liquid water at 25°C is the product.[2]

For homogeneous gas reactions, that is, reactions taking place entirely between gaseous products and reactants, a good approximation in many cases is to consider that the gases obey the ideal gas laws.

For a chemical reaction between ideal gases

$$\Delta G = \Delta G^\circ + RT \sum \nu_i \ln P_i \qquad (6)$$

where $+\nu_i$ is the Stoichiometric number of moles of a product and $-\nu_i$ is the number of moles of reactant, and P_i is the individual partial pressure of each substance.(3)

For an ideal gas, the ratio of the partial pressure at the state under consideration to the partial pressure at an arbitrary standard state is called the activity,

$$a_A = P_A / P_A^\circ \qquad (7)$$

It can be seen that if we define the standard state as one atmosphere, the activity becomes equal to the partial pressure at the state in question,

$$a_A = P_A \qquad (8)$$

For the generalized reaction $aA + bB \rightleftharpoons cC + dD$ the equilibrium constant, K, is defined by

$$K = \frac{P_C^c \, P_D^d}{P_A^a \, P_B^b} \tag{9}$$

where P_I are the individual partial pressures. Then it can be shown that

$$\sum \nu_i \ln P_i^{\nu_i} = \ln \frac{(P_C)^c (P_D)^d}{(P_A)^a (P_B)^b} = \ln K \tag{10}$$

Therefore,

$$\Delta G = \Delta G^\circ + RT \ln \frac{(A_C)^c (A_D)^d}{(A_A)^a (A_B)^b} \tag{11}$$

which is valid for a reaction in equilibrium.

If n equivalents of reactant are converted to products and the electrons released pass through an external metallic circuit between a positive cell EMF, E, the electrical work done on the cell is -nFE. It can then be shown that this work is equal to the free energy change of the reaction,[4]

$$\Delta G = -nFE \tag{12}$$

Using this relation in equation (11) the equilibrium reversible (open circuit) cell voltage can be obtained as

$$E = E^{\circ} - \frac{RT}{nF} \ln \frac{(A_C)^c (A_D)^d}{(A_A)^a (A_B)^b} \tag{13}$$

which is a form of the Nernst equation.

Using this relationship the theoretical open circuit voltage for a hydrogen-oxygen reaction producing liquid H_2O at 25°C is 1.23 volts. At open circuit, when no current is drawn from the cell, the potential developed across the cell is equal to the potential corresponding to the reversible free energy change in transforming reactant to product. As current is drawn from the cell the potential across the cell begins to fall. Part of the energy used to maintain open circuit voltage is now expended in moving the electrons involved in the reaction through the circuit. The reaction, therefore, can proceed only as fast as the external resistance will allow the current to flow with Ohm's Law applying.

This loss of potential is termed polarization and is represented mathematically as

$$\eta = E_r - E \tag{14}$$

where E_r is the reversible emf and E is that emf which exists across the cell. Polarization is a function of the current drawn from the cell and therefore can be expressed in terms of the resistance in the external circuit. Depending upon the properties of the individual cell and the amount of current drawn, various mechanisms can control polarization. In each case the polarizing mechanism is the rate-controlling mechanism of the reaction.

The output characteristic of a cell, its voltage-current relation, (E-I curve) is dependent upon electrochemical kinetics and mass transport within the cell. The concept of electrode kinetics can be used to explain why a cell is polarized when a current is drawn.

C. Kinetic Theory of Cell Operation

There are three major phenomena to which the loss of cell potential has been attributed, i.e., activation polarization, cell resistance, and concentration polarization. Activation polarization results from the slowness of chemical and electrochemical

reactions at the given conditions. At room temperature, hydrogen and oxygen would combine to form water at an infinitessimally slow rate if just mixed together. Energy must be added to the system in order for the reaction to occur. This activation energy can be supplied by heat or by a catalytic agent. The catalyst, which can be platinum in the case of hydrogen and oxygen, serves as an accelerator for the reaction so that it will proceed relatively rapidly at room temperatures. But there is no guarantee that the substances will combine at a rate sufficient to produce the theoretical free energy potential at the electrode. As the voltage is decreased from the ideal equilibrium value (open circuit), the reaction rate is increased and produces a measureable current. At equilibrium conditions a very minute exchange current flows through the cell and the free energy of the reaction is used to maintain the potential across the electrodes. The maximum voltage produced by the cell depends on the free energy change of the reaction which depends upon the concentrations of the reactants and products.

The cell resistance or IR polarization of the cell depends largely upon the mobility of the ions formed and electrons released at the electrodes and their ability to traverse the distance from their entrance to the cell to a reaction site. Major contributors to this "Internal Resistance" of the cell are the conductivity of the electrolyte and the contact resistance between the current collectors and the electrodes.

When high currents are dfawn from the cell, the third cause of polarization, concentration polarization becomes the controlling process. Since a reaction can occur only as fast as the reactants are fed to the reaction site and the products are cleared away, limitations on the physical movement of the fuel and oxidant restrict the increase of reaction rate. A typical voltage-current plot for a fuel cell, illustrating the types of polarization, plotted on linear coordinates, is shown in Figure 15A.

1. Open Circuit Voltage

Let us consider an electrode which is brought in contact with an electrolyte and which has absorbed on its surface one of the reactants to be used in the cell. Assume the over-all reaction to be: $aA + bB + C \rightleftharpoons xX + yY + nx$ (15)

A, B, C, etc., are atoms, molecules or active surface sites.

Under open circuit equilibrium condictions the sum of the currents associated with the reduction side of the reactions must equal the sum of the currents associated with the oxidation side of the reactions of each electrode.[1] Since the system under consideration has only one redox reaction, the reaction rates for each electrode can be expressed as currents,

$$\vec{i}_c = \overleftarrow{i}_c = i_{oc} \quad \text{(cathode)} \qquad (16)$$

$$\overleftarrow{i}_a = \vec{i}_a = i_{oa} \quad \text{(anode)}$$

where $\leftarrow$ indicates reduction and $\rightarrow$ indicates oxidation, and i_{oa} and i_{oc} are termed the exchange currents for each reaction occurring at the two electrodes.

As the oxidation reduction reactions proceed at each electrode, electrons build up on its surface. Eventually the electrons stabilize with the positive ions in the electrolyte to produce the single cell potential, (OCV). There exists a potential difference between the molecular layer of electrolyte adjacent to the electrode, termed the plane of closest approach, and the surface of the electrode. If the electrode is freely conducting, the voltage change across the double layer can be considered as made up of a section, φ, across the plane of closest approach and a section, φ_o, which extends into the diffuse part of the electrolyte. Thus $\varphi + \varphi_o = E$, the potential at the electrode. (17)

2. Activation Polarization[4]

The rate of reactions requiring appreciable activation energy can be predicted, using Eyring's absolute rate equations

$$v_f = k_a T/h \gamma_{\pm} (A)^a (B)^b C e^{-\alpha F \varphi / RT} \quad (18)$$

where v_f is the rate of forward reaction (electrode to electrolyte), (A) and (B) are the activities of reactants, and C is the concentration of a reactant which determines the units of the rate of reaction.

$\gamma^{\ddagger}$ is the activity coefficient of the activated intermediate and $\Delta F^{\ddagger}$ is the truncated standard state free energy of activation.

This rate theory assumes that the reaction occurs by the formation of an activated complex from the reactants. The rate of reaction is the rate at which the complex multiples transform to a complex which is in equilibrium with the products. The reaction would be

$$aA + bB + C \rightleftharpoons C^{+} \quad \text{(activated surface complex)}.$$

The forward reaction rate can be written

$$\nu_f = k (A)^a (B)^b C e^{-\Delta F^{\ddagger}/RT} \tag{19}$$

The rate of the back reaction would be

$$\nu_b = k (X)^x (Y)^y e^{-\Delta F^{\ddagger} - \Delta F_0/RT} \tag{20}$$

ΔF_0 is the standard state free energy change of the reaction from left to right per gm. mole of C. One of the activities must be a surface activity (catalyst).

From eq. (12) it follows that a change in a free energy change is given by

$$\Delta(\Delta F) = \eta F \Delta V \tag{21}$$

and therefore the existence of a voltage gradient across the cell changes the relative standard-state free energy levels of any reactant or product which carries a charge.

It can be shown that for a reaction taking place in a potential field, the rate can be expressed as:

$$\nu_f = k(A)^a(B)^b C e^{-\Delta F^{\ddagger}/RT} e^{-\alpha n F \psi/RT} \tag{22}$$

and:

$$\nu_b = k(X)^x(Y)^y e^{-(\Delta F^{\ddagger} - \Delta F_o)/RT} e^{(1-\alpha) n F \psi/RT} \tag{23}$$

where α is the fraction of free energy change caused by the field, ψ, by the time the activated intermediate complex is formed.

Considering a half-cell reaction and defining activation polarization as $\eta = E_r - E$ (14), where E_r is the reversible potential, the reaction from left to right is aided by lower E, where E_r and E are defined as changes from the electrode to the electrolyte. Then, using:

$$\nu_f = K(e) e^{-\Delta F^{\ddagger}/RT} e^{\alpha n F(\eta - E_r)/RT}$$

$$\nu_b = K(P) e^{-(\Delta F^{\ddagger} - \Delta F_o)/RT} e^{(1-\alpha) n F (E_r - \eta)/RT} \tag{24}$$

where (R) and (P) are the activities of reactants and products raised to the appropriate molecularities.

Substituting:

$$nFE_r = -\Delta F_o + RT \ln [(R)^r/(P)^p] \tag{13}$$

and considering the current density in the forward direction to be:

$$(\nu_f - \nu_b) n_1 F = i \tag{25}$$

the current density produced is:

$$i = n_1 F k (R)^{1-\alpha} (P)^{\alpha} e^{-(\Delta F_+^{\ddagger} - \alpha \Delta F_o)/RT} e^{\frac{\alpha n F \eta}{RT}} - e^{-(1-\alpha)\frac{nF\eta}{RT}}$$

To simplify this equation, an exchange current, I, is defined as the rate of reaction per unit area in each direction at equilibrium, $\eta = 0$.

$$I = n_1 F k (R)^{1-\alpha} (P)^{\alpha} e^{-(\Delta F_+^{\ddagger} - \alpha \Delta F_o)/RT} \tag{26}$$

and

$$i = I(e^{\alpha n F \eta/RT} - e^{-(1-\alpha) n F \eta/RT}) \tag{27}$$

$\frac{i}{i_c}$ can now be considered the fraction of polarization that aids the current in the direction considered, and $\frac{I}{i_c}$ is the fraction which retards the back reaction.

When η is very small, the exponentials can be expanded and higher powers of $\alpha n F \eta / RT$ neglected,

$$i = i_c \alpha n F \eta / RT \tag{28}$$

When η is large, the back reaction is insignificant and the forward reaction is predominant. Therefore,

$$i = I e^{\alpha n F \eta / RT} \tag{29}$$

and

$$\eta = RT/\alpha n \ln i \pm (RT/\alpha n F) \ln 1/2 \tag{30}$$

which can be written as

$$E_T = E^\circ - B \ln i/I_o \tag{31}$$

in terms of polarized potential, E, across the cell, where E^o is the open circuit voltage and I_o is the exchange current (not current density) at open circuit. This is termed the Tafel equation. It must be remembered that these equations are for <u>half cell reactions</u>. To get the equation describing activation polarization across the whole cell, the potentials of the electrodes must be subtracted. Using the reversible potential difference between the half cells

at standard state E_{oc}, as the standard state OCV of the cell, the terminal voltage E_T can be expressed as,

$$E_T = E_{oc} - \beta_c \ln(i/I_{oc}) - \beta_a \ln(i/I_{oa}) \quad (32)$$

where subscripts c and a refer to cathode and anode. Greene and Greene[1] defined a term, the cell current constant, I_{cc}, evaluated at $E_T = E_{oc}$ in the above equation. Then E_T could be expressed in terms of I_{cc} to give:

$$E_T = E_{oc} - \gamma \ln i/I_{oc} \quad (33)$$

where:

$$I_{cc} = I_{oc}(I_{oa}/I_{oc})^{\beta_a/\beta_c+\beta_a} \quad (34)$$

and γ is equal to the sum of the values of the individual electrode Tafel slopes

$$\gamma = \beta_a + \beta_c \quad (35)$$

and is to be called the cell voltage constant. This, therefore, is an equation of the form of a Tafel equation which can be used to given the current-voltage relation of a full fuel cell. Figure 11-2 shows the general shape of Eq. (33) on linear coordinates.

3. Internal Resistance

Polarization of a total cell is the sum of the half cell effects, considered above, and the ohmic polarization. This latter effect deals largely with the conductivity of the electrolyte and the connections between electrodes and metering devices. In the electrolyte, the resistance is embodied in the manner in which a charged particle can move through an electric field. The simplest relationship is direct linearity

$$\eta = IR \tag{36}$$

$$E = E_r - IR \tag{37}$$

Internal resistance is usually the rate controlling effect through the range of moderate current production, from the Tafel effect region of activation polarization to the concentration polarization region. The cell of interest for the pO_2 sensor has a low internal resistance and additional circuit resistance can be eliminated by properly securing the current collectors to the electrode surfaces.

CURRENT
VOLTAGE
A-18

4. Mass Transport Effect-Concentration Polarization

Fuel cells which use liquid electrolytes as conducting media involve problems associated with the transport of reactant through the electrolyte to the reaction site which gives rise to ionic concentration gradients in the electrolyte. The exact solution to the mass transport problem is usually impossible to perform, generally involving the solution of the Navier-Stokes equation allowing for electrical forces. An approximate solution can be obtained by assuming that the ions follow a relationship similar to Fick's law which states that the diffusion rate is proportional to the concentration gradient and inversely proportional to the thickness over which the gradient extends.

$$q_r = D(c_2 - c_1)/\delta \tag{38}$$

This line of reasoning can be pursued further and an expression will be obtained which describes the final portion of the polarization curve, the current limiting region. But in the cell being discussed here a slightly different approach is needed, even though the result is similar. The cell under discussion does not have a liquid electrolyte but rather a solid organic membrane serves as the ionic path. Electrolyte concentration gradients are not important in this system because of the nature of the membrane

itself and because it is on the order of a few milli-inches thick, presenting a very short path to the ions. Concentration polarization becomes rate determining only at very high current densities, when a problem arises in connection with the transportation of the reactants to the electrodes from outside the cell. This occurs when air is used as the oxidant and the oyxgen must diffuse through the nitrogen. Also, when the water produced accumulates in a film on the surface of the catalyst, the oxygen must diffuse through it to be adsorbed.

For this case, assuming Ficks' law to hold, the rate of diffusion of the reactants to the active surface is given by

$$q = D_{eff} (C_B - C_s)/\delta$$

where D_{eff} is the effective diffusion coefficient, C_B and C_S are reactant bulk surface concentrations and δ is the film thickness. Assuming that everything that gets to the surface takes part in the reaction, then the current density will be

$$i = nF D_{eff} (C_b - C_s)/\delta \qquad (39)$$

The maximum rate at which current will be produced is given when C_S tends to zero at steady state

$$i_L = (nFD/\delta) C_b \qquad (40)$$

where i_L is the limiting current density. Then the current at less than the limiting case will be:

$$i = i_L / C_b \left(C_b - C_s \right) \tag{41}$$

since

$$nFD/\delta = i_L / C_b$$

Using eq. (27) modified to take into account a concentration gradient:

$$i = L\left(R/R_b \, e^{\alpha n F \eta / RT} - P/P_b \, e^{-(1-\alpha) n F \eta / RT} \right) \tag{42}$$

and assuming product accumulation is not detrimental to the reaction

$$i = L\left(1 - i/i_L \right)^a e^{\alpha n F \eta / RT} - e^{-(1-\alpha) n F \eta / RT} \tag{43}$$

Assuming a first order reaction, a = 1.

Examining the situation in which the reaction is irreversible and the back reaction signified by the term on the right hand side, above, is negligible ($\alpha \rightarrow 1$), it can be shown (4) that :

$$\eta = \left[(RT/\alpha nF) \ln (i_L/i) + (RT/\alpha nF) \ln \frac{i}{i_L - i} \right] \quad (44)$$

where η is the polarization of the half cell due to activation and concentration polarization. Using $E_T = E_r - \eta$ to find the terminal voltage of the cell and the previous definition of I_{oc},

$$E_T = E_r - (RT/nF) \ln (i/I_{oc}) - (RT/nF) \ln i/i_L - i \quad (45)$$

This equation when plotted gives the usual Tafel form at low i and the current limited drop in E_T at high currents as shown by Fig. (3).

In the case of the pO_2 sensor, where gas diffusion to the electrodes is the main current limiting mechanism, the concentrations, C, in equation (38) through (41) can be replaced by partial pressures.

A complete form of the equation for the polarization curve would also include the ohmic losses. Assuming the polarization is a linear function of the current, the IR term can be added to the polarization expression and the equation for terminal voltage becomes

$$E_T = E_r - RT/nF \ln (i/I_{oc}) - RT/nF \ln i_L/i_L - i - iR \quad (46)$$

Each term this equation becomes predominant over a certain range of i

5. Polarizing Effects

Impurities in the reactants can produce two pronounced effects. One is by reacting with each other and producing currents which tend to polarize the cell's output. The second is to block off the active sites on the catalytic surface by being strongly chemisorbed thereby interfering with the main reactions.

Assume that an impurity exists in very small amounts and is producing a current associated with its own redox couple. If its exchange current is high compared to the cell's exchange current it will produce a marked polarization of the cell. Since the concentration of impurity is low and its exchange current is high, it will react in a diffusion limited manner over most of the voltage range. If αi is the impurity current density, the measured current density i_m is:

$$i_m + \alpha i = I\left(e^{\alpha n F_n/RT} - e^{-(1-\alpha) n F_n/RT}\right) \qquad (47)$$

since two currents of similar magnitude exist at the same voltage.

Thus:

$$i_m + \alpha i = I\, e^{\alpha n F_n/RT} - e^{-(1-\alpha) n F_n/RT} \qquad (48)$$

At open circuit, $\dot{i}_m = 0$ and $-a\dot{i}^\circ = I\left(e^{\alpha n F \eta / RT} - e^{(1-\alpha) n F \eta / RT}\right)$ (49)

and a large polarization results even though no current is drawn through the external circuit. If we are investigating a reaction with a low exchange current I, we will not get the ideal reversible potential at open circuit unless the system has been sufficiently purified to make $a\dot{i}^\circ$ small compared to I.

An example which applies to the case in point is that of oxygen getting to the hydrogen side of the membrane and visa-versa. Small eddy currents are produced on one side of the cell since the presence of both reactants and the catalyst provides favorable conditions for side reactions. The potential associated with the current produced tends to generate a sizeable reduction in cell output. If enough of the reactants exist on the same side of the cell, combustion may even occur, resulting in irreversible cell damage.

Electrochemical reactions usually proceed via active surface sites on the electrode. Whenever gas is part of the reaction system at least two consecutive steps transpire: gas absorption - desorption and the electrochemical reaction. It is generally accepted that when gas is used at an electrode the process of transferring an electron to or from the surface leaves the gas in a chemisorbed state on the surface. The influence of the adsorption-desorption

rates of the catalyst on the polarization depends upon their relative magnitudes as compared with the reaction rate of the cell. If adsorption is fast it doesn't become a controlling factor and its rate is not appreciably changed by potential changes or pressure variations. Large currents result, surface coverage is almost constant and polarization is a function mainly of the electrochemical reaction. The surface coverage of the catalyst is its effective activity in ionic discharge reactions and therefore the rates of adsorption-desorption can affect the polarization relations.

Let us assume that the cell in which we are interested has electrodes with a catalyst that has a fast adsorption-desorption rate and is always at a state near equilibrium. For the hydrogen electrode in an acid electrolyte the reactions can be represented as :

$$2 \text{ ACTIVE SITES} + H_2 \rightleftharpoons 2(H)$$

$$(H) + H_2O \rightleftharpoons H^+ \cdot H_2O + (e) + \text{ACTIVE SITE} \qquad (50)$$

where (H) is a chemisorbed atom. Let Cm be the maximum number of active absorption sites per cm^2 of surface in gm moles. Then equation (26) and (27)

$$\dot{i} = I\left(e^{\alpha n F\eta/RT}\right) - e^{-(1-\alpha)nF\eta/RT}$$

where:

$$I = \eta_1 FK(R)^{(1-\alpha)} P^{\alpha} e^{-(\Delta F^{\ddagger} - \alpha \Delta F_0)/RT}$$

can be written in the form,

$$\dot{i} = K(R)^{1-\alpha}(P)^{\alpha} e^{-(\Delta F^{\ddagger} - \alpha \Delta F_0)/RT} Q' \qquad (51)$$

where $K = nFk c_m$ and Q' stands for:

$$Q' = e^{\alpha n F\eta/RT} - e^{-(1-\alpha)nF\eta/RT} \qquad (52)$$

The activities (R) and (P) will contain terms involving chemisorbed surface concentrations.

An expression relating the amount of catalytic surface area covered to the pressure and equilibrium constant, termed Langmuir's isotherm, is written

$$P(1-\theta_e)^2 = K\theta_e^2 \qquad (53)$$

where θ_e is the fractional degree of coverage and activities can be taken as $\theta/\frac{1}{2}$ since at standard state, surface coverage is assumed at $\theta = \frac{1}{2}$. The concentration of chemisorbed species is then θ_{cm}.

The standard state free energy related to chemisorption can be expressed as

$$\Delta F_{oc} = RT \ln\left[P(1-\theta_e)^2/\theta_e^2\right] \qquad (54)$$

It can be shown that the influence of the free energy of chemisorption on the reaction is contained purely in the effect it has on θ and $1-\theta$. Also, exchange current density for metals with the same active area and number of active sites will vary as a function of θ and $1-\theta$ and therefore with the standard state free energy. The relationship between exchange current and free energy is logarithmic, of the form:

$$\log(1/I) \propto |\Delta F_{oc}| \tag{55}$$

This expression plotted out shows that the maximum exchange current occurs when the surface has a zero energy of chemisorption. Weak chemisorption occurs when ΔF_{oc} has a high positive value and therefore it is harder for the gas to be chemisorbed. Since there is very little gas on the surface, the reaction is slowed. A highly negative ΔF_{oc} causes strong chemisorption in which gas can easily adhere to the surface. The surface is easily saturated but the gas is held too strongly to react, thus causing a low reaction rate.

Thus, a good catalyst is one which has a ΔF_{oc} near zero. The catalyst would react fast and not be the rate determining process.

6. Effect of pO_2 on Cell Output

Variation of O_2 partial pressure has a definite effect on the voltage output of the fuel cell and upon the current-voltage curve. Under equilibrium conditions, at open circuit, the Nernst equation can be used to describe the variation of voltage output with pO_2.

$$E_r = E_o + RT/nF \ln R^r/p^p \qquad (13)$$

In experiments using flat plate and porous electrodes in an alkaline electrolyte, Hartner, Vertes, Medina and Oswin found the polarization decreases in a non-linear fashion as pO_2 increased.[5] Their studies were performed on cells operated at current densities sufficiently high to cause concentration polarization to be the rate limiting process. The resistance to the mass transport of O_2 through the liquid electrolyte to the reaction zone caused this polarization. Using the relationship expressing current in the concentration polarized region as $\dot{i} = DnF(c_1 - c_2)/\delta$ equation 39 above, and concentration polarization as $\eta_c = RT/nF \ln \dot{i}/\dot{i}_L - \dot{i}$ from equation 45 above, and $\dot{i}_L = DnF(c_1)/\delta$

from equation (40); it can be seen a drop in concentration polarization may be obtained by increasing limiting current. This can be accomplished by increasing D, the diffusion constant, by increasing temperature; decreasing δ through agitation or increasing C_1. Keeping the first two constant and varying C_1, the polarization in terms of pO_2 was found to be of the form $\eta_c = RT/nF \ln\left[\frac{f(pO_2)}{f(pO_2)-K}\right]$ at constant current. Assuming that the catalytic activation effect was negligible, they found that the current in the concentration polarization region is a function of $(pO_2)^{\frac{1}{2}}$ that is $i_{c_1} = A \ln pO_2 + B$ where A is 0.5. Normalizing,

$$i_{c_1}/i_{c_2} = [(pO_2)_1/(pO_2)_2] \tag{56}$$

which is based on their experimental results.

There are two possible mechanisms which could exist in the event that concentration polarization is the rate limiting process. The first is liquid phase diffusion of dissolved oxygen, the other is interphase mass transfer of oxygen from the gas into the liquid phase. Should ordinary diffusion in the liquid phase be the rate controlling step, and the liquid surface in contact with the gas is saturated with O_2, the current would vary linearly with pO_2 at V = C. Since the relationship found was a function of

$(pO_2)^{\frac{1}{2}}$, pure diffusion was eliminated as being the mass transfer rate controlling step in these experiments.

These results illustrate the fact that the output of a fuel cell does vary with pO_2.

To get an insight into the dependence of E_1 on pO_2 equations (13), (26), (34), and (45) can be combined and expanded to give

$$E_T = E_0 + \frac{RT}{nF}\ln\frac{(R)^r}{(P)^p} - \frac{RT}{nF}\left(\frac{\alpha_a+\alpha_b}{\alpha_a\alpha_b}\right)\ln\left(\frac{2R_b(\alpha_b-1)P_b^{-\alpha_b}}{I_{ob}}\left[\frac{I_{oa}(R_a)^{(1-\alpha_a)}P_a^{\alpha_a}}{I_{ob}R_b^{(1-\alpha_b)}P_b^{\alpha_b}}\right]^{\frac{-\alpha_b}{\alpha_a+\alpha_b}}\right.$$

$$\left. - \frac{RT}{nF}\left(\frac{\alpha_a+\alpha_b}{\alpha_a\alpha_b}\right)\ln\left[\frac{(R_L)}{R_L - \dot{i}\,\delta_s/nFD_s}\right]\right] - \dot{i}R \qquad (57)$$

This relates E_t to $\dot{i}$ and pO_2. It is the equation for the family of E-I curves run at various pO_2.

If the cell is operated with a resistor R_L across its terminals the above equation can be modified to yield:

$$E_T = \frac{\dot{i}R_L}{R_L+R}\ln\left(\frac{R_L nFD_s P^s}{E_T\delta_s} - 1\right) -$$

$$\frac{E_0R_L}{R_L+R} + \frac{\dot{i}RR_L}{R_L+R}\ln\left[\frac{(R)^{rK/a}}{(P)^{pK/a}}\cdot I_{ob}R_b^{(1-\alpha_b)}P_b^{\alpha_b}\left(\frac{I_{oa}}{I_{ob}}\cdot\frac{R_a^{(1-\alpha_a)}}{R_b^{(1-\alpha_b)}}\frac{P_a^{\alpha_a}}{P_b^{\alpha_b}}\right)\frac{\delta_s}{nFD_sP^s}\right. \qquad (58)$$

which is the general equation for any E_T vs pO_2 curve for the cell.

Since the cell will be operated in the current limited region this equation can be simplified to:

$$E_T = E_o + \frac{RT}{nF} \ln (pO_2)^r (pH_2)^r - \frac{RT}{nF} \ln \left(1 - \frac{E_T}{pO_2} \frac{\delta}{R_L n F D}\right) - K_a - \frac{E_T R}{R_L} \quad (59)$$

which applies only to concentration polarized cells. This gives an insight into the general logarithmic shape to be expected in the E_T vs pO_2 curve at constant R_L. This equation should apply to this development.

APPENDIX B

DETAILED DRAWINGS AND PARTS LIST

PARTIAL PRESSURE OXYGEN SENSOR

REVISIONS			
SYM	ZONE	DESCRIPTION	DATE	APPROVED

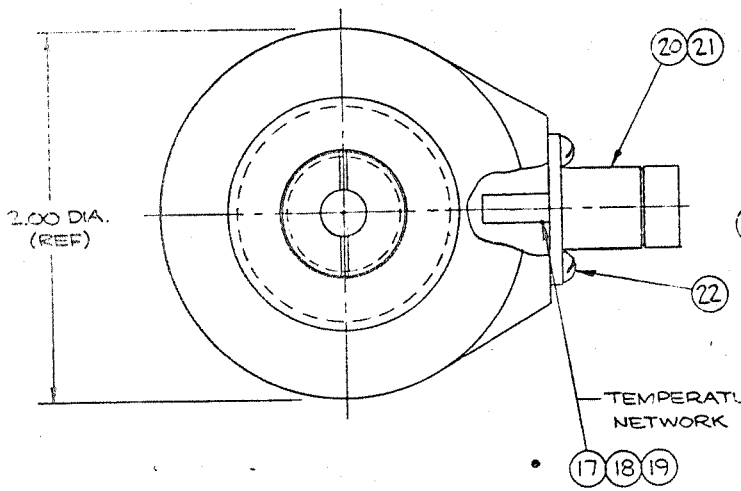

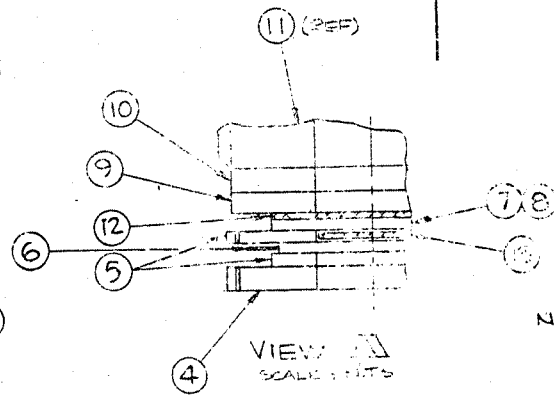

NOTE
1. REFER TO OPERATOR INSTRUCTIONS

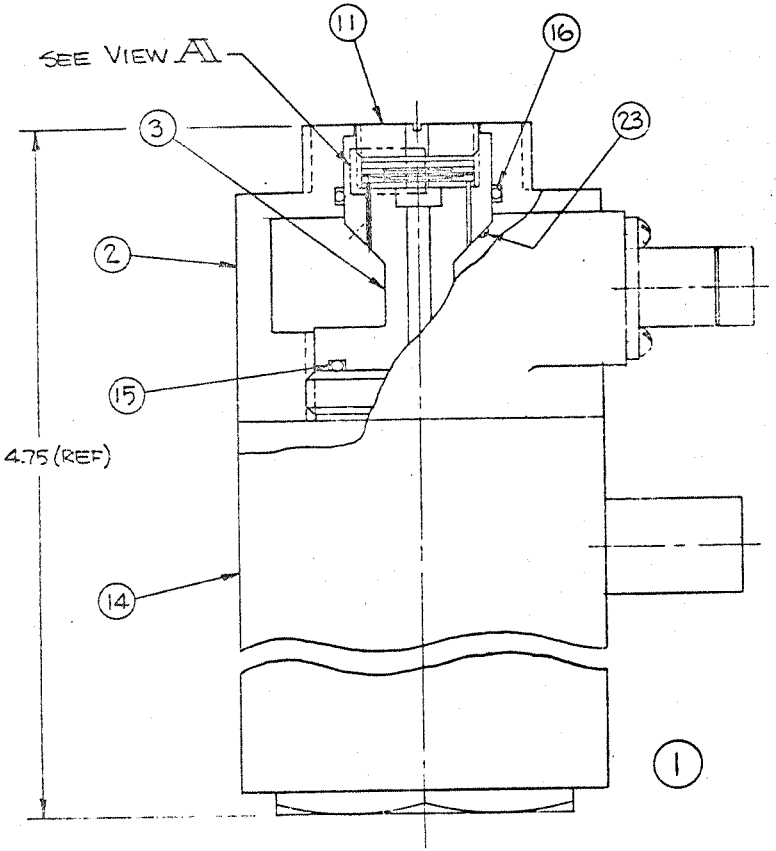

NO REQ'D	IDENTIFICATION NO.	F/N	DESCRIPTION	STOCK SIZE	MATERIAL
2	———	23	SCREW, RD HD	#0-80 NF-3A×⅛ LG	BRASS
4	MS 35206-11	22	SCREW, PAN HD	#4-40 UNC-2A×.18 LG	
1	PT 02P-8-22	21	CONNECTOR	BENDIX AVIATION CORP, SIDNEY, NY	
1	PT 02P-8-22	20	CONNECTOR	BENDIX AVIATION CORP, SIDNEY, NY	
1	CB1571	19	THERMISTOR	FENWALL INCORPORATED, ASHLAND, MASS	
1	200-66-1/S30	18	POTENTIOMETER	DAYSTRON	
1	NF 170N	17	RESISTOR	20Ω 1/8 WATT	
1	2-19-V495-7	16	O RING	PARKER SEAL CO CLEVELAND OHIO	
1	2-20-V495-7	15	O RING	PARKER SEAL CO. CLEVELAND, OHIO	
1	1790 001	14	REGULATOR & RESERVOIR	CARLETON CONTROLS CORP, EAST AURORA, NY	
1	133B2820-P2	13	SCREEN		
1	133B2820-P1	12	SCREEN		
1	133B2813-P1	11	SCREW, RETAINER		
1	133B2819-P1	10	WASHER		
1	133B2817-P1	9	SEAL, UPPER		
1	133B2818-P2	8	BARRIER, SINGLE GAS } INTERCHANGEABLE		
1	133B2818-P1	7	BARRIER, MULTI-GAS } SEE NOTE 1		
1	133B2815 P1	6	ION, EXCHANGE MEMBRANE		
2	133B2812-P1	5	CURRENT COLLECTOR		
1	133B2816-P1	4	SEAL, LOWER		
1	133B2805-P1	3	INSERT		
1	113C8514-P1	2	HOUSING		
X	113C8517-G1	1	ASSEMBLY		

LIST OF MATERIAL

UNLESS OTHERWISE SPECIFIED DIMENSIONS ARE IN INCHES—
TOLERANCES ON:
2-PLACE DECIMALS ±
3-PLACE DECIMALS ±
ANGLES ±
ALL SURFACES ✓

MATERIAL—
GOVT OR COML
GE

SIGNATURES		DATE
DRAWN	J.H. Saunders	8-10-64
CHECKED		
ISSUED		
ENGRG		
MTG		
MATLS		

GENERAL ELECTRIC
MSD DEPT LOC PHILA, PA (STC)

TITLE
OXYGEN SENSOR
ASS'Y

CONTRACT NO.

CODE IDENT NO.	SIZE	DWG NO.
15227	C	113C8517

SCALE 2/1 WT CALC ACTUAL SHEET OF

REV 113C8517 SIZE C

SIZE C 113C 8514 REV A

REVISIONS				
SYM	ZONE	DESCRIPTION	DATE	APPROVED
A		REDESIGNED & REDRAWN, FORMERLY WAS 133B2804	6-9-67	LH

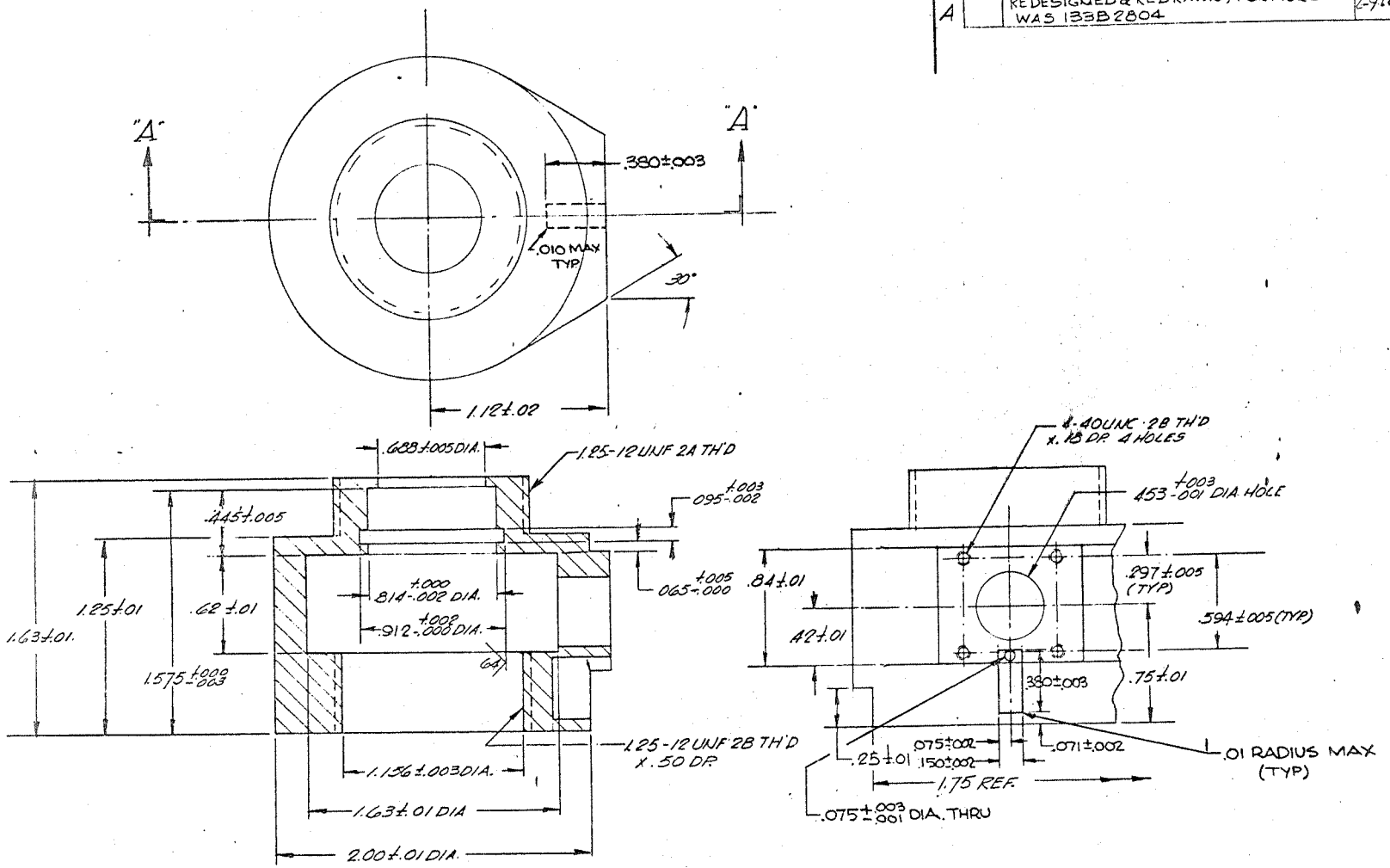

SECTION "A" - "A"

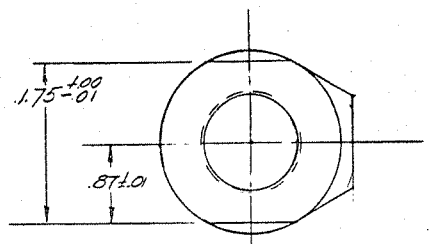

BOTTOM VIEW
SCALE 1-1

(1) FORMERLY WAS DWG-133B2804

UNLESS OTHERWISE SPECIFIED DIMENSIONS ARE IN INCHES—
TOLERANCES ON:
2-PLACE DECIMALS ±
3-PLACE DECIMALS ±
ANGLES ±
ALL SURFACES ✓

MATERIAL—
GOVT OR COML
ALUM. ALY 6061-T6
GE

SIGNATURES		DATE
DRAWN		
CHECKED		
ISSUED		
ENGRG		
MFG		
MATLS		

GENERAL ELECTRIC
MSD DEPT LOC. PHILA, PA. (STC)

TITLE
HOUSING,
OXYGEN SENSOR

CONTRACT NO.

CODE IDENT NO.	SIZE	DWG NO.
15227	C	113C8514

SCALE 2-1 WT CALC ACTUAL SHEET 1 OF 2

SIZE C 113C8514 REV A

FOLD

FORM NO. P (2-63) PRINTED IN U.S.A.

B-34

FOLD

SIZE	133B2805	SHEET	REV
B			A

REVISIONS

SYM	DESCRIPTION	DATE	APPROVED
A	RE DESIGNED	6-9-64	LSL

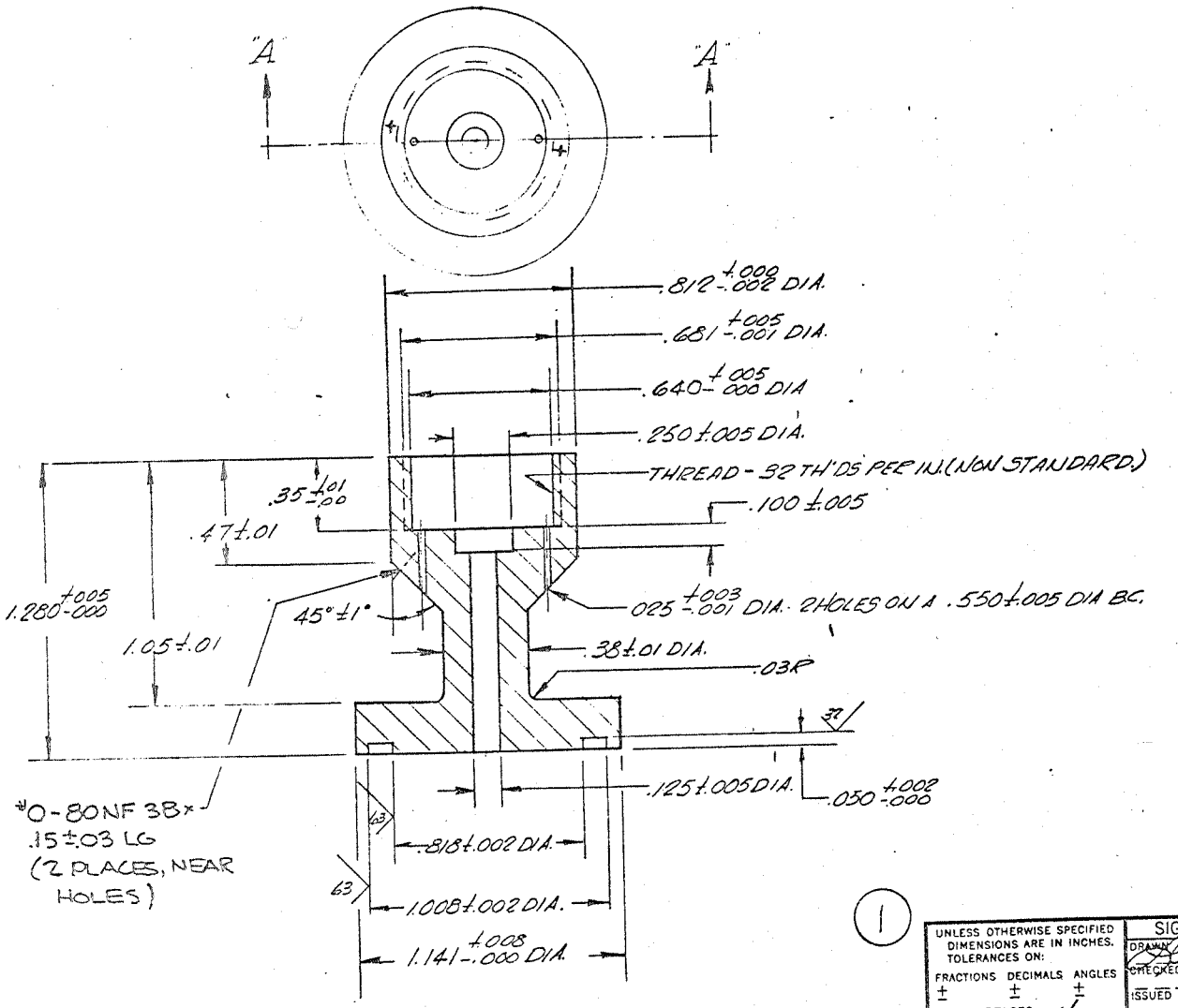

SECTION "A"-"A"

(1)

UNLESS OTHERWISE SPECIFIED DIMENSIONS ARE IN INCHES. TOLERANCES ON: FRACTIONS ± DECIMALS ± ANGLES ± ALL SURFACES √	SIGNATURES	DATE
MATL – GOVT OR COML METHYLMETHACRYLATE MIL-M-10851 GE	DRAWN	6-8-64
	CHECKED	
	ISSUED	
	ENGRG	
	MFG	
	MATLS	

GENERAL ELECTRIC MSD DEPT LOC PHILA, PA. (STC)

TITLE: INSERT, OXYGEN SENSOR

CONTRACT NO.

CODE IDENT NO.	SIZE	DWG NO.
15227	B	133B2805

SCALE 2-1 | WT CALC ACTUAL | SHEET 1

PRINTS TO

FN 502-P (6-63) PRINTED IN U.S.A.

FOLD

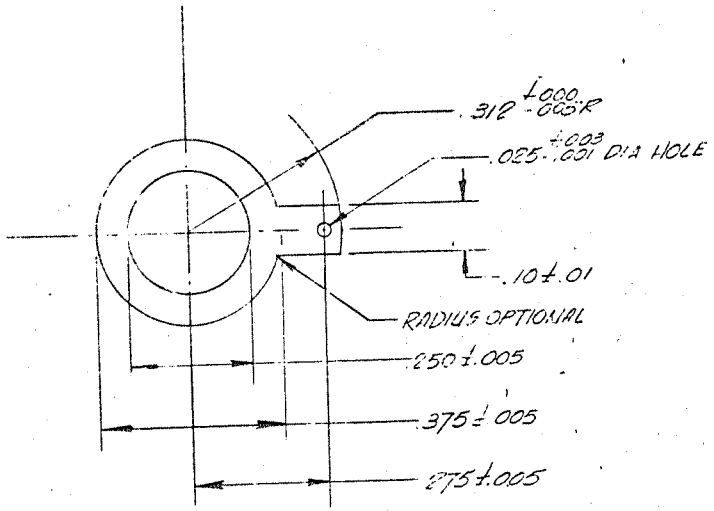

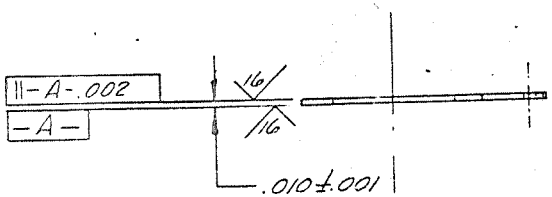

133B2812 SHEET

REVISIONS

SYM	DESCRIPTION	DATE	APPROVED

FOLD

UNLESS OTHERWISE SPECIFIED DIMENSIONS ARE IN INCHES. TOLERANCES ON:
FRACTIONS ± DECIMALS ± ANGLES ±
ALL SURFACES √
MATL-GOVT OR COML
TANTALUM
GE

SIGNATURES		DATE
DRAWN	Rassul	6-10-64
CHECKED		
ISSUED		
ENGRG		
MFG		
MATLS		

GENERAL ELECTRIC
MSD DEPT LOC PHILA, PA. (STC)

TITLE CURRENT COLLECTOR, OXYGEN SENSOR

CONTRACT NO.

CODE IDENT NO. 15227 | SIZE B | DWG NO. 133B2812

SCALE 4-1 | WT CALC ACTUAL | SHEET 1

PRINTED IN U.S.A.

PARTS TO

FOLD

FOLD

SIZE		SHEET	REV
B	133B2813		

REVISIONS

SYM	DESCRIPTION	DATE	APPROVED

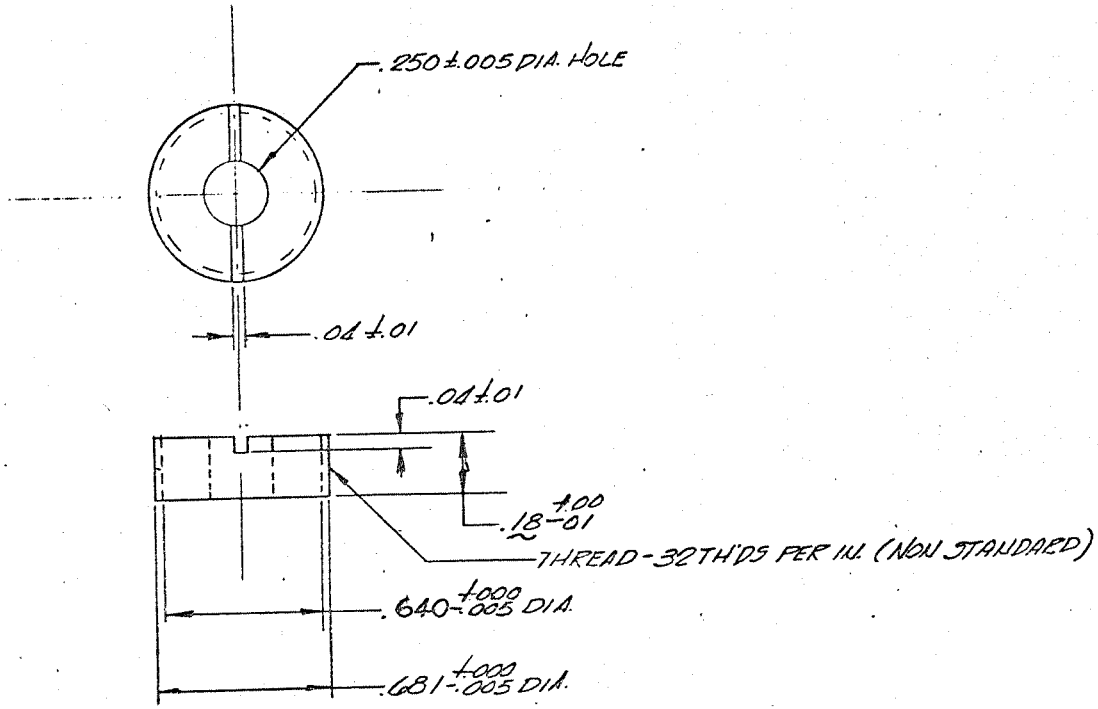

UNLESS OTHERWISE SPECIFIED DIMENSIONS ARE IN INCHES. TOLERANCES ON:	SIGNATURES	DATE	GENERAL ELECTRIC
FRACTIONS ± DECIMALS ± ANGLES ±	DRAWN Connel	6-10-64	MSD DEPT LOC PHILA, PA (STC)
ALL SURFACES ✓	CHECKED		TITLE SCREW, RETAINER-SPECIAL OXYGEN SENSOR
MATL—GOVT OR COML CRES STL TYPE 303 OR 304	ISSUED		CONTRACT NO.
CE	ENGRG		CODE IDENT NO. 15227 / SIZE B / DWG NO. 133B2813
	MFG		SCALE 2-1 / WT CALC ACTUAL / SHEET
	MATLS		

PRINTS TO

FOLD

FOLD

SIZE	133B2815	SHEET	REV
B			

REVISIONS

SYM	DESCRIPTION	DATE	APPROVED

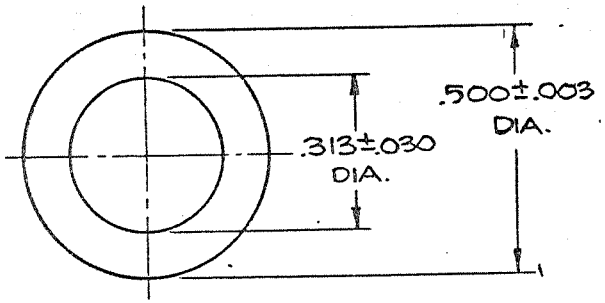

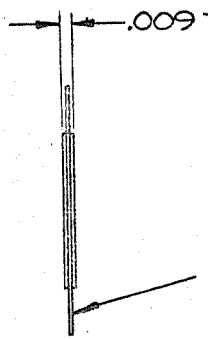

NOTE
1 MATERIAL FROM GENERAL ELECTRIC DIRECT ENERGY CONVERSION ORGANIZATION

UNLESS OTHERWISE SPECIFIED DIMENSIONS ARE IN INCHES. TOLERANCES ON:	SIGNATURES	DATE
FRACTIONS ± DECIMALS ± ANGLES ±	DRAWN J.H. Saunders	8/6/68
ALL SURFACES ✓	CHECKED	
MATL—GOVT OR COML	ISSUED	
SEE NOTE 1	ENGRG	
GE	MFG	
	MATLS	

GENERAL ELECTRIC MSD DEPT LOC PHILA PA (STC)

TITLE ION, EXCHANGE MEMBRANE

CONTRACT NO.

CODE IDENT NO.	SIZE	DWG NO.
15227	B	133B2815

SCALE | WT CALC ACTUAL | SHEET

PRINTS TO

FOLD

FOLD

SIZE	133B2816	SHEET	REV
B			

REVISIONS

SYM	DESCRIPTION	DATE	APPROVED

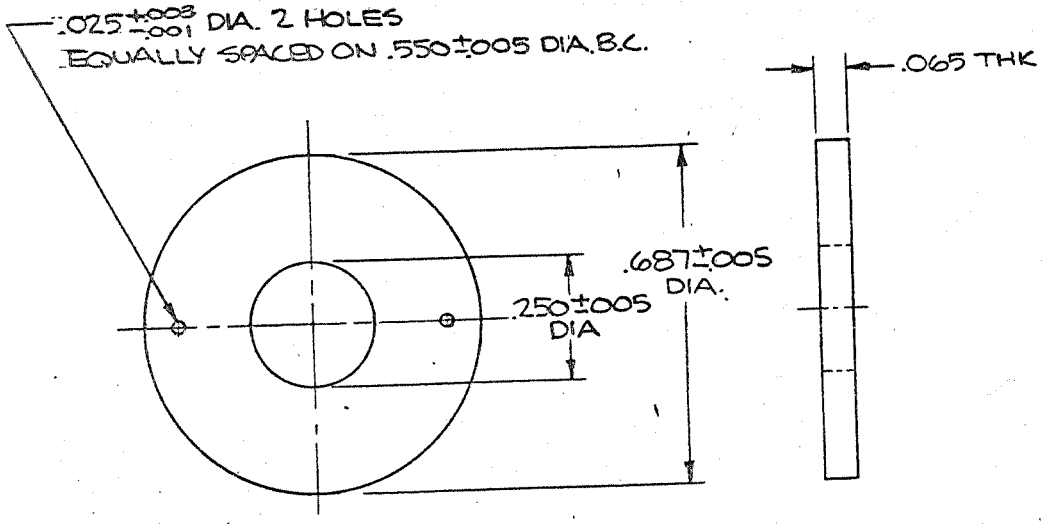

UNLESS OTHERWISE SPECIFIED DIMENSIONS ARE IN INCHES. TOLERANCES ON:	SIGNATURES	DATE
FRACTIONS ± DECIMALS ± ANGLES ±	DRAWN J.H. Saunders	8/9/68
ALL SURFACES √	CHECKED	
MATL—GOVT OR COML	ISSUED	
VITON 985	ENGRG	
GE	MFG	
	MATLS	

GENERAL ELECTRIC

MSD DEPT LOC PHILA, PA. (STC)

TITLE SEAL, LOWER

CONTRACT NO.

CODE IDENT NO.	SIZE	DWG NO.
15227	B	133B2816

SCALE | WT CALC ACTUAL | SHEET

PRINTS TO

FOLD

FOLD

SIZE	133B2817	SHEET	REV
B			

REVISIONS

SYM	DESCRIPTION	DATE	APPROVED

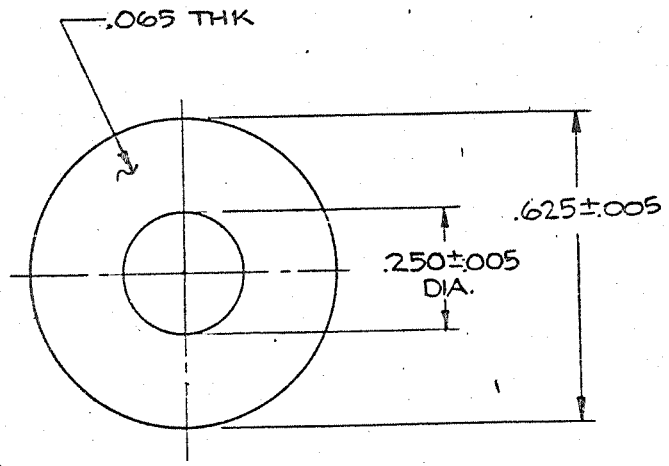

UNLESS OTHERWISE SPECIFIED DIMENSIONS ARE IN INCHES. TOLERANCES ON:	SIGNATURES	DATE
FRACTIONS ± DECIMALS ± ANGLES ±	DRAWN J.H. Saunders	8/6/68
ALL SURFACES ✓	CHECKED	
MATL–GOVT OR COML	ISSUED	
VITON #985	ENGRG	
GE	MFG	
	MATLS	

GENERAL ELECTRIC — MSD DEPT — LOC PHILA PA (STC)

TITLE: SEAL, UPPER

CONTRACT NO.

CODE IDENT NO.	SIZE	DWG NO.
15227	B	133B2817

SCALE	WT CALC ACTUAL	SHEET

PRINTS TO

FN,002-P (1-68) PRINTED IN U.S.A.

FOLD

SIZE	DRAWING NO.	SHEET	REV
B	13382818		

REVISIONS

SYM	DESCRIPTION	DATE	APPROVED

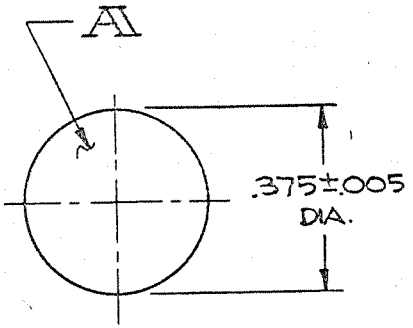

Pc. No	DIM. A	NAME
1	.003 THK	MULTI-GAS
2	.001 THK	SINGLE GAS

(1) (2)

UNLESS OTHERWISE SPECIFIED DIMENSIONS ARE IN INCHES. TOLERANCES ON:
FRACTIONS ± DECIMALS ± ANGLES ±
ALL SURFACES √

MATL—GOVT OR COML
SILICONE RUBBER
GE

SIGNATURES		DATE
DRAWN	J.H. Saunders	8/6/64
CHECKED		
ISSUED		
ENGRG		
MFG		
MATLS		

GENERAL ELECTRIC
MSD DEPT LOC PHILA PA (STK)

TITLE
BARRIER

CONTRACT NO.

CODE IDENT NO.	SIZE	DWG NO.
15227	B	13382818

SCALE	WT CALC. ACTUAL	SHEET

PRINTS TO

FM 552 P (1-63) PRINTED IN U.S.A.

SIZE	DWG NO.
B	133B2819

REVISIONS

SYM	DESCRIPTION

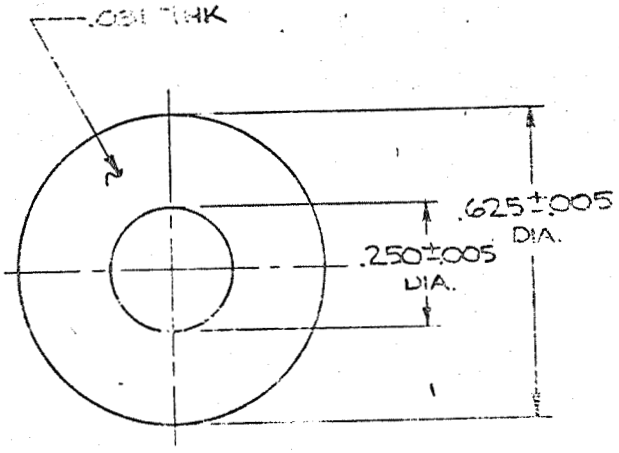

UNLESS OTHERWISE SPECIFIED DIMENSIONS ARE IN INCHES. TOLERANCES ON:

DECIMALS	ANGLES
±	±
ALL SURFACES	✓

MATCH DWG NO. COML

FINISH

BREAK

SIGNATURES		DATE
DRAWN	J.H. Saunders	3/6/64
CHECKED		
ISSUED		
ENGRG		
MFG		
MATLS		

GENERAL ELECTRIC

MSD DEPT LOC PHILA, PA (STC)

TITLE: WASHER

CONTRACT NO.

CODE IDENT NO.	SIZE	DWG NO.
15227	B	133B2819

SCALE	WT LBS ACTUAL	SHEET

PRINTS TO

FM 902-P (4-63) PRINTED IN U.S.A.

FOLD

SIZE	133B2820	SHEET	REV
B			

REVISIONS

SYM	DESCRIPTION	DATE	APPROVED

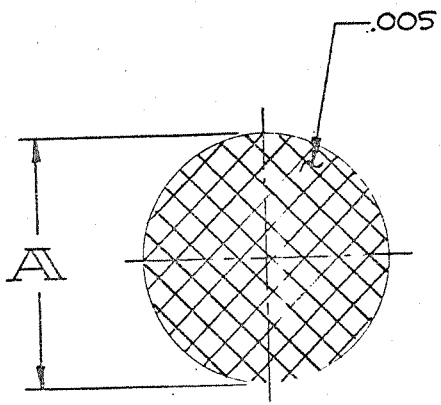

PC NO	DIM A
1	.375±.005 DIA.
2	.240±.005 DIA.

NOTE

1 MATERIAL FROM GENERAL ELECTRIC DIRECT ENERGY CONVERSION ORGANIZATION

UNLESS OTHERWISE SPECIFIED DIMENSIONS ARE IN INCHES. TOLERANCES ON: FRACTIONS ± DECIMALS ± ANGLES ± ALL SURFACES ✓	SIGNATURES	DATE
MATL–GOVT OR COML: SEE NOTE 1	DRAWN J.H. Saunders	8-10-64
GE	CHECKED	
	ISSUED	
	ENGRG	
	MFG	
	MATLS	

GENERAL ELECTRIC

MSD DEPT LOC PHILA PA (STC)

TITLE: SCREEN

CONTRACT NO.

CODE IDENT NO.	SIZE	DWG NO.
15227	B	133B2820

SCALE | WT CALC ACTUAL | SHEET

PRINTS TO

PRINTED IN U.S.A.

FN-502-P (2-63)

FOLD

APPENDIX C

BIBLIOGRAPHY

1. Greene, S. B. and Greene, N. D., Theoretical Analysis of Electrochemical Energy Conversion Systems, Electrochemical Technology - Sept.-Oct., 1963.

2. Phillips, Studies of Development and Future Prospects for the Ion-Exchange Membrane Fuel Cell. General Electric Report

3. Moore, Walter J., Physical Chemistry, 3rd Ed., Prentice Hall, 1962.

4. Austin, L. G., Electrode Kinetics of Low Temperature Hydrogen-Oxygen Fuel Cells in "Fuel Cells", Young, G. J. Reinhold Publishing Co., N.Y. (1960)

5. Hartner, A. J., Vertes, M. A., Median, V. E., and Oswin, H. G., Effects Of Oxygen Partial Pressure on Fuel Cell Cathodes, presented before the Div. of Fuel Chemistry, American Chemical Society, N. Y., September 8-13, 1963.

6. Tuwinder, Sidney B., Diffusion and Membrane Technology, Reinhold Publishing Co., 1962.

7. Warner, H., An Oxygen Partial Pressure Sensor, presented during the "Fourth International Medical Electronics Conference", July, 1961.

APPENDIX D

Component Specification For A Hydrogen Pressure Regulating Valve and Reservoir

1.0 Scope - This specification establishes the design and fabrication of an integral regulating valve and reservoir, for use with pure hydrogen gas.

2.0 Functional Schematic

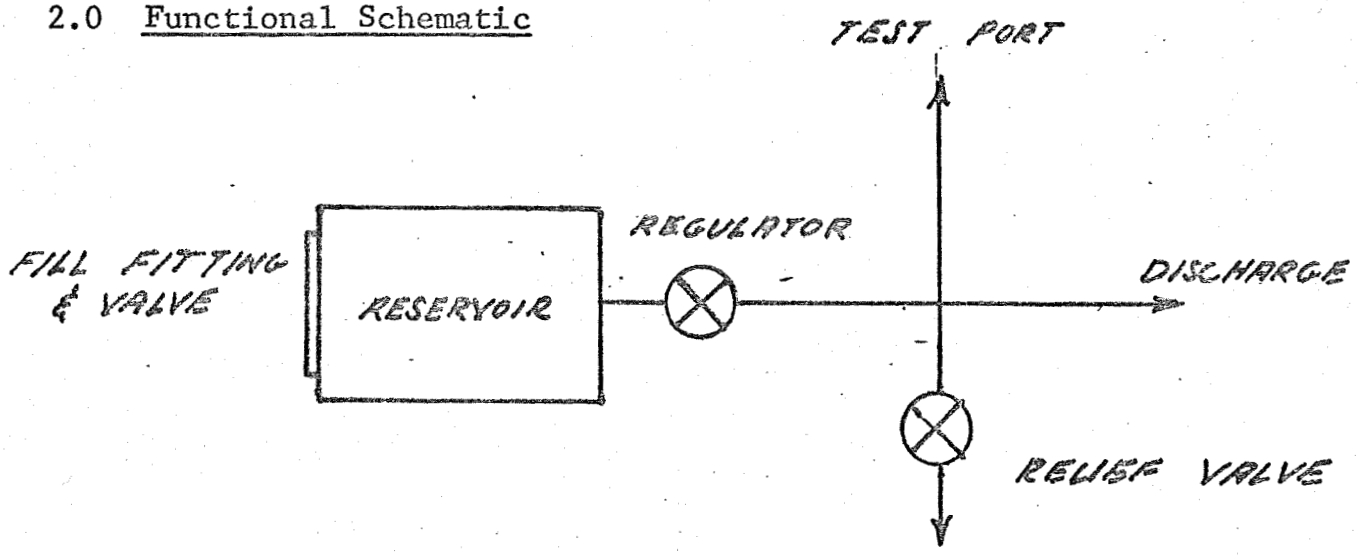

3.0 Requirements

3.1 Inlet Pressure - 20 to 2000 psig @70°F

3.1.1 Proof Pressure - 3200 psig @110°F

3.1.2 Burst Pressure - 4300 psig @110°F

3.2 Outlet Pressure - The regulated outlet pressure shall be adjustable from 12 to 17 psia with a holding tolerance of ±0.5 psi. This adjustment feature need not be accessible.

3.3 Flow Rate - Valve shall be designed for a maximum flow rate of 0.13 Sec/Min., hydrogen gas.

3.4 Relief Valve - A relief valve shall be positioned on the regulating valve discharge. This valve will crack at 25 ±5 psig and shall be capable of flowing 0.25 Scc/Min. minimum.

3.5 Storage Reservoir - The reservoir shall be designed to hold 0.5 grams of hydrogen gas at 2000 psig and 70°F.

3.6 Temperature Range - 35°F to 110°F.

3.7 Envelope - The size of the valve and reservoir shall not exceed 13.8 cubic inches. Detail mounting requirements will be negotiated at a future date.

3.8 Weight - The weight of the valve and reservoir assembly shall not exceed 10 ounces.

4.0 Protective Treatment - When any materials utilized are subject to deterioration due to environmental conditions, they shall be suitably protected. The use of any coatings that might crack, chip or scale shall be avoided.

5.0 Design - This valve and reservoir shall be designed to meet the general requirements of MIL-E-5727C although no qualification test shall be performed.

5.1 Interface - The GE Regulator Vendor interface shall consist of 1¼-12-UNF-2A thread. Depth shall be controlled between 0.275 and 0.30 inches.

5.2 Unit shall be designed to operate in any arbitrary attitude.

6.0 Acceptance Tests - The following acceptance tests shall be performed on each unit shipped in the order stated. General Electric personnel shall have the right to witness these tests at the vendor's facility.

6.1 Proof Pressure Test - With outlet port capped the unit shall be pressurized to 3500 psig at room ambient conditions.

6.2 Performance Test - With the reservoir charged to 2000 psi the regulator shall demonstrate stability by holding the outlet pressure to 14.5 ±0.5 psia. This test shall be repeated with the reservoir charged to 20 psig. This performance shall be demonstrated in any arbitrary attitude selected.

6.3 Relief Valve Performance Test - The outlet pressure shall be artificially raised until the relief valve cracks at 25 $\pm$3 psig.

6.4 Leakage Test - With the reservoir charged to 2000 psig and the outlet port capped external leakage shall not exceed 1 x 10^{-6} cc/sec at room temperature. Test gas is optional.